National River Conservation Directorate
Ministry of Jal Shakti,
Department of Water Resources,
River Development & Ganga Rejuvenation
Government of India

Cyclone Monitoring Information

Periyar River Basin

March 2026

cPeriyar
IIT PALAKKAD
cGanga

Cyclone Monitoring Information

Periyar River Basin

cPeriyar

IIT PALAKKAD

National River Conservation Directorate (NRCD)

The National River Conservation Directorate, functioning under the Department of Water Resources, River Development & Ganga Rejuvenation, and Ministry of Jal Shakti providing financial assistance to the State Government for conservation of rivers under the Centrally Sponsored Schemes of 'National River Conservation Plan (NRCP). National River Conservation Plan to the State Governments/ local bodies to set up infrastructure for pollution abatement of rivers in identified polluted river stretches based on proposals received from the State Governments/ local bodies, www.nrcd.nic.in.

Centres for Periyar River Basin Management Studies (cPeriyar)

The Centres for Periyar River Basin Management Studies (cPeriyar) is a Brain Trust dedicated to River Science and River Basin Management. Established in 2024 by IIT Palakkad and NIT Calicut, under the supervision of cGanga at IIT Kanpur, the center serves as a knowledge wing of the National River Conservation Directorate (NRCD). cPeriyar is committed to restoring and conserving the Periyar River and its resources through the collation of information and knowledge, research and development, planning, monitoring, education, advocacy, and stakeholder engagement, www.cperiyar.org.

Centre for Ganga River Basin Management and Studies (cGanga)

cGanga is a think tank formed under the aegis of NMCG, and one of its stated objectives is to make India a world leader in river and water science. The Centre is headquartered at IIT Kanpur and has representation from most leading science and technological institutes of the country. cGanga's mandate is to serve as think-tank in implementation and dynamic evolution of Ganga River Basin Management Plan (GRBMP) prepared by the Consortium of 7 IITs. In addition to this, it is also responsible for introducing new technologies, innovations, and solutions into India, www.cganga.org.

Acknowledgment

This report is a comprehensive outcome of the project jointly executed by IIT Palakkad (Lead Institute) and NIT Calicut (Fellow Institute) under the supervision of cGanga at IIT Kanpur. It was submitted to the National River Conservation Directorate (NRCD) in 2026. We gratefully acknowledge the individuals who provided information and photographs for this report.

Team

Dr. Sarmistha Singh, cPeriyar, IIT Palakkad
Dr B Sridharan, cPeriyar, IIT Palakkad
Dr. Athira P, cPeriyar, IIT Palakkad
Dr. Neenu K, cPeriyar, IIT Palakkad
Drisiya J, cPeriyar, IIT Palakkad
Akhila K, cPeriyar, IIT Palakkad
Dr. Santosh G Thampi, cPeriyar, NIT Calicut
Dr. S K. Pramada, cPeriyar, NIT Calicut
Anand V, cPeriyar, NIT Calicut
Aditya Harikumar, cPeriyar, NIT Calicut
Dr Vinod Tare, cGanga, IIT Kanpur

Preface

Cyclones are among the most destructive hydro-meteorological hazards affecting the Indian subcontinent, bringing intense rainfall, strong winds, storm surges waves, flooding, and widespread socio-economic disruption. In the context of Kerala and particularly river basins such as the Periyar, cyclonic systems in the Arabian Sea are increasingly influencing rainfall variability, reservoir inflows, flood risks, landslides, and coastal vulnerabilities. With emerging evidence of changing cyclone patterns under a warming climate, the need for systematic monitoring, timely information dissemination, and science-based risk assessment has become more critical than ever.

This Cyclone Monitoring Information Report presents a comprehensive analysis of cyclonic activity affecting Kerala, with particular emphasis on its implications for the Periyar River Basin. The report integrates meteorological observations, reanalysis datasets, spatial mapping, hydrological linkages, and impact assessments to evaluate cyclone frequency, intensity trends, rainfall characteristics, and associated hydrological responses. Special attention is given to extreme rainfall events, reservoir dynamics, flood potential, and cascading impacts on infrastructure, ecosystems, and communities.

By combining data-driven analysis with geospatial techniques and basin-scale interpretation, this report aims to strengthen early warning capabilities, enhance preparedness planning, and support resilient water resource management. It also provides a structured information framework that can assist policymakers, disaster management authorities, researchers, and local stakeholders in making informed, timely decisions during cyclone events.

We sincerely acknowledge the contributions of meteorological agencies, research institutions, technical experts, and field teams whose efforts have enabled the development of this report. Their commitment to advancing scientific understanding and operational preparedness has been invaluable. It is our hope that this report will serve not only as a technical reference but also as a strategic tool supporting proactive risk reduction, climate adaptation, and sustainable basin management in the face of evolving cyclone dynamics.

Centres for Periyar River Basin
Management Studies (cPeriyar)
IIT Palakkad & NIT Calicut

Contents

List of Figures

List of Tables

1. Background

Periyar River Basin (PRB), the longest river in Kerala, originates from the Sivagiri Hills in the Western Ghats and flows westward for approximately 260.7 km before draining into the Vembanad Lake. PRB spans ecologically sensitive highlands, midland agricultural zones, and densely populated lowlands, including major urban and industrial centres. This diverse physiographic and socio-economic setting makes the basin highly sensitive to extreme hydro-meteorological events, particularly cyclones and associated heavy rainfall systems. Although Kerala lies along the western coast of India, traditionally considered less cyclone-prone compared to the eastern seaboard, recent decades have witnessed an increasing frequency and intensity of cyclonic systems over the Arabian Sea. Warmer sea surface temperatures, altered atmospheric circulation patterns, and climate variability have contributed to stronger and more moisture-laden storms. Even when cyclones do not make direct landfall in Kerala, their associated rainbands and low-pressure systems often produce extreme rainfall over the Western Ghats and adjoining river basins along the coast, they can also increase wave heights.

Basin's steep topography, dense drainage network, and A reservoir-regulated flow system amplifies the hydrological response to high-intensity rainfall. Major reservoirs such as Idukki and Idamalayar play a critical role in hydropower generation and flood moderation; however, intense short-duration rainfall during cyclonic events can result in rapid inflow surges, reservoir stress, downstream flooding, and landslide occurrences in vulnerable highland regions. Urban centres such as Kochi and industrial belts like Eloor–Edayar increase exposure and vulnerability to cyclone-induced hazards. High population density, infrastructure concentration, and land-use alterations in floodplains further compound the risk. In addition to direct impacts such as wind damage and flooding, cyclones influence water quality, sediment transport, reservoir operations, and groundwater recharge dynamics. With climate change projections indicating potential increase in the frequency of cyclone tracks shifts in cyclone tracks, intensity, and rainfall characteristics, the need for systematic cyclone monitoring and basin-specific risk identification has become increasingly important. Accurate prediction of cyclone path, real-time monitoring of hourly meteorological parameters, and integration with hydrological assessments are essential for strengthening preparedness, minimizing damage, and supporting adaptive water resource management.

In this context, a structured Cyclone Monitoring and Information framework is necessary to bridge the gap between large-scale meteorological forecasting and basin-level decision-making. Such a framework enables early identification of risk zones, supports reservoir operation planning, and enhances coordination among disaster management authorities, research institutions, and local administrations.

1.2 Objectives

The objective of this report is to monitor and analyze historical cyclones affecting the Periyar river basin in order to identify potential risks and support timely decision-making.

This includes:

1. Predicted path of the cyclone – To assess the historical trajectory, intensity, and movement of cyclonic systems and evaluate their potential influence on the Periyar river basin.
2. Hourly meteorological changes – To examine temporal variations in rainfall, wind speed, atmospheric pressure, temperature, and related parameters to understand the evolving severity and associated hydrological risks.

2. Introduction

A “Cyclonic Storm’ or a “Cyclone” is an intense vortex or a whirl in the atmosphere with very strong winds circulating around it in anti-clockwise direction in the Northern Hemisphere and in clockwise direction in the Southern Hemisphere (Indian Meteorological Department (IMD), 2021). The word “cyclone” comes from the Greek word “kyklos” (often written as “cyclos”), which means “a coil” or “a circle.” The term was introduced by Henry Piddington, who carefully studied tropical storms over the Bay of Bengal (BoB) and the Arabian Sea (ARB) (IMD, 2021). These powerful storms looked like giant sea serpents coiling over the ocean, and inspired by this image, he named them “cyclones”. Around the world, these intense tropical storms are known by different names depending on where they form. Over the Atlantic Ocean, they are called hurricanes; over the Pacific Ocean, they are known as typhoons; around the Australian region, they are sometimes referred to as willy-willies; and over the North Indian Ocean (NIO), including the BoB and the ARB, they are simply called cyclones (Niyas et al., 2009; IMD, 2021; Kumar & Gupta, 2023).

Tropical cyclone (TCs) is the term used globally to cover tropical weather systems in which winds equal or exceed ‘gale force’ (minimum of 62 kmph or 34 knots) (IMD, 2021). India has a coastline encompassing the mainland and various islands exceeding 7,500 km; about 76% of the coastline in India is prone to cyclones (National Disaster Management Authority (NDMA), 2008). An analysis of cyclone frequencies on the East and West coasts of India during 1891-2000 shows that nearly 308 cyclones (103 of which were severe) affected the East Coast (NDMA, 2019). In the NIO, cyclones predominantly originate over the BoB and the ARB and subsequently move under the influence of large-scale atmospheric steering currents (Priya et al., 2022). The frequency of TCs in the BoB is higher relative to that over the ARB. However, in recent years, it has been observed that a greater number of TCs are forming in the ARB than in the BoB (Deshpande et al., 2021). According to IMD records, only 25 per cent of cyclones that develop over the ARB approach the west coast (IMD, 2013).

TCs can lead to extreme rainfall, flash floods, riverine flooding, landslides, and significant infrastructure damage, necessitating systematic monitoring and early warning systems. In India, the responsibility for tracking, forecasting, and issuing warnings for such disturbances is undertaken by IMD. Although the BoB and ARB generate only about 7 % of the world's cyclones, their impacts are highly destructive, particularly along the densely populated, low-lying coasts of eastern India and Bangladesh bordering the North Bay of Bengal (Gupta et al., 2019). Most tropical cyclones in the NIO form in the BoB (~74%) compared to the ARB (~26%), with BoB storms typically tracking northward toward India, Bangladesh, and Myanmar, while ARB cyclones generally move westward toward Oman and Yemen, and about 25% dissipate before landfall. Cyclone activity peaks during the post-monsoon season (October–November, ~45%), followed by pre-monsoon (~22%) and monsoon (~18%) seasons, whereas winter (December–February, ~15%) remains the least active period (Wahiduzzaman, 2024).

According to the United Nations Framework Convention on Climate Change (UNFCCC), anthropogenic climate change influences tropical cyclones by altering their frequency, intensity, spatial distribution, and duration. Rising sea surface temperatures enhance cyclone formation and intensification, while sea-level rise increases the severity of storm surges and associated coastal flooding during cyclonic events (Wu et al., 2022; Wang et al., 2023). According to the World Meteorological Organization (WMO), the year 2016 recorded exceptionally high global temperatures, reduced Arctic sea-ice extent, continued sea-level rise, and increased ocean heat content. These warming trends contribute to enhanced cyclone-related hazards. According to the Intergovernmental Panel on Climate Change (IPCC) Sixth Assessment Report (AR6), based on multiple independent scientific analyses, observational evidence, theoretical studies, and climate model simulations, there is high confidence that the accumulation of greenhouse gases in the Earth's atmosphere is warming the climate system. This warming is increasing the likelihood of extreme and unpredictable weather events, including tropical cyclones.

In India, the coastal states and Union Territories (UTs), covering a total of 84 coastal districts, are exposed to tropical cyclone impacts. Among them, four states on the east coast, such as Tamil Nadu, Andhra Pradesh, Odisha, and West Bengal, along with the Union Territory of Puducherry, are highly vulnerable to cyclone hazards. On the west coast, Gujarat is also recognized as highly susceptible to cyclonic disturbances.

2.1 Classification of Cyclonic Disturbances

Cyclones are intense low-pressure systems characterized by a central region of minimum atmospheric pressure, with pressure gradually increasing outward from the centre. The magnitude of the central pressure drop and the surrounding pressure gradient determine the cyclone's intensity and wind strength (IMD, 2021). The classification criteria used by IMD for categorizing low-pressure systems over the Bay of Bengal and the Arabian Sea, as adopted from the World Meteorological Organization (WMO), are presented in Table 1.

Table 1 Classification used in India for tropical cyclones (*Source: NDMA, 2019*)

Sl. No	Type	Wind Speed (km/h)	Wind Speed (Knots)
1	Low Pressure Area	< 31	< 17
2	Depression	31 – 49	17 – 27
3	Deep Depression	50 – 61	28 – 33
4	Cyclonic Storm	62 – 88	34 – 47
5	Severe Cyclonic Storm	89 – 118	48 – 63
6	Very Severe Cyclonic Storm	119 – 221	64 – 119
7	Super Cyclone	> 221	> 119

a) Structure of Tropical Cyclone

TCs are warm-core, low-pressure systems characterized by a large rotating vortex in the atmosphere. They are powered by the release of latent heat from convective clouds that develop over warm ocean waters (IMD, 2013). The structure of a mature TCs is a complex, three-dimensional system characterized by a distinct central eye, a surrounding eyewall, and outer spiral rainbands (Kumar et al., 2025) (Figure 1). The eye is a relatively calm region of minimum atmospheric pressure and subsiding air, which leads to a warm-core structure where lower tropospheric temperatures are significantly higher than the surrounding environment (Kumar et al., 2025). Surrounding this core is the eyewall, a ring of intense convective activity where the steepest radial pressure gradients exist, generating the storm's maximum sustained wind speeds (Bell & Montgomery, 2008). Beyond the eyewall, spiral rainbands extend outward, characterized by intense wind shear and steep wind speed gradients that contribute to the storm's overall destructive potential (Kumar et al., 2025).

A fully developed cyclone is an intense atmospheric whirl, typically 150–1000 km in diameter and 10–15 km in height, with wind speeds of 150–250 km/h or higher. The central pressure is usually 30–100 hPa lower than the normal sea-level pressure (IMD, 2013; Sharma et al., 2025).

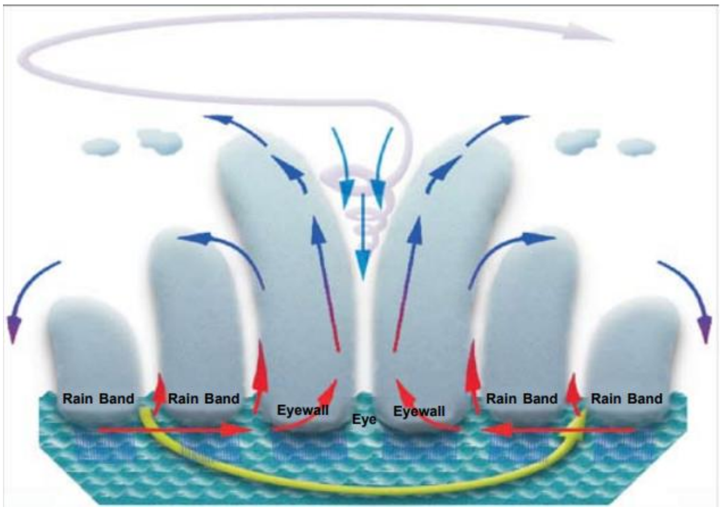

Figure 1 Schematic diagram of a cyclone (S*ource: IMD, 2013*)

b) Life Cycle of Tropical Cyclone over the North Indian Ocean

Over NIO, tropical cyclones typically last 4-5 days and evolve through four stages: formative, immature, mature, and decaying. Cyclogenesis begins over warm waters (SST > 26.5° C) under favourable conditions such as sufficient Coriolis force, low vertical wind shear, high humidity, and atmospheric instability (IMD, 2021). The formative stage involves pressure fall and organization of circulation, followed by rapid intensification in the immature stage, marked by increasing winds, falling central pressure, and development of an eye and spiral rainbands. The mature stage represents peak intensity with maximum sustained winds (Bell & Montgomery, 2008; Priya et al., 2022). In the decaying stage, the system weakens over land or cooler waters due to reduced moisture supply and increased friction. The longest recorded NIO cyclone track occurred in October 1921, originating over the South China Sea and traversing Vietnam, the BoB, South India, the ARB, and Oman (Figure 2).

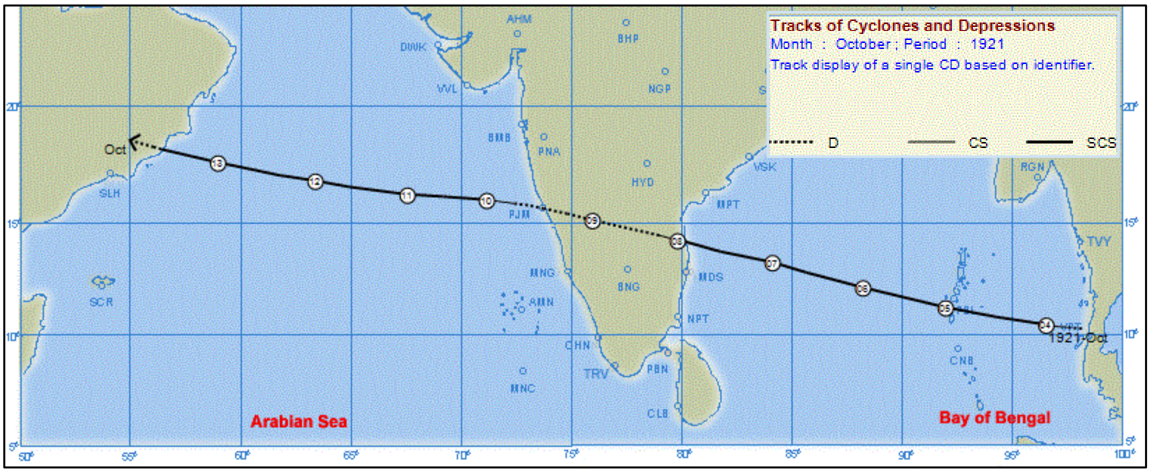

Figure 2 Longest life period of 1921 cyclone over the NIO (*Source: IMD, 2013*)

c) Institutions for cyclone forecasting and dissemination of warnings

Early warning is a key component of disaster risk management. In India, cyclone forecasting and dissemination are primarily handled by the IMD and the Indian National Centre for Ocean Information Services (INCOIS) under the Ministry of Earth Sciences (MoES).

India Meteorological Department (IMD)

The IMD operates a three-tier cyclone warning system:

- Area Cyclone Warning Centres (ACWCs) at Chennai, Mumbai, and Kolkata
- Cyclone Warning Centres (CWCs) at Visakhapatnam, Ahmedabad, and Bhubaneswar
- The Cyclone Warning Division (New Delhi) functions as the Regional Specialized Meteorological Centre (RSMC) for the World Meteorological Organization (WMO) / United Nations Economic and Social Commission for Asia and the Pacific (ESCAP) region.

Cyclone warnings in India are issued in four stages by the IMD to ensure timely preparedness and response. The first stage, Pre-Cyclone Watch, is issued 72 hours in advance, indicating the potential development of a cyclonic disturbance. This is followed by the Cyclone Alert (48 hours in advance), providing details on the storm's location, intensity, and likely impact areas. The Cyclone Warning stage (24 hours in advance) gives precise forecasts of landfall location, time, and associated hazards such as heavy rainfall, strong winds, and storm surge. The final stage, Post Landfall Outlook (12 hours in advance), describes the cyclone's movement inland and expected weather conditions over interior regions. These warnings are also associated with colour codes - Yellow (Alert), Orange (Warning), and Red (Post-landfall outlook) - to indicate increasing severity.

In addition to these warnings, the IMD disseminates information through multiple channels, including port warnings, coastal and marine bulletins, and special advisories for fishermen. Ports are instructed to hoist storm warning signals, while regular updates are issued for the Indian Navy and coastal regions. Warnings are broadcast to the public via radio and television, particularly through All India Radio and Doordarshan, and are relayed through state authorities to coastal communities. Fishermen receive frequent updates, especially during disturbed weather, ensuring effective communication and risk reduction.

For monitoring, IMD uses Doppler weather radars (more concentrated along the east coast due to higher vulnerability) and satellite data (Indian National Satellite System (INSAT-3D/3DR), and disseminates warnings via fax, email, SMS, and telephonic alerts to state authorities. The earlier Cyclone Warning Dissemination System (CWDS) is being upgraded with 500 new Direct-To-Home-based systems by the joint initiative led by the IMD in collaboration with the Indian Space Research Organisation (ISRO) and the MoES.

Indian National Centre for Ocean Information Services (INCOIS)

INCOIS provides ocean-related advisories, including ocean state forecasts, high wave alerts, storm surge guidance, tsunami warnings, and potential fishing zone advisories. It issues weather forecasts twice daily for the NIO, increasing frequency during cyclones. The Forecasts are transmitted through maritime systems such as International Maritime Satellite System (INMARSAT) and Navigational Telex (NAVTEX), mainly serving shipping and marine sectors. However, these systems are less accessible to small-scale fishing communities due to technological and cost constraints.

3. Cyclone Monitoring

Cyclone monitoring refers to the continuous observation, tracking, and forecasting of a cyclone position, intensity, structure, and associated rainfall using integrated meteorological techniques. Cyclone monitoring involves the systematic collection, analysis, and integration of meteorological data from multiple observational platforms to determine the cyclone location, intensity (strength), direction of movement, and its likely evolution over the subsequent few days. This continuous monitoring enables timely forecasting and early warning dissemination.

a) Satellite Observations

Satellite observations are the primary source of information for monitoring cyclones, particularly when the system is located over the open ocean where in-situ observations are limited. In this context, geostationary satellites continuously capture images of the Earth's atmosphere, enabling real-time assessment of cloud structure, rotational organization, eye formation, and cloud-top temperatures. Among the various satellite products, infrared (IR) imagery is especially useful during night-time for estimating cloud-top temperature and storm intensity, while visible (VIS) imagery provides detailed information on cloud patterns during daylight hours. In addition, water vapour (WV) imagery helps in analysing upper-level moisture distribution and convective activity, thereby improving the overall understanding of cyclone structure and evolution.

In India, cyclone monitoring is supported by the INSAT series of geostationary satellites operated under the framework of the IMD. Cyclone intensity over the ocean is commonly estimated using the Dvorak technique, a satellite-based empirical method that relates cloud pattern characteristics to wind speed and central pressure. Satellite-derived information is assigned greater importance when the cyclone is far from land, where conventional surface and radar observations are limited.

b) Doppler Weather Radar (DWR) Observations

When a cyclone approaches the coastline, Doppler Weather Radar (DWR) becomes an essential tool for detailed monitoring and short-range forecasting. Unlike satellites, which primarily provide large-scale cloud imagery, radar systems offer high-resolution and real-time observations of the cyclone's internal structure and wind characteristics near land. DWR generates reflectivity and radial velocity products, where reflectivity is used to determine rainfall intensity and the distribution of spiral rainbands, and radial velocity provides information on wind speed and direction within the storm system. These observations enable accurate measurement of near-surface winds, identification of the cyclone eye and eyewall structure, and estimation of spatial rainfall intensity. Radar data become increasingly reliable and critical as the system approaches landfall, and due to their high temporal resolution, they significantly enhance short-range forecasts of up to 24 hours, particularly in predicting landfall location, wind impact zones, and heavy rainfall distribution (Zhao et al., 2012; Srivastava & Bhardwaj, 2014; IMD, 2021).

c) Surface and Ocean Observations

Surface and ocean observations play a crucial role in cyclone monitoring by providing direct, ground-based measurements of atmospheric and oceanic conditions. These observations are obtained from Automatic Weather Stations (AWS), coastal observatories, ships operating in the ocean, moored and drifting buoys, and routine synoptic observations recorded at three-hour intervals. Unlike satellite imagery, which provides indirect estimates, these platforms supply real-time in-situ measurements of key meteorological parameters, including wind speed, wind direction, atmospheric pressure, air temperature, and rainfall (IMD, 2021; Singh et al., 2022).

Among these parameters, atmospheric pressure is particularly significant in cyclone analysis. A continuous and rapid fall in central pressure is one of the strongest indicators of cyclone intensification, as it reflects the strengthening of the low-pressure core and the associated increase in wind speed. The integration of surface and ocean observations with satellite and radar data improves the accuracy of intensity assessment and short-term forecasting, especially during the approach and landfall stages of a cyclone.

d) Upper Air Observations

Upper air observations are essential for understanding the atmospheric conditions above the Earth's surface that influence cyclone development, movement, and intensity changes. These observations are obtained using radiosonde instruments and wind profilers, which provide vertical profiles of atmospheric parameters at different altitudes.

A radiosonde is a balloon-borne instrument that measures temperature, humidity, pressure, and wind speed and direction from the surface up to the upper troposphere. Wind profilers use radar technology to continuously monitor wind patterns at various atmospheric levels. These datasets are crucial for assessing vertical wind shear, which refers to the change in wind speed and direction with height (Zhang et al., 2019; IMD, 2021; Mashao et al., 2024). Low vertical wind shear is favourable for cyclone intensification, as strong shear can disrupt the cyclone's vertical structure and weaken the system. Therefore, upper air observations play a significant role in forecasting cyclone strengthening or weakening trends.

e) Numerical Weather Prediction (NWP) Models

Numerical Weather Prediction (NWP) models are advanced computer-based systems that simulate the behaviour of the atmosphere using mathematical equations representing physical laws such as conservation of mass, momentum, and energy. These models use observed atmospheric and oceanic parameters as input data, including temperature, atmospheric pressure, wind speed and direction, humidity, and sea surface temperature (Kotal et al., 2014; Ashrit et al., 2020; Yip et al., 2026). Based on these initial conditions, the models compute the future state of the atmosphere at regular time intervals.

Using these simulations, NWP models generate forecasts of the cyclone's future position (track), wind intensity, central pressure, and associated rainfall distribution. To enhance forecast reliability, multiple models are run simultaneously and their outputs are combined using ensemble forecasting techniques. This approach reduces uncertainty by accounting for variations in initial conditions and model physics (IMD, 2021).

Cyclone forecasting in the North Indian Ocean typically utilizes global models such as the Global Forecast System (GFS) and the European Centre for Medium-Range Weather Forecasts (ECMWF) model, as well as high-resolution regional models like the Weather Research and Forecasting (WRF) model and the Hurricane Weather Research and Forecasting (HWRF) model (Srivastava & Bhardwaj, 2014; Tallapragada et al., 2014). In addition, Multi-Model Ensemble (MME) approaches and Ensemble Prediction Systems (EPS) are employed to provide probabilistic forecasts and improve track and intensity prediction accuracy (IMD, 2021).

4. Historical Tracks of Tropical Cyclones

The tropical cyclone (TCs) track data used in this study were obtained from the IMD and the International Best Track Archive for Climate Stewardship (IBTrACS). The IMD provides cyclone track information through its Cyclone eAtlas, primarily in JPEG format, which requires additional georeferencing and digitization in GIS platforms such as ArcGIS for further spatial analysis. Cyclone eAtlas, is an electronic database that provides detailed information on the tracks of cyclones and depressions (C & Ds) over the NIO basin from 1891 to the most recent years. This dataset includes spatial and temporal characteristics of each system, making it highly useful for long-term climatological and trend analysis.

The IBTrACS is a comprehensive global repository of tropical cyclone data that integrates records from multiple meteorological agencies, enabling reliable inter-agency comparisons. It includes data contributed by the Joint Typhoon Warning Center (JTWC), which is widely used for estimating key cyclone parameters such as maximum sustained wind speed and minimum central pressure. In this study, the shapefile obtained from IBTrACS, incorporating JTWC best-track data, was utilized to analyse cyclone tracks over the NIO for the selected study period.

IBTrACS represents the most comprehensive global collection of TCs best-track data. It integrates historical and recent cyclone records from multiple international agencies, providing a unified, quality-controlled dataset. Developed in collaboration with various WMO Regional Specialized Meteorological Centres and other global partners, IBTrACS enables consistent inter-agency comparisons and enhances the reliability of cyclone track analysis.

5. History of Cyclones in Kerala

Cyclone monitoring in Kerala is provided by the Cyclone Warning Centre, Thiruvananthapuram, of the India Meteorological Department. The Centre also issues warnings about low-pressure systems that develop in the ARB and BoB, which may pose a danger to fishermen in Kerala. Though Kerala has had many instances of localised coastal cyclones, the state has been relatively free from severe cyclonic storms. Kerala has experienced five major cyclonic events over the past 127 years (KSDMA, 2021). The list of cyclones affecting the PRB is presented in Table 2.

Table 2 Cyclones Affecting the PRB

Cyclone Name	Basin	Date	Category
Gaja	Bay of Bengal	08/11/2018 - 22/11/2018	VSCS
Ockhi	Bay of Bengal	29/11/2017 - 06/12/2017	VSCS
Tauktae	Arabian Sea	13/05/2021 - 18/05/2021	ESCS
Fanoos	Bay of Bengal	04/12/2005 - 12/12/2005	VSCS
Unnamed	Bay of Bengal	19/11/1912 - 22/11/1912	SCS
Unnamed	Bay of Bengal	06/11/1925 - 10/11/1925	SCS
Unnamed	Bay of Bengal	11/11/1935 - 17/11/1935	SCS
Unnamed	Bay of Bengal	29/11/1959 - 06/12/1959	DD
Unnamed	Bay of Bengal	08/11/1966 - 14/11/1966	SCS
Unnamed	Bay of Bengal	17/11/1978 - 29/11/1978	SCS
Unnamed	Bay of Bengal	06/11/1992 - 17/11/1992	SCS
Unnamed	Arabian Sea	05/11/1993 - 16/11/1993	VSCS
Unnamed	Bay of Bengal	02/11/1997 - 14/11/1997	SCS

VSCS - Very Severe Cyclonic Storm ESCS **-** Extremely Severe Cyclonic Storm **SCS -** Severe Cyclonic Storm **DD** - Deep Depression

6. Identified Cyclones in the Periyar River Basin

Periyar river basin is generally less susceptible to cyclones and is categorized under low to moderate cyclone proneness. Maximum sustained wind speeds during such events are typically 34 - 37 knots (63 - 69 km/h), and the basin is within a moderate wind hazard risk zone (Building Materials & Technology Promotion Council (BMTPC), 2019) (Figure 3). The Ernakulam district, which forms part of the PRB, frequently witnesses mild cyclonic disturbances and associated impacts such as heavy rainfall, riverine flooding, urban inundation, and slope instability in upstream regions, during the Southwest Monsoon (June–August) and Northeast Monsoon (September - November) (Kerala State Disaster Management Authority (KSDMA), 2015).

Cyclone Gaja formed over the BoB in November 2018 and made landfall in Tamil Nadu. After crossing the peninsula, its weakened remnant moved westward across southern India and emerged into the ARB as a low-pressure system (Salim & Monolisha, 2022). Although its core landfall occurred outside Kerala, the system contributed rainfall to parts of the Periyar region. Notably, since the IMD began systematic cyclone monitoring in 1990, Gaja was among the rare systems to traverse from the Bay of Bengal to the Arabian Sea across southern India. Similarly, Cyclone Ockhi moved over the ARB in November 2017 and passed close to the Kerala coast without making landfall in the Periyar basin, yet it produced intense rainfall and strong winds in central Kerala (Singh et al., 2020). Cyclone Tauktae, which moved parallel to the Kerala coastline in May 2021, also did not make landfall in the basin but caused heavy rainfall and significant hydrometeorological impacts within the Periyar catchment (Kannaujiya et al., 2024). Cyclone Fannos in December 2005 also had a trajectory over the southern parts of the PRB.

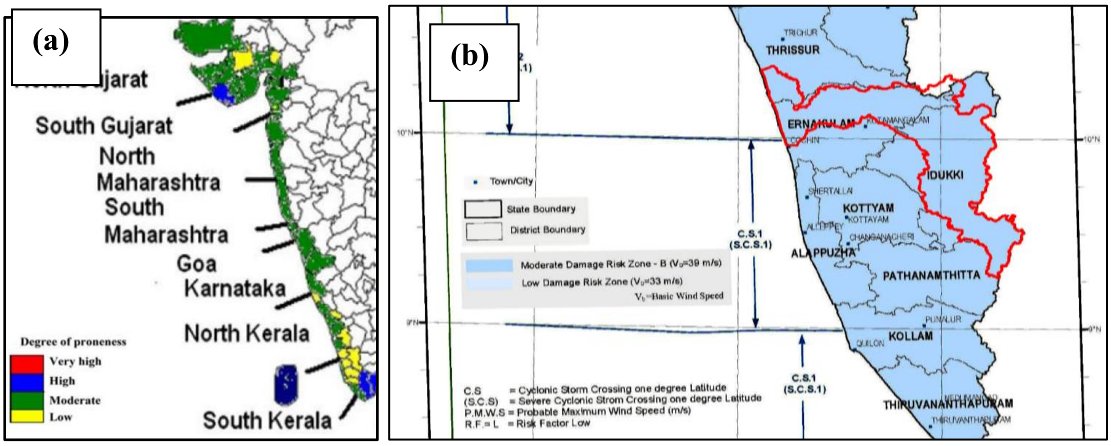

Figure 3 (a) Cyclone hazard prone (b) Wind hazard map (*Source: BMTPC*)

a) Cyclone Gaja

Very Severe Cyclonic Storm (VSCS) Gaja was a significant tropical cyclone that developed over the BoB on 8th November 2018 and made landfall along the Tamil Nadu–Puducherry coast on 16th November. The system caused widespread impacts across southern India, including heavy rainfall and associated hazards in Kerala, particularly within the PRB (IMD, 2018).

Monitoring

Cyclone Gaja was continuously monitored and forecast by the IMD from 7th November 2018, prior to its genesis as a low-pressure area over the BoB using satellite observations (INSAT-3D/3DR, SCATSAT, polar-orbiting satellites), Scatterometer inputs, Doppler Weather Radars at Karaikal, Chennai, Thiruvananthapuram, and Kochi, and available ship and buoy observations. Numerical weather prediction models were used to forecast its track and intensity. Based on these observations and model outputs, IMD issued regular bulletins to WMO/ESCAP Panel countries, national and state disaster management agencies, the public, and the media, and the system was placed under radar surveillance from the morning of 15th November (IMD, 2018). The observed track of Cyclone Gaja is shown in Figure 4.

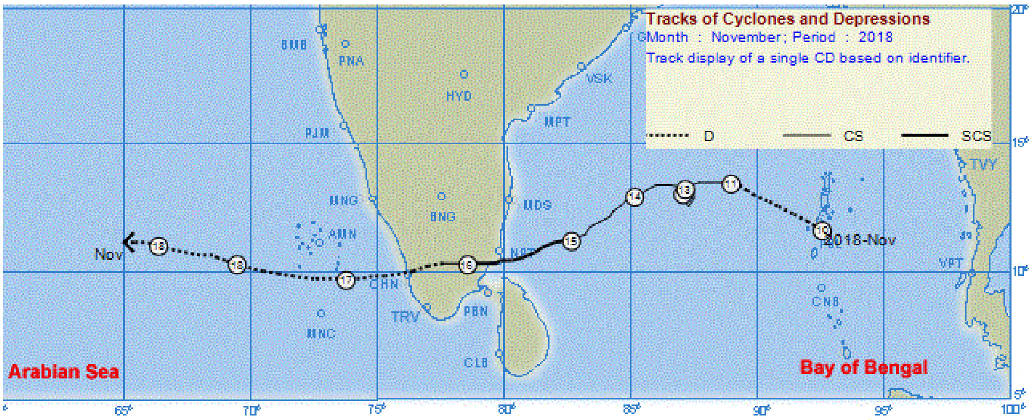

Figure 4 Observed track of VSCS GAJA *(Source: IMD, Cyclone eAtlas)*

Genesis, Intensification and Movement

On VSCS Gaja originated as a low-pressure area over the Gulf of Thailand and adjoining the Malay Peninsula on 8th November 2018 and moved west-north-westward into the BoB under favourable environmental conditions, including sea surface temperatures of 28 - 29° C, strong lower-level convergence (20×10^{-5} s^{-1}), significant cyclonic vorticity (100×10^{-6} s^{-1}), adequate upper-level divergence (15×10^{-5} s^{-1}), and low vertical wind shear (10-15 knots), all of which supported its organization and intensification (IMD, 2018). It intensified into a depression on 10th November and, on 11th November, further into a cyclonic storm.

The cyclone initially moved westward until early 12th November, then recurved south-south-westwards, following an anticlockwise looping track until 13th November morning, before resuming a westward track. It reached its peak intensity as a Very Severe Cyclonic Storm on 15th November, with maximum sustained wind speeds of about 130–140 km/h over the southwest BoB (IMD, 2018).

Gaja made landfall along the Tamil Nadu coast on 16th November with wind speeds of approximately 130 km/h, gusting up to 145 km/h, and weakened rapidly thereafter due to land interaction (Thenmozhi et al., 2024). The remnant system moved westward across Tamil Nadu and entered central Kerala as a depression on 16th November, passing through the Idukki and Ernakulam Districts and significantly influencing rainfall over the PRB before emerging into the ARB. Figure 5 shows the observed track of VSCS Gaja based on JTWC data.

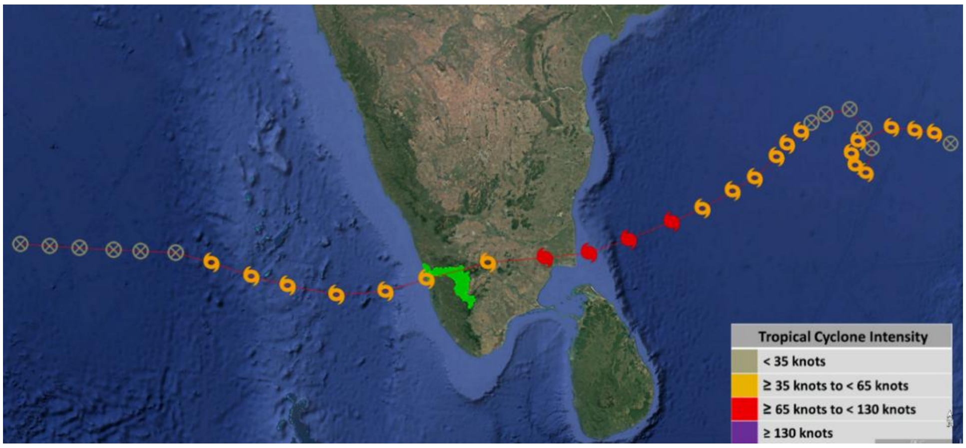

Figure 5 Observed track of VSCS Gaja in Google Earth Imagery (*Source: JTWC*)

The mean wind speed in the middle and deep tropospheric layer around the cyclone centre is shown in Figure 6. The middle - lower tropospheric wind shear remained below 10 knots until 0000 UTC of 14th November, increased to ~15 knots by 0000 UTC of 16th November, and peaked at ~25 knots at 0600 UTC of 16th November, before rapidly decreasing to <5 knots and remaining low until 19th November (IMD, 2018). In contrast, the upper-lower tropospheric shear was ~15 knots until 0600 UTC on 15th November, increased to ~20 knots by 0600 UTC on 16th November, and gradually declined to ~10 knots by 0000 UTC on 19th November.

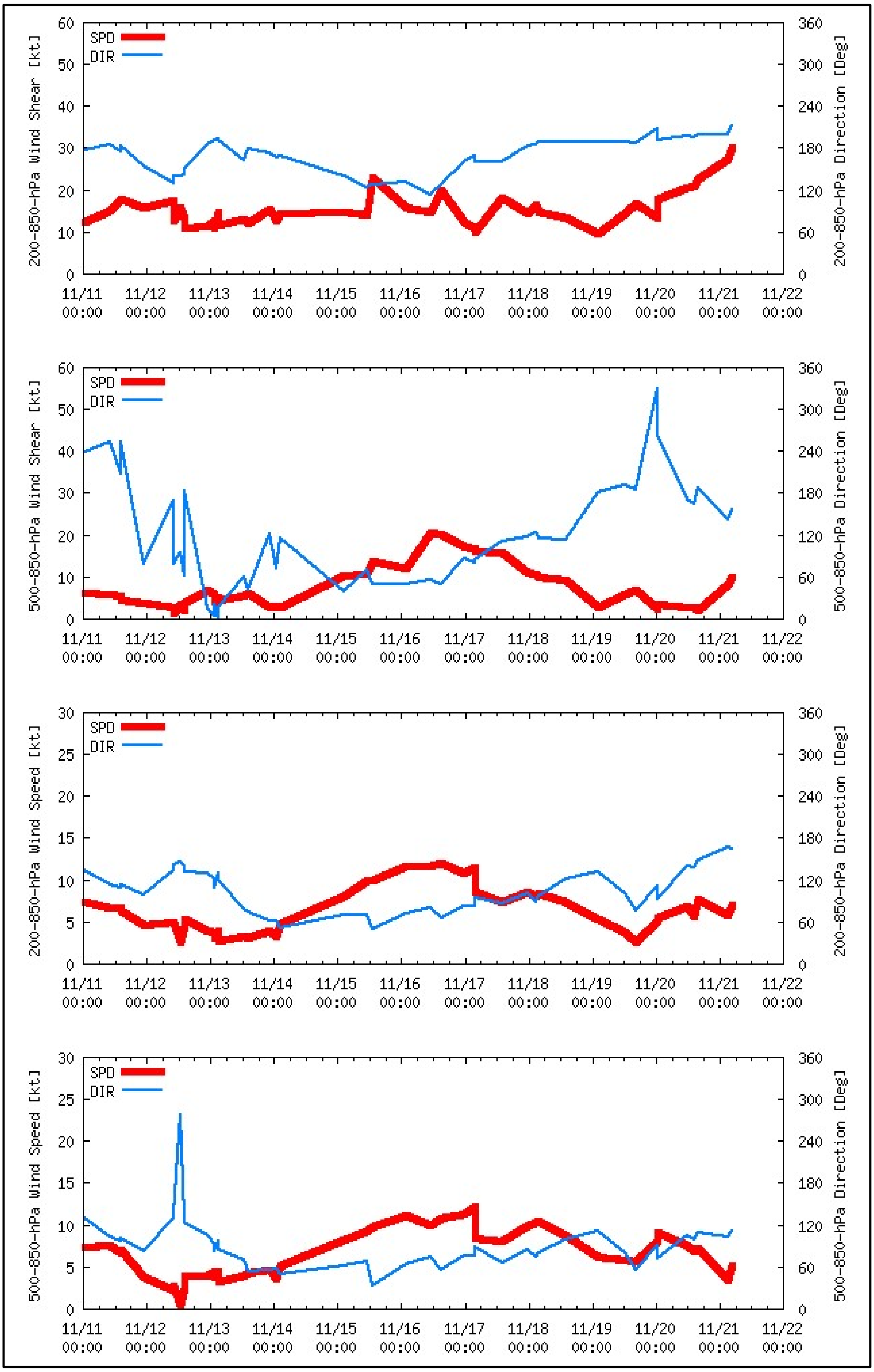

Figure 6 Wind shear and wind speed in the middle and deep layer around the system during VSCS Gaja (*Source: IMD, 2018*)

Impacts and Damages

Kerala, particularly the PRB, was affected by heavy rainfall on 17th November 2018, with a basin-wide average of 61 mm. The maximum rainfall was observed at the Upper Perinjankutty rain gauge station (9.90°N, 77.08°E), which received 185 mm, followed by Pambla Dam Premises (9.96°N, 76.96°E) with 147 mm. Although the cyclone did not make landfall in Kerala, its weakened system contributed significant precipitation over the Western Ghats region, particularly in the upper catchment areas of the basin.

The intense rainfall triggered landslides and mudslides in Idukki district, partially destroying a house and damaging agricultural land in Vattavada, along with damage to a bridge (Figure 7). Sections of National Highway 49 were inundated. In Ernakulam district, which forms the downstream part of the PRB, two houses were destroyed and 199 houses were damaged. The total damage in Ernakulam was estimated at ₹3,800,000. Additionally, fallen trees damaged electrical infrastructure, as reported by The Times of India (17 November 2018).

Figure 7 Inundated cultivation land in Idukki (left) and a car trapped in mud following a landslide at Panniyarkutty near Adimali, Idukki (right). (*Source: The News Minute*)

b) Cyclone Ockhi

VSCS Ockhi was a significant TC that developed over the southwest BoB and rapidly intensified as it moved westward, severely impacting Tamil Nadu, Kerala, and the Lakshadweep Islands with heavy rainfall, strong winds, and rough seas, causing significant damage to infrastructure and loss of lives, particularly among fishermen, before weakening over the ARB and dissipating near Gujarat (IMD, 2017).

Monitoring

Cyclone Ockhi was continuously monitored by the IMD using satellite observations (INSAT-3D/3DR, SCATSAT, ASCAT), along with ship, buoy, and coastal observations. DWR located at Chennai, Thiruvananthapuram, Kochi, and other stations supported real-time tracking of the system. Forecasting was aided by multiple numerical weather prediction models, including IMD-GFS, WRF, HWRF, ECMWF, and NCEP-GFS. Based on these observations and model outputs, IMD issued regular advisories and warnings to disaster management agencies and the public (IMD, 2017). The observed track of VSCS Ockhi over the BoB is shown in Figure 8.

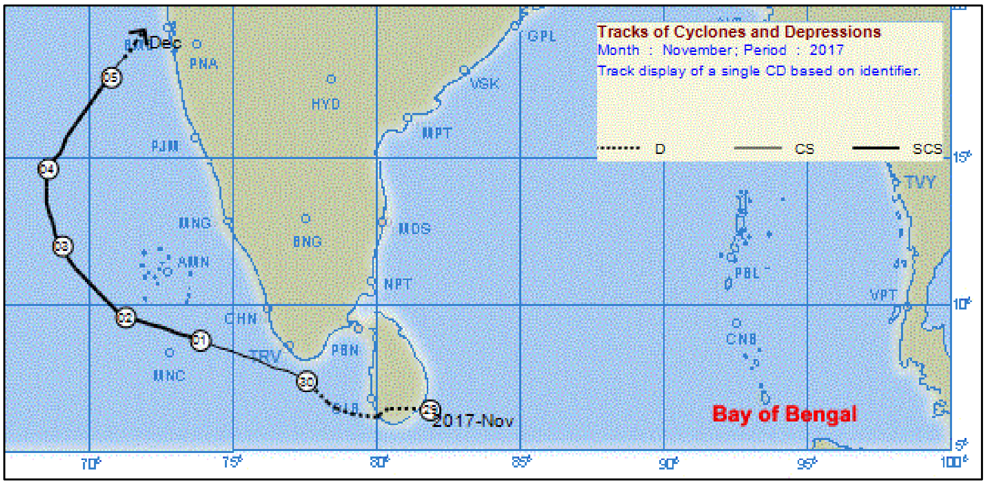

Figure 8 Observed track of VSCS Ockhi (*Source: IMD, Cyclone eAtlas*)

Genesis, Intensification and Movement

Cyclone Ockhi originated as a low-pressure system over the southwest BoB and adjoining Sri Lanka region on 28th November 2017 and intensified into a depression on 29th November (IMD, 2017). After crossing Sri Lanka, the system rapidly intensified over the Comorin Sea into a deep depression and cyclonic storm within hours, and further into a severe cyclonic storm.

Favourable environmental conditions, including warm sea surface temperatures (28–30°C) and low to moderate vertical wind shear, supported its further intensification into a Severe Cyclonic Storm on 1st December and subsequently into a VSCS over the southeast ARB. The cyclone attained its peak intensity during 2nd–3rd December, with maximum sustained wind speeds of about 150–160 km/h and a minimum central pressure of approximately 976 hPa.

The cyclone initially moved westward, then west-south-westward, and later west-north-westward under the influence of large-scale atmospheric circulation. It travelled approximately 2538 km with an average forward speed of about 15 km/h. The cyclone gradually weakened due to increasing vertical wind shear and reduced ocean heat content, and finally crossed the south Gujarat coast between Surat and Dahanu as a well-marked low on 6 December (IMD, 2017) (IMD, 2017). Figure 9 shows the observed track of VSCS Ockhi based on data from the JTWC.

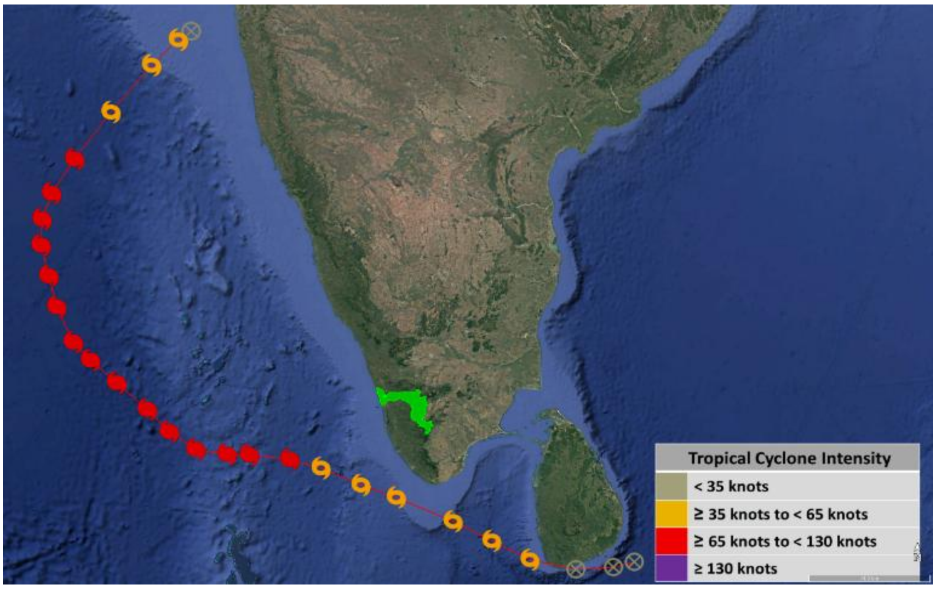

Figure 9 Observed track of VSCS Ockhi in Google Earth Imagery (*Source: JTWC*)

The mean wind speed in the middle and deep tropospheric layers around the cyclone centre is presented in Figure 9.

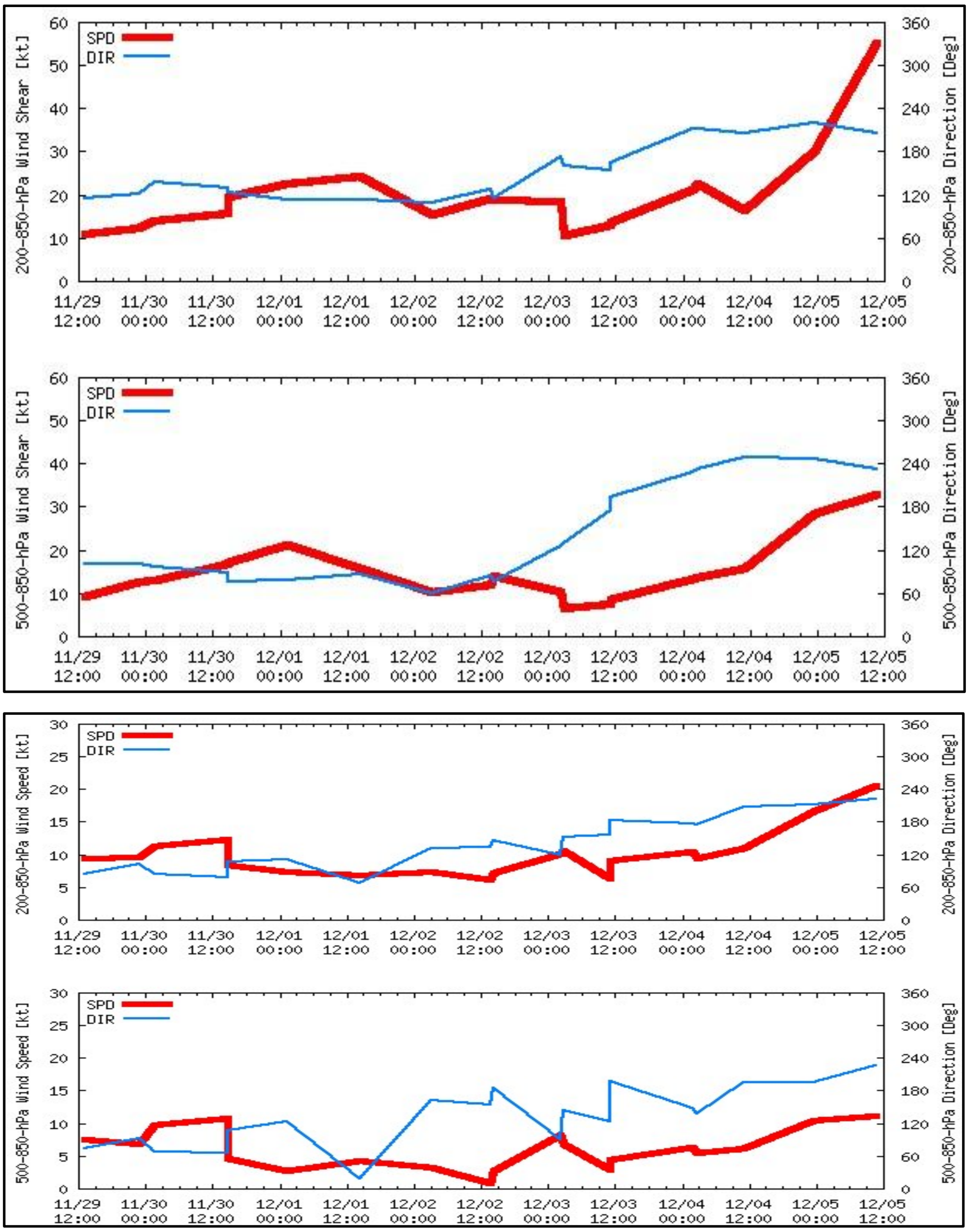

Figure 10 Wind shear and wind speed in the middle and deep layer around the system during VSCS Ockhi (*Source: IMD, 2017*)

Impacts and Damages

The rainfall in the PRB due to Cyclone Ockhi was highest on 1st December 2017, with a basin-wide average of 22 mm. The maximum rainfall was recorded at Kumili (9.6˚ N, 77.17˚ E) with 112.6 mm, followed by Nedumkandam (9.83˚ N, 77.16˚ E), which received 80.2 mm. As per the KSDMA report, the damages caused by Cyclone Ockhi are presented in Table 3.

Figure 11 Damage and Flooding Caused by Cyclone Ockhi *(Source: The Times of India (left) and www.thequint.com (right))*

Table 3 Details of damage as furnished by the Kerala State Disaster Management Authority (KSDMA) (as on 17th January, 2018)

Sl. No	Items	Count
1	Human lives lost	51 (Kerala)
2	Injuries	• 40 (Ernakulam) • >1week hospitalisation – 40 (Ernakulam)
3	Livestock	Nil
4	No. of missing fishermen	108 (Malayalees) + 81 (Non Malayalees)
5	Houses damaged	*Pucca* Thrissur – 42 (Fully), 812 (Severely Damaged) Ernakulam– 10 (Fully), 464 (Severely Damaged) Idukki – 5 (Fully), 109 (Severely Damaged) *Huts* Thrissur – 17 Ernakulam– 6 Idukki – 50
6	Infrastructure Damage	• Boats (fully damaged/lost) - 23 (Thrissur), 106 (Ernakulam) • Loss of road- 1 km (Thrissur), 10 km (Ernakulam). • Damage to Supply Tanks – 430
7	Total crop area affected (in hectares)	*Perennial* Thrissur - 80 Ernakulam– 74.05 Idukki – 7.97 *Irrigated* Thrissur - 215.00 Ernakulam- 101.50 Idukki - 599.68

Cyclone Taukatae

Extremely Severe Cyclonic Storm (ESCS) Tauktae was a major tropical cyclone that developed over the Arabian Sea in May 2021 and moved northward along the west coast of India (Figure 12). The system intensified rapidly and made landfall along the Gujarat coast on 17th May, causing widespread impacts including heavy rainfall, strong winds, and coastal flooding across western India (IMD, 2021).

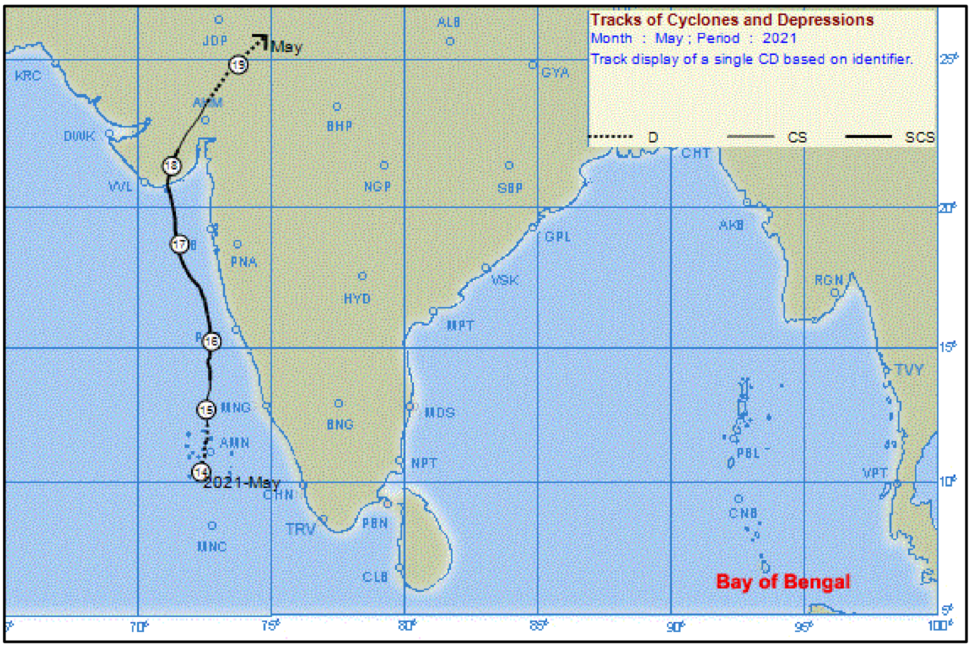

Figure 12 Observed track of ESCS Tauktae (*Source: IMD, Cyclone eAtlas*)

Monitoring

The IMD carried out continuous monitoring of Cyclone Tauktae using satellite observations (INSAT-3D, INSAT-3DR, SCATSAT, and polar-orbiting satellites), along with data from ships, buoys, and coastal stations. DWR at Thiruvananthapuram, Kochi, and Goa provided additional real-time observations. Forecasting of the cyclone's genesis, track, intensity, and landfall was supported by multiple numerical weather prediction models operated by the MoES, along with global and dynamical-statistical models. IMD issued timely warnings and advisories to support disaster preparedness and mitigation (IMD, 2021).

Genesis, Intensification and Movement

Cyclone Tauktae originated as a low-pressure system over the southeast ARB and adjoining Lakshadweep region on 13th May 2021, associated with enhanced convection and strengthening cross-equatorial flow (IMD, 2021). It intensified into a depression on 14th May and rapidly strengthened into a cyclonic storm on the same day under favourable environmental conditions, including warm sea surface temperatures and low vertical wind shear.

The system moved nearly northward and intensified into a Severe Cyclonic Storm on 15th May over the east-central ARB and a VSCS by the same day. From 16th May, it shifted to a north-north-westward track and underwent rapid intensification and reached the stage of an ESCS on 17th May, attaining peak intensity with maximum sustained wind speeds of about 180–190 km/h (gusting up to 210 km/h) and a minimum central pressure of around 950 hPa.

Cyclone Tauktae subsequently moved north-north-westward and made landfall along the Saurashtra coast near Diu on 17th May with wind speeds of approximately 160–170 km/h, gusting up to 185 km/h. After landfall, the system weakened rapidly while moving inland across Gujarat and adjoining Rajasthan, eventually dissipating as a depression by 18th May (IMD, 2021).

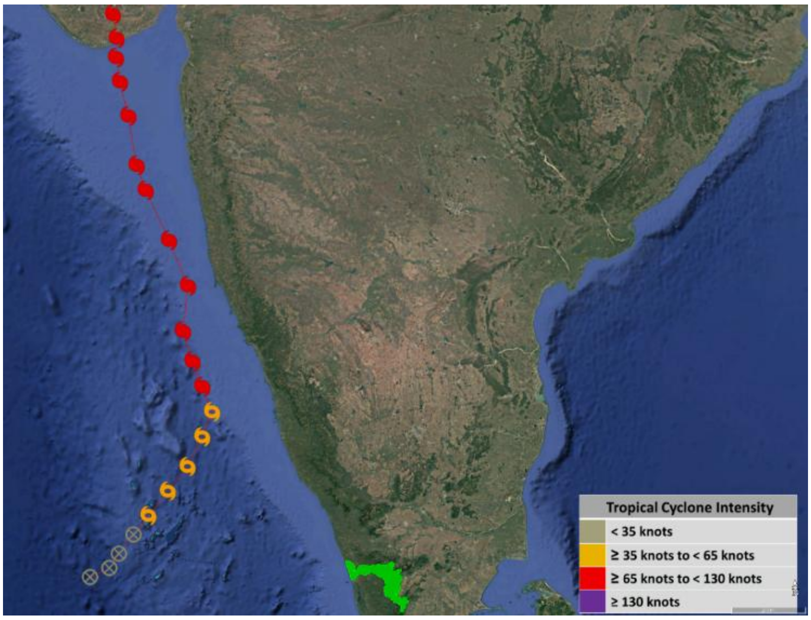

Figure 13 Observed track of ESCS Tauktae in Google Earth Imagery (*Source: JTWC*)

The mean wind speed and vertical wind shear in the middle and deep atmospheric layers are presented in Figure 12. The deep-layer vertical wind shear decreased significantly to below 10 knots during the rapid intensification phase (from the morning of 16th May to the morning of 17th May), creating highly favourable conditions for vertical alignment and strengthening of the system. The mean wind shear in the middle layer remained consistently low from the genesis stage until landfall, with a slight further reduction observed during the rapid intensification period. Additionally, the mean wind direction in the deep layer indicated a predominantly northward steering flow, which closely corresponded with the observed near-northward movement of the cyclone during its mature phase (IMD, 2021).

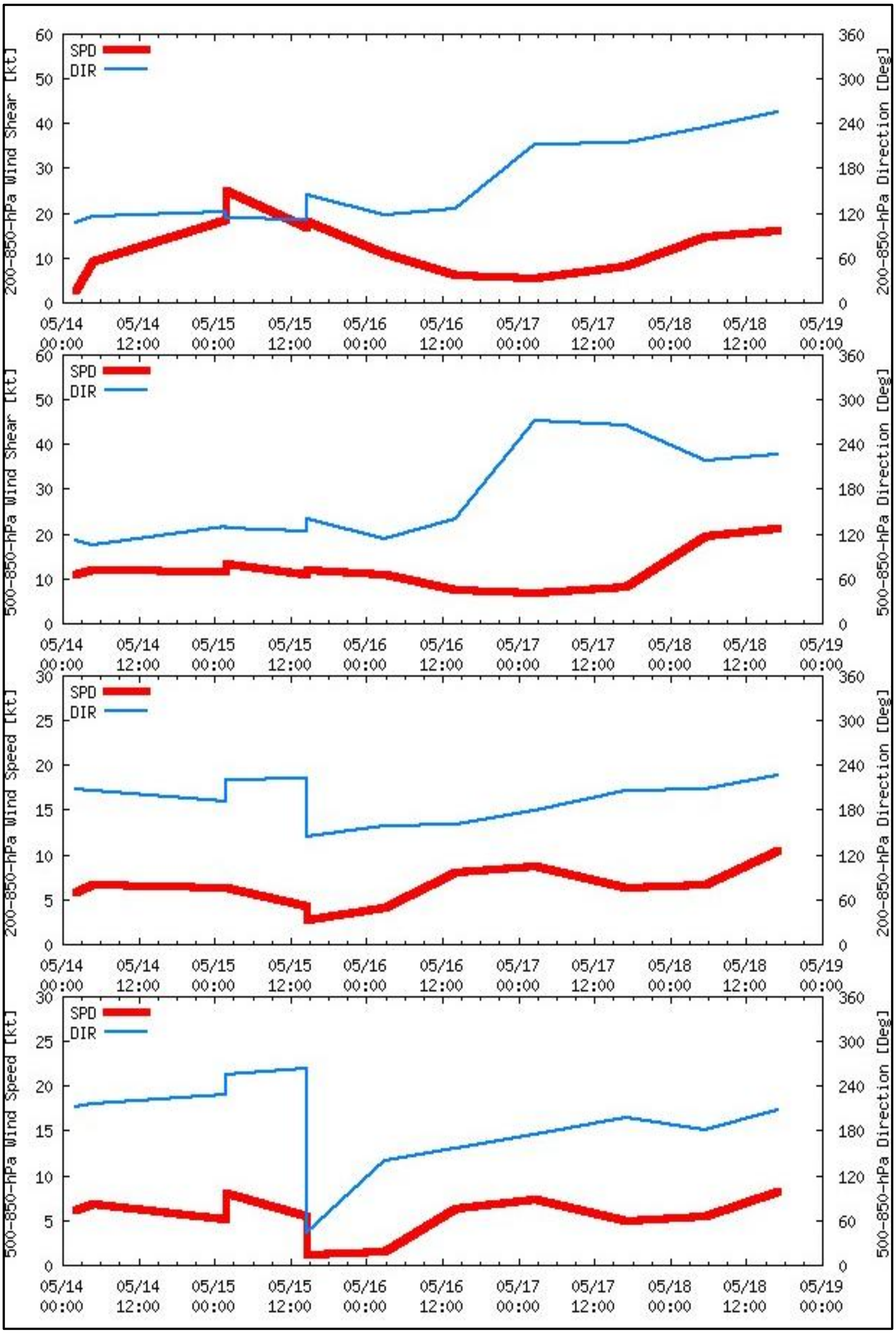

Figure 14 Wind shear and wind speed in the middle and deep layers around the system during ESCS Tauktae *(Source: IMD 2021)*

Impacts and Damages

The PRB recorded maximum rainfall on 15th and 16th May 2021, with basin-wide averages of 71 mm and 68 mm, respectively. On 15th May 2021, the highest rainfall was observed at Painavu (9.85˚ N, 76.94˚ E) with 174.4 mm, followed by Pindimedu (10.13˚ N, 76.81˚ E) with 170 mm. On 16th May 2021, the maximum rainfall was recorded at Idamalayar Dam (10.22˚ N, 76.71˚ E) with 156.4 mm, followed by Pindimedu, which received 140 mm. A total of 11 people lost their lives due to the impact of Cyclone Tauktae in Kerala (KSDMA, 2021). The cyclone also caused damage to houses and infrastructure, power outages, coastal erosion, flooding in low-lying areas, and disruption to fishing activities (Figure 15). Details of the damage caused by the cyclone in Idukki, Ernakulam and Thrissur Districts, in which the Periyar basin is located, are listed in Table 4.

Table 4 Damages caused by Cyclone Tauktae *(Source: District Emergency Operations Centres)*

Sl. No	District	No. of LSGIs effected	No. of Human Fatalities 11.05.2021 to 20.05.2012)	No. of Damaged Houses	
				Completely	Partially
1	Thrissur	38	0	25	81
2	Ernakulam	13	1	35	420
3	Idukki	28	2	6	372

Figure 15 Indian Navy in the coastal village of Chellanam in Ernakulam district (Kerala), which was heavily hit by tidal waves (Left) (*Source: IMD 2021; Flooded roads in Ernakulam (right) Source***:** *District Emergency Operations Centre, Ernakulam)*

d) Cyclone Fanoos

Cyclonic Storm Fanoos was a tropical cyclone that developed over the BoB in December 2005 and moved westward towards the Tamil Nadu coast (Figure 16). The system reached moderate intensity before weakening and making landfall near Vedaranniyam, subsequently affecting parts of southern India, including Kerala (IMD, 2005).

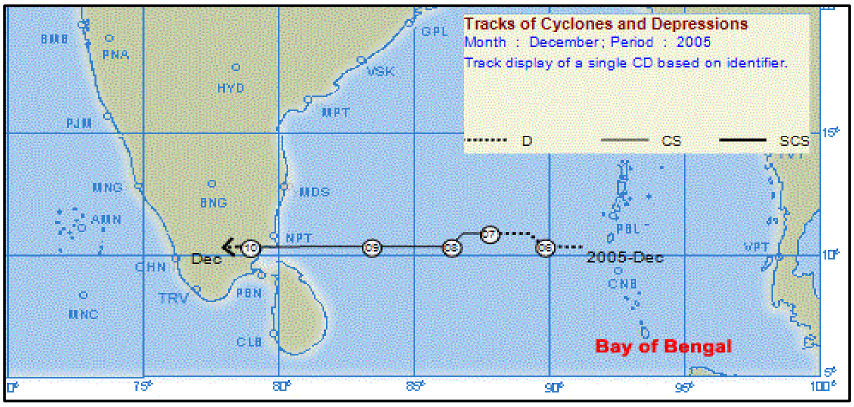

Figure 16 Observed track of VSCS Fanoos (*Source: IMD, Cyclone eAtlas*)

Monitoring of the Cyclone

Cyclone Fanoos was monitored using satellite imagery and radar observations. Satellite data were used to assess the intensity and structural evolution of the system. Radar observations from DWR Chennai and Cyclone Detection Radar (CDR) Karaikal supported tracking of the cyclone's position and structure, including the identification of spiral rain bands and the vortex centre. These observations, despite occasional limitations (due to slow internet connectivity), enabled continuous monitoring of the system (IMD, 2005; Rao et al., 2009).

Genesis, Intensification and Movement

Cyclone Fanoos originated as a low-pressure area over the south Andaman Sea on 4th December and moved north-westwards into the southeast BoB by 5th December 2005, where it intensified into a well-marked low-pressure area (IMD, 2005). It intensified into a depression on 6th December and further into a deep depression and cyclonic storm by 7th December while continuing its westward movement. The system maintained a predominantly westward track, with slight variations in direction, and reached its peak intensity during 7th–9th December, with maximum sustained wind speeds of about 100–110 km/h and a minimum central pressure of approximately 980–984 hPa. It then began to weaken and crossed the Tamil Nadu coast near Vedaranniyam on 10th December as a weakening system.

After landfall, the cyclone weakened further while moving westward across south Tamil Nadu and adjoining Kerala with wind speeds decreasing to 45 - 55 km/h, eventually dissipating into a low-pressure area by 11th December. The remnant system influenced weather conditions over parts of Kerala during its weakening phase (Rao et al., 2009). Figure 17 shows the observed track of VSCS Fanoos based on data from the JTWC.

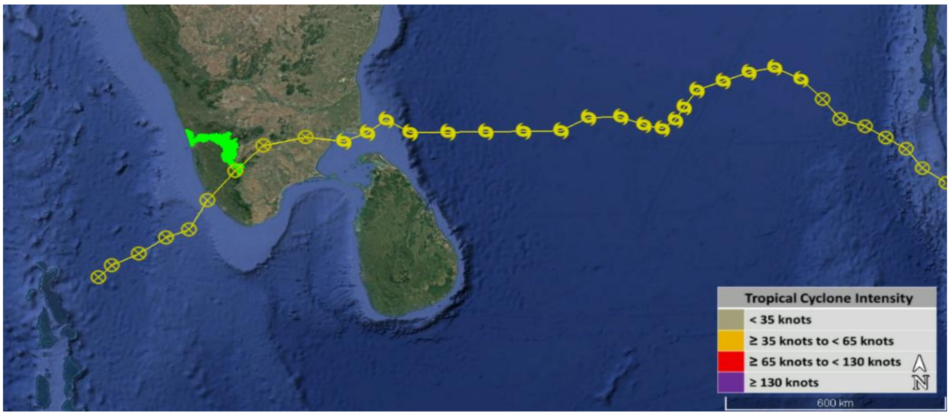

Figure 17 Observed track of VSCS Fannos in Google Earth Imagery (*Source: JTWC*)

Impacts and Damages

Cyclone Fanoos caused severe damage mainly in Tamil Nadu and parts of Andhra Pradesh, bringing heavy rainfall, strong winds, and widespread flooding (Figure 18). Coastal districts of Tamil Nadu experienced extensive damage to houses, infrastructure, and agricultural lands, along with disruption of power and communication systems. The cyclone also led to loss of lives, displacement of people, and significant economic losses, particularly affecting fishing and farming communities. The effects of Cyclone Fanoos in Kerala were relatively limited, particularly within the PRB, compared to other states. On 11th December 2005, Valara (10.04˚ N, 76.84˚ E) recorded 153.7 mm of rainfall, followed by Kumili (9.61˚ N, 77.17˚ N) with 28.8 mm, while the basin average rainfall was 14 mm.

Figure 18 Flood impacts due to Cyclone Fanoos (2005) *(Source: Rao et al. (Andhra University)*

7) Other Cyclones

a) Cyclones in 1912 & 1925 - Severe Cyclonic Storm

There were two cyclonic systems in 1912 (19th - 22th November and 17th - 19th December) and one in November 1925 (6th - 10th November) that developed over the Comorin Sea, located south of Kerala and Tamil Nadu and west of Sri Lanka (Figure 19). The November and December 1912 cyclones affected the southern coastal regions of Kerala and Tamil Nadu. The November 1912 system, identified as a severe cyclonic storm, followed a track similar to Cyclone Ockhi: it crossed southern Tamil Nadu and Kerala, moved northwestward over the Arabian Sea, and later recurved northeastward to make a second landfall over Maharashtra (IMD, 2017).

The December 1912 system, a cyclonic storm, remained offshore and skirted along the Kerala coast without making a direct landfall. In contrast, the November 1925 system was a severe cyclonic storm that moved northward and crossed the north Kerala coast on 10th November.

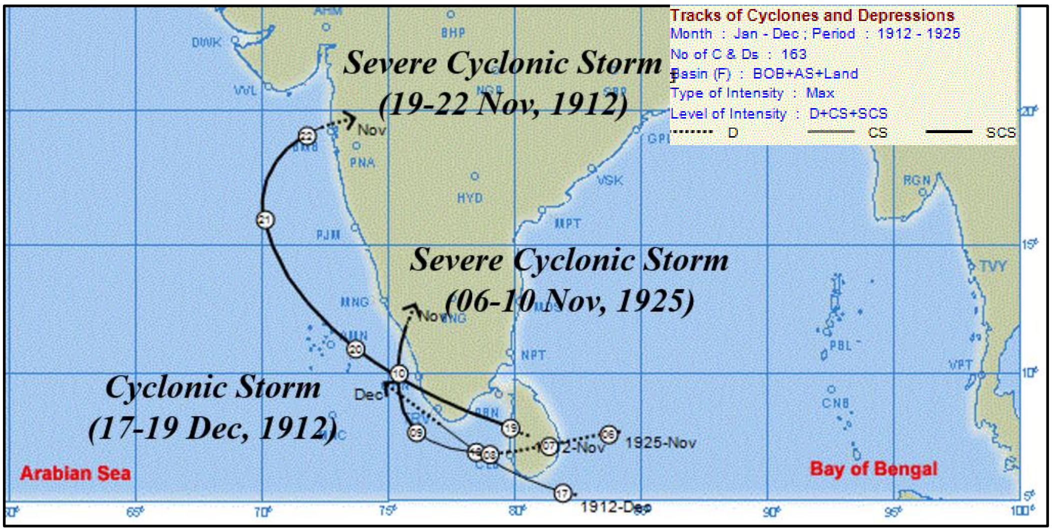

Figure 19 Observed track of 1912 and 1925 cyclones *(Source: IMD, Cyclone eAtlas)*

b) Cyclone in 1935 - Severe Cyclonic Storm

The cyclone of November 1935 (11th - 17th November) developed over the BoB. It intensified into a cyclonic storm on 13th November and further strengthened into a severe cyclonic storm on 14th November (Figure 20). However, before making landfall over Tamil Nadu on 15th November, the system weakened into a depression. It then moved westward across southern India, passing through parts of Kerala, including the PRB. The system eventually emerged into the ARB and dissipated near Lakshadweep on 17th November.

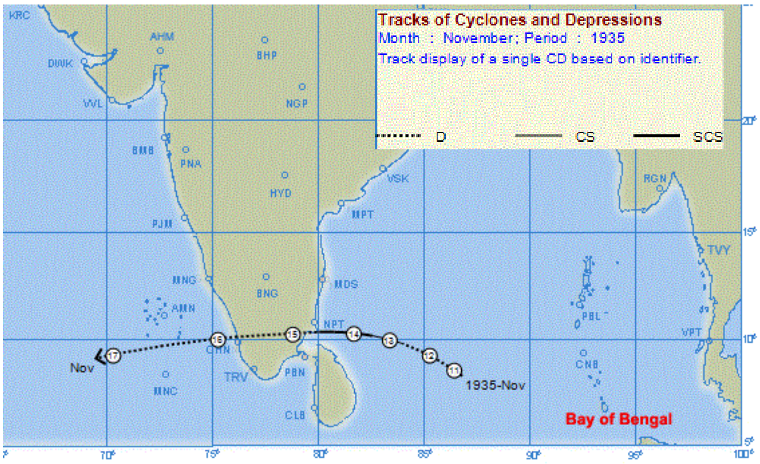

Figure 20 Observed track of 1935 cyclone *(Source: IMD, Cyclone eAtlas)*

c) Cyclone in 1959 – Deep Depression

The cyclonic system formed over the southwest BoB on 28th November 1959, centred about 300 km east-southeast of Nagapattinam at 0830 IST. It remained at the depression stage throughout its lifecycle and did not intensify into a cyclonic storm. The system moved westward with a relatively long track and crossed the east coast of India between Nagapattinam and Pamban on the night of 28th - 29th November (IMD, 1959).

By the morning of 29th November, the system had traversed inland across southern India, passing through parts of Kerala, including the PRB, and emerged into the ARB. It likely maintained deep depression intensity while moving westward over the Arabian Sea, reaching the southwest Arabian Sea by 4th December. The system continued westward and could be tracked until it moved west of 60°E longitude by the morning of 6th December 1959, after which it dissipated (Figure 21). During its passage over Kerala, it brought fairly widespread rainfall across the state, contributing to increased river discharge and localized waterlogging (IMD, 1959).

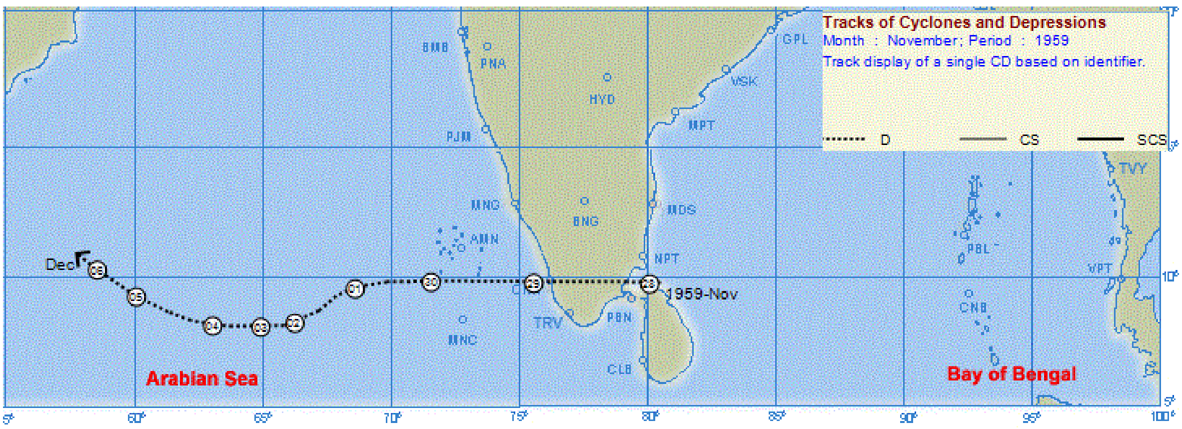

Figure 21 Observed track of 1959 cyclone *(Source: IMD, Cyclone eAtlas)*

d) Cyclone in 1966 – Severe Cyclonic Storm

In November 1966, a depression formed over the BoB on 8th November and intensified into a cyclonic storm on 9th November. It moved westward and crossed Sri Lanka, after which it weakened into a depression and entered Tamil Nadu. The system remained weak while traversing central Kerala towards the north. On 11th November, near the north Kerala coast, it re-intensified into a cyclonic storm and further strengthened into a severe cyclonic storm on 12th November. It then moved northwestward and crossed the Maharashtra coast, after which it gradually weakened. By 14th November, the system had weakened into a depression and eventually dissipated (Figure 22).

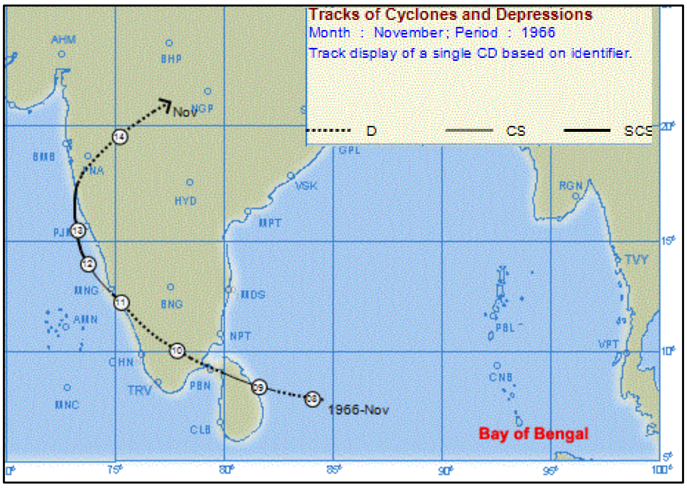

Figure 22 Observed track of 1966 cyclone *(Source: IMD, Cyclone eAtlas)*

e) Cyclone in 1978 – Severe Cyclonic Storm

The cyclonic system formed over the southwest BoB on 17th November 1978 and intensified gradually (Figure 23). By 18th November, it was classified as a depression, and it strengthened into a cyclonic storm on 20th November, further intensifying into a severe cyclonic storm on 21st November. The system continued to intensify and reached its peak intensity on 23rd November, with estimated maximum sustained winds of about 220 km/h (≈120 knots) (IMD, 1997), while the JTWC classified it as a Category 2 equivalent cyclone. The cyclone made its first landfall near Batticaloa in Sri Lanka on the night of 23rd November at peak intensity. After crossing Sri Lanka, it emerged into the Gulf of Mannar on 24th November in a weakened state. Later the same day, it made a second landfall near Kilakkarai along the Tamil Nadu coast, with reduced intensity (around 85 km/h) (IMD, 1980).

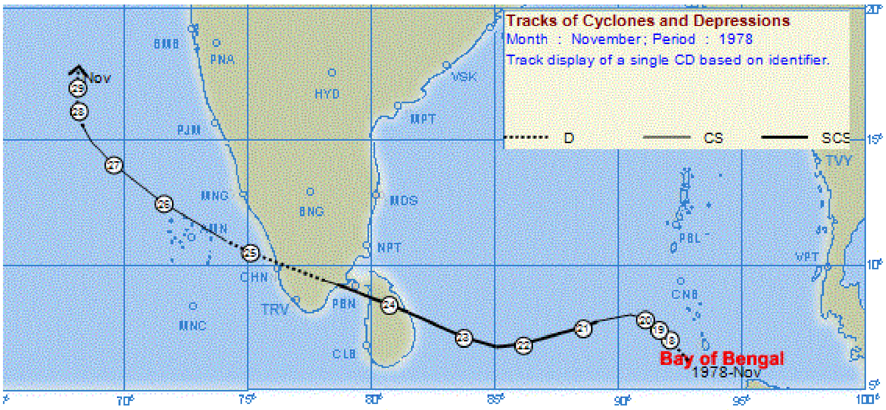

Figure 23 Observed track of 1978 cyclone *(Source: IMD, Cyclone eAtlas)*

Subsequently, the system weakened further into a depression while moving westward across southern India, traversing parts of Kerala, including the PRB, and emerging into the ARB along the Kerala coast on 25th November (Figure 24). Over the ARB, the system briefly re-intensified into a cyclonic storm; however, it gradually weakened thereafter, degenerating into a depression. The system finally dissipated over the ARB on 29th November 1978 (Morford, 1979). Although the cyclone caused catastrophic damage in Sri Lanka, its impact in India was relatively minor. In Kerala and the Lakshadweep Islands, the system mainly resulted in rainfall, with no major reported destruction, while only limited damage to huts was recorded in parts of Tamil Nadu.

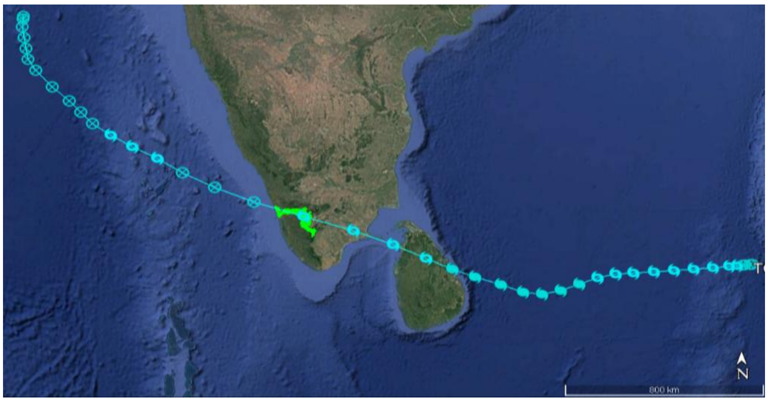

Figure 24 Observed track of 1978 cyclone in Google Earth Imagery *(Source: JTWC)*

f) Cyclone in 1992 – Severe Cyclonic Storm

A cyclonic disturbance over the South China Sea developed into a weak tropical depression on 6th November 1992. The system moved westward, crossed the Malay Peninsula, and entered the BoB by 8th November. It gradually intensified and, by 11th November, reached tropical storm intensity over the BoB near Sri Lanka (IMD, 1997). The system made landfall over Sri Lanka on 12th November with an intensity of about 55 - 65 knots (≈100 - 120 km/h). While traversing the island, it weakened slightly, with wind speeds decreasing to around 40 knots, but re-emerged into the sea later the same day and began to intensify again while moving toward the Indian coast (Figure 25).

It subsequently made landfall near Uvari along the Tamil Nadu coast, became a cyclone with an intensity of approximately 70 knots before hitting southern India. After landfall, the system moved westward across southern India, passing through central Kerala and affecting parts of the PRB, while gradually weakening. It emerged into the ARB near Munambam on 14th November. Over the Arabian Sea, the system continued moving north-westward but remained relatively weak. It made another landfall near Karwar in Karnataka on 17th November, with an intensity of about 35 knots, and weakened rapidly thereafter, dissipating on the same day (Figure 26).

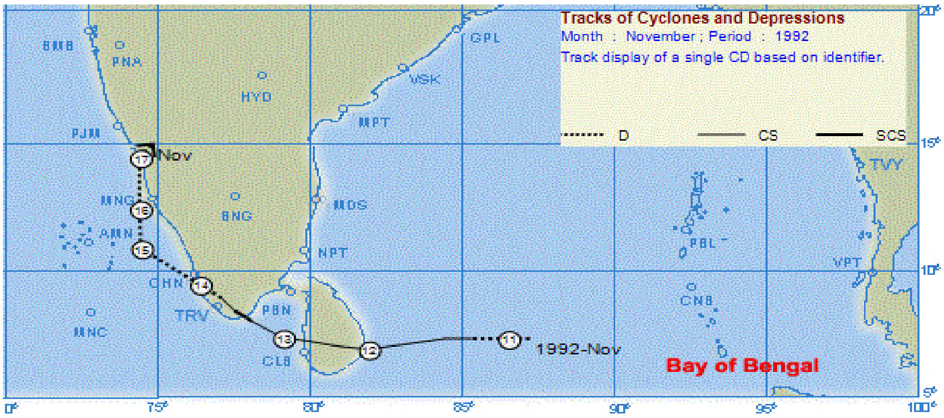

Figure 25 Observed track of 1992 cyclone *(Source: IMD, Cyclone eAtlas)*

In Kerala, the cyclone primarily caused heavy rainfall leading to flooding and dam overflow, notably at Thenmala, which necessitated evacuation of downstream residents with assistance from the Indian Army. Compared to neighboring states, especially Tamil Nadu, which experienced widespread destruction and significant loss of life, the impacts in Kerala were moderate and largely associated with hydrological effects rather than severe structural damage.

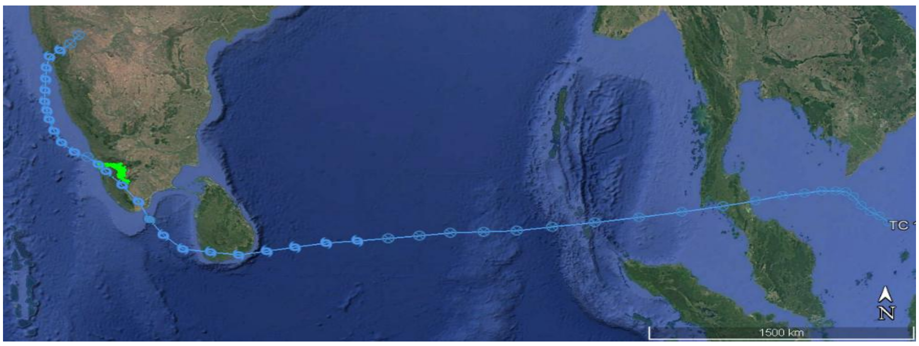

Figure 26 Observed track of 1992 cyclone in Google Earth Imagery *(Source: JTWC)*

g) Cyclone in 1993 - Very Severe Cyclonic Storm

On 5th November 1993, a cyclonic disturbance associated with the Intertropical Convergence Zone (ITCZ) was first observed southwest of India, near the Maldives, with an initial intensity of about 20 knots (JTWC, 1993) (Figure 27 and 28). By 8th November, the IMD classified the system as a depression over the ARB. The system moved north-eastward and made landfall near Thoothukudi on 9th November, weakening into a remnant low-pressure area while crossing southern India, including parts of Kerala. Subsequently, the remnant system turned north-westward and re-emerged into the ARB, where it reorganized. On 12th November, it re-intensified into a depression, and later the same day, the JTWC designated it as TCs. As the system moved north to northeast, it intensified further based on ship observations. The IMD upgraded it to a VSCS on 14th November, with estimated peak winds of about 120 km/h (≈65 knots), while the JTWC estimated higher winds of up to 150 km/h (≈80 knots).

As the system approached the Gujarat coast, increasing vertical wind shear displaced convection away from the center, leading to rapid weakening. The storm slowed, changed direction toward the southeast, and gradually lost intensity. By 16th November 1993, it had weakened into a remnant low-pressure area over the ARB, remaining offshore (about 100 km from the coast) and dissipating without making a second landfall.

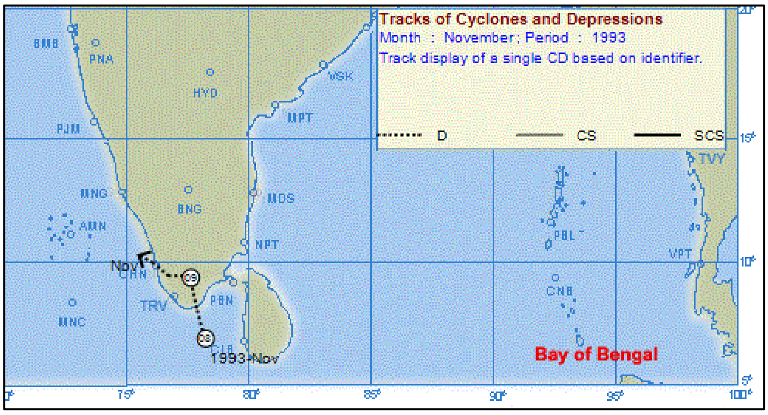

Figure 27 Observed track of 1993 cyclone *(Source: IMD, Cyclone eAtlas)*

In Kerala, the depression had minimal direct impact, with no significant damage reported. The system, however, produced heavy rainfall and gusty winds across parts of western India and Pakistan, resulting in flooding, power outages, and rough sea conditions. The most severe impacts were observed in Pakistan, where storm-induced flooding led to substantial loss of life and large-scale displacement, indicating that the cyclone’s effects were considerably more intense outside Kerala.

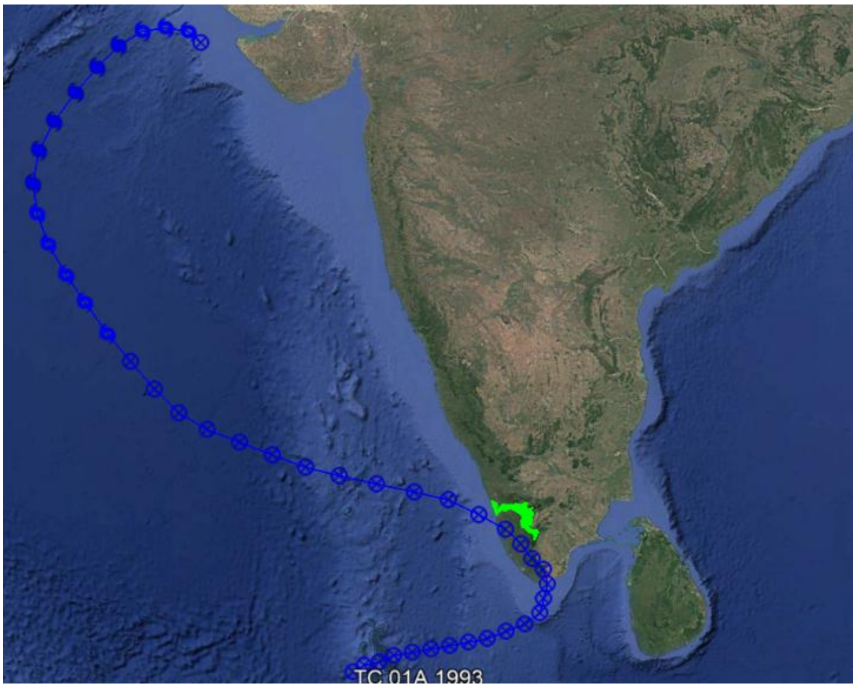

Figure 28 Observed track of 1993 cyclone in Google Earth Imagery *(Source: JTWC)*

h) Cyclone in 1997 – Severe Cyclonic Storm

A tropical depression originated off the eastern coast of Sri Lanka on 2nd November 1997, with an initial intensity of about 15 knots. It moved southwestward into Sri Lanka, maintaining relatively low intensity. By 4th November, the system changed its track and moved northward, with a slight increase in intensity to around 20 knots (JTWC, 1997). On 6th November, it exited Sri Lanka near its northern tip and subsequently took a westward course. The system entered the Tamil Nadu coast near Sethubavachatram on 7th November, with an intensity of approximately 20 knots. It then moved westward across the region and passed through the northern parts of the PRB on 8th November, maintaining similar intensity. Later the same day, it emerged into the ARB near Perinjanam in Thrissur District (Figure 29).

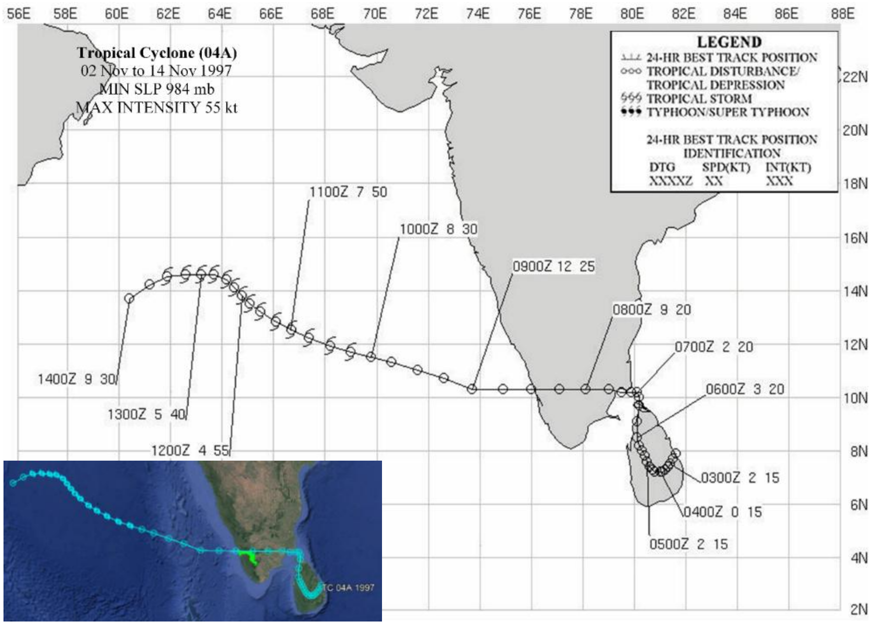

Figure 29 Observed track of 1997 cyclone in Google Earth Imagery *(Source: JTWC)*

Over the ARB, the system began to intensify gradually, reaching about 25 knots, and on 9th November it shifted to a north-westward direction near the Lakshadweep Islands. The intensity further increased to around 35 knots on 10th November, at which point it was upgraded to a tropical storm over the ARB, and it continued to strengthen, attaining its peak intensity with maximum sustained winds of about 65 mph (105 km/h), equivalent to approximately 55 knots. After reaching its peak, the system turned south-westward and began to weaken gradually, with increasing wind shear contributing to its decay, and it eventually dissipated over the open waters of the Arabian Sea on 14th November 1997.

Mitigation and preparedness

Disaster risk reduction requires an integrated approach that ensures coordination across all phases of the disaster management cycle. While the institutional mechanism at the national, state, district, and taluk levels functions in a top-down manner, community-based disaster risk reduction follows a bottom-up approach. In practice, disaster response reflects a combination of both approaches (NDMA, 2019).

In Kerala, preparedness and mitigation measures for cyclones includes the implementation of Local Self Government Disaster Management Plans (LSG DMP), activation of Standard Operating Procedures (SOP) as per the Orange Book of Disaster Management; Monsoon Preparedness and Response Guidelines 2021 (Edition 2), dissemination of multilingual warnings and IEC materials, and the establishment of Multi-Purpose Cyclone Shelters (MPCS) under the National Cyclone Risk Mitigation Project (NCRMP) (NDMA, 2019; KSDMA, 2021).

The NCRMP in Kerala is implemented through a State Project Implementation Unit headed by the Additional Chief Secretary, Revenue and Disaster Management, with day-to-day operations managed by a State Project Manager. The project consists of four components: Early Warning Dissemination Systems, Cyclone Risk Mitigation Infrastructure, Capacity Building, and Project Management and Implementation Support. Sites for constructing MPCS were finalized through GO (Rt) No. 641/2016/DMD dated 28-01-2016, and three model designs were prepared. The project commenced in August 2015 and was scheduled for completion in 2020 (KSDMA, 2016). The list of MPCS located in the Ernakulam and Thrissur districts of the PRB is shown in Table 3.

Table 3 List of MPCS as on 23rd September 2021 *(Source: NCRMP Kerala)*

Sl. No.	LSGI where MPCS is located	District	Adjoining Coastal LSGIs Served by the MPCS
1	Vadakekkara (Thuruthipuram)	Ernakulam	Pallippuram, Eriyad (Kozhikode), Chittattukara, Chendamangalam
2	Pallippuram	Ernakulam	Kuzhuppily, Eriyad, Edavanakkade, Chittattukara, Ezhikara
3	Kadappuram	Thrissur	Chavakkad Municipality, Orumanayor, Engandiyur
4	Eriyad (Azhikode)	Thrissur	Edavilangu, Pallippuram, Kodungallur Municipality

8. Hourly Meteorological Variation During Cyclone Events

8.1 Temporal Variation of Meteorological Parameters Along the Cyclone Track

a) Hourly Meteorological Changes – Unnamed 1935

The Unnamed Cyclone of November 1935 initially developed as a tropical depression on 11 November 1935 over the Bay of Bengal (path shown in Figure 27), with sustained wind speeds of approximately 56 km/h (30 kt). During the initial two days (11–12 November), the system maintained nearly steady intensity, indicating a weak but persistent cyclonic circulation, with minimal variation in associated meteorological parameters such as rainfall and pressure. On 13th November, gradual intensification was observed as wind speeds increased from 59 km/h (32 kt) to 63 km/h (34 kt), marking the transition from a depression to a deep depression as per the IMD classification. Later on, the same day, wind speeds further increased to 91 km/h (49 kt), indicating strengthening into a cyclonic storm stage. This intensification phase is typically associated with increased convection, resulting in enhanced rainfall activity and a drop in central pressure. The cyclone reached its peak intensity on 14th November 1935, with maximum sustained wind speeds of 119 km/h (64 kt), classifying it as a Severe Cyclonic Storm (SCS) according to IMD standards. This stage likely corresponded with peak rainfall intensity over the affected regions, driven by strong moisture convergence and organized cloud bands. However, the intensification was short-lived, and the system weakened rapidly within a few hours, with wind speeds decreasing to 87 km/h (47 kt), reverting to a cyclonic storm. As the wind speed decreased further, the system weakened into a deep depression and subsequently into a depression by the afternoon of 14th November. From 15 to 17 November, the system persisted as a weak depression with wind speeds around 56 km/h (30 kt), indicating gradual dissipation. During this weakening phase, a noticeable reduction in rainfall intensity would have occurred, with precipitation becoming more scattered and less organized. The weakening of wind circulation reduces moisture convergence and vertical uplift, leading to diminished cloud formation and rainfall. Central pressure tends to rise, and temperature variations become less pronounced as the system loses its cyclonic structure.

b) Hourly Meteorological Changes – Cyclone 1959

Cyclone of late November–December 1959 initially appeared on 27 November 1959 over the Bay of Bengal (path shown in Figure 17), with an unreported classification (NR) and no recorded wind speed. By 28 November 1959, the system was identified as a depression, with sustained wind speeds of approximately 46 km/h (25 kt), as per IMD classification. From 28th November to 6 December 1959, the system maintained a relatively steady intensity, with wind speeds consistently around 46 km/h (25 kt). This indicates that the cyclone persisted in a weak depression stage throughout its observed period, without intensifying into a deep depression or cyclonic storm. The persistence of nearly constant wind speeds suggests that the system likely experienced unfavorable environmental conditions for intensification, such as weak sea surface temperature gradients, limited moisture availability, or high vertical wind shear. As a result, convective activity would have remained weak and poorly organized. In terms of associated meteorological parameters, the weak and steady wind circulation implies that rainfall activity was likely light to moderate and spatially scattered, rather than intense or concentrated. The absence of strong upward motion and moisture convergence would have limited the development of deep convective clouds. Central pressure variations would have been minimal, and temperature fluctuations relatively subdued, reflecting the system's weak and stable structure. The cyclone remained a low-intensity system, with its behavior primarily characterized by stable wind speeds and limited atmospheric interaction, leading to negligible intensification and modest rainfall impacts.

e) Hourly Meteorological Changes – Cyclone 1966

Cyclone of November 1966 was first noted on 7th November 1966 with an unreported classification (NR). By 8th November 1966, the system developed into a depression over the Bay of Bengal (path shown in Figure 18), with sustained wind speeds of approximately 46 km/h (25 kt), indicating the formation of a weak cyclonic circulation as per the IMD classification. On 9th November, the system briefly intensified into a deep depression with wind speeds of about 65 km/h (35 kt). However, this strengthening was short-lived, and the cyclone weakened back to a depression later the same day. During 9–11th November, the system remained relatively weak, with wind speeds around 46 km/h (25 kt), suggesting limited atmospheric support for sustained intensification. Consequently, rainfall during this phase would have been light to moderate and scattered, associated with weak convection and limited moisture convergence. A significant strengthening phase began on 11th November, clearly highlighted in Figure 29, where wind speeds increased to 65 km/h (35 kt), marking the transition again to a deep depression. This phase represents the onset of organized convection, with increasing rainfall intensity and improved cyclonic structure. The cyclone intensified rapidly and reached its peak intensity on 12th November 1966, with sustained wind speeds of approximately 120 km/h (65 kt), classifying it as SCS under IMD standards. This peak intensity was maintained for nearly a day and would have corresponded to maximum rainfall activity, driven by strong moisture inflow, enhanced vertical uplift, and well-organized cloud bands. A noticeable drop in central pressure and increased wind-driven convergence would have further supported intense precipitation. After reaching its peak, the system began to weaken on 13th November, with wind speeds decreasing to 65 km/h (35 kt), reverting to a deep depression, and subsequently weakening further to a depression with wind speeds around 46 km/h (25 kt) (Figure 30). During this weakening phase, rainfall intensity would have reduced significantly, becoming more scattered as the cyclonic circulation weakened, convection diminished, and central pressure gradually increased. By 14th November 1966, the cyclone persisted as a weak depression, indicating the dissipation phase of the system, with minimal organized rainfall and loss of cyclonic structure.

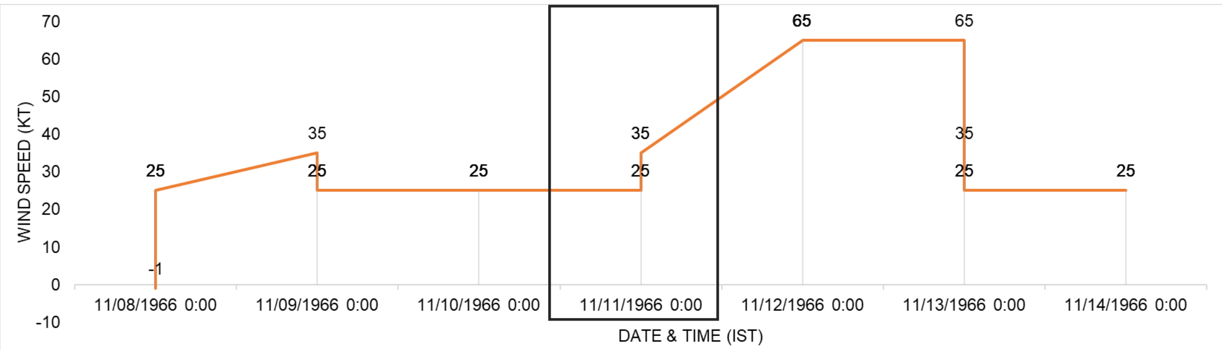

Figure 30 Temporal variation of wind speed highlighting intensification on 11 November and subsequent weakening on 13 November 1966.

d) Hourly Meteorological Changes – Cyclone 1978

Cyclone of November 1978 initially appeared on 19th November 1978 with an unreported classification (NR) (Figure 19). Later that day, the system developed into a depression over the Bay of Bengal, with sustained wind speeds of approximately 56 km/h (30 kt), indicating the formation of a cyclonic circulation as per IMD classification. The system intensified rapidly on 20th November, strengthening into a cyclonic storm, with wind speeds increasing from 65 km/h (35 kt) to 74 km/h (40 kt). This phase would have been associated with enhanced convective activity, resulting in moderate to heavy rainfall due to increased moisture convergence and cloud organization. Over the following two days (21–22 November), the cyclone continued to strengthen steadily, with wind speeds increasing from 83 km/h (45 kt) to 111 km/h (60 kt), marking its transition into SCS. This strengthening phase likely resulted in widespread rainfall with increasing intensity, supported by stronger vertical uplift and falling central pressure. By 22th November, the system intensified further into a Very Severe Cyclonic Storm (VSCS), with wind speeds around 130–148 km/h (70–80 kt). At this stage, the cyclone would have exhibited well-developed spiral rainbands, producing heavy to very heavy rainfall over the affected regions. The cyclone reached its maximum intensity on 23 November 1978, when sustained wind speeds increased to approximately 167 km/h (90 kt), maintaining its classification as a VSCS under IMD standards. This peak phase would have corresponded to maximum rainfall intensity, driven by strong moisture inflow, intense convection, and a well-organized cyclonic structure. After reaching this peak, the system gradually weakened later on 23 November, with wind speeds decreasing to the SCS category and further weakening into a cyclonic storm by 24th November. During this weakening phase, rainfall intensity would have started to decline, becoming less organized as convection weakened and central pressure began to rise. During 25–26th November, the cyclone weakened further, transitioning between cyclonic storm, deep depression, and depression stages, with wind speeds ranging between 46 and 65 km/h (25–35 kt). This phase would have been associated with light to moderate and scattered rainfall, reflecting reduced convection and weakening circulation. By 27th November, the system weakened significantly and persisted as a depression, with wind speeds around 37–46 km/h (20–25 kt) (Figure 31). At this stage, the cyclone lost its organized structure, and rainfall would have become minimal and highly scattered, indicating the dissipation phase of the system.

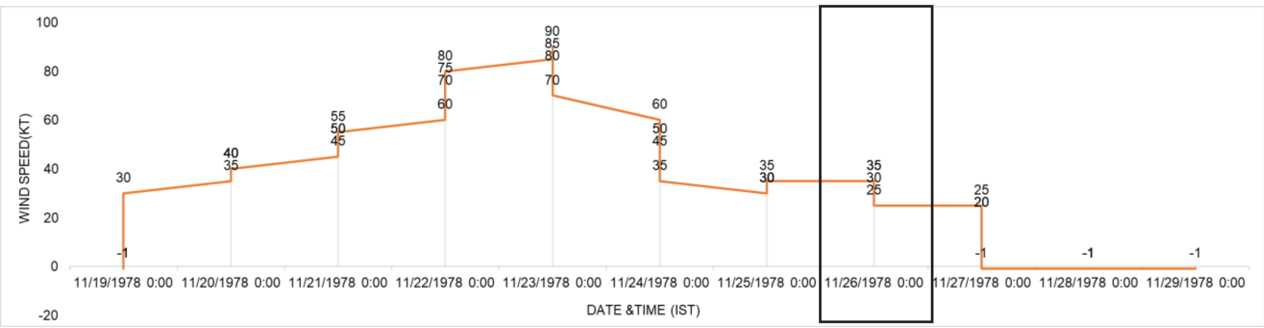

Figure 31 Observed variation of Wind speed

e) Hourly Meteorological Changes – Cyclone 1992

Cyclone of November 1992 initially developed as a weak system on 6th November 1992, with sustained wind speeds ranging between 19 and 28 km/h (10–15 kt) (Figure 22). At this stage, the system can be considered below depression intensity as per IMD classification. During the early phase (6–9 November), the system remained weak, with wind speeds fluctuating between 19 and 37 km/h (10–20 kt), indicating limited organization and weak convective activity. Rainfall during this period would have been minimal to light and highly scattered due to weak moisture convergence and insufficient vertical uplift. Gradual intensification began on 10th November, when wind speeds increased to 37–46 km/h (20–25 kt), marking the formation of a depression over the Bay of Bengal. This phase likely corresponded to increasing cloud organization and moderate rainfall activity, supported by improving atmospheric conditions. By 11th November, the cyclone intensified further into a cyclonic storm, with wind speeds increasing from 65 km/h (35 kt) to 93 km/h (50 kt) within the same day. The system continued to strengthen and maintained cyclonic storm intensity on 12th November, with wind speeds reaching 102 km/h (55 kt). This strengthening phase would have been associated with moderate to heavy rainfall, driven by enhanced convection, moisture inflow, and decreasing central pressure. A significant intensification occurred on 13th November, when wind speeds increased to approximately 130 km/h (70 kt), classifying the system as a VSCS under IMD standards. This peak phase would have corresponded to maximum rainfall intensity, characterized by strong spiral rainbands, intense convection, and high moisture convergence. However, this peak intensity was short-lived, and the cyclone weakened back to a cyclonic storm later the same day. From the 14th to the 16th of November, the system fluctuated between cyclonic storm, deep depression, and depression stages, with wind speeds ranging between 56 and 102 km/h (30–55 kt), indicating intermittent phases of deintensification and weakening. During this period, rainfall would have varied accordingly, with periods of moderate to heavy rainfall during strengthening phases and reduced, scattered rainfall during weakening phases. By 17th November 1992, the cyclone weakened further to a depression, with wind speeds around 46–56 km/h (25–30 kt), marking the dissipation phase of the system (Figure 32). At this stage, the cyclone lost its organized structure, and rainfall would have become light and scattered, reflecting diminished convection and weakening circulation.

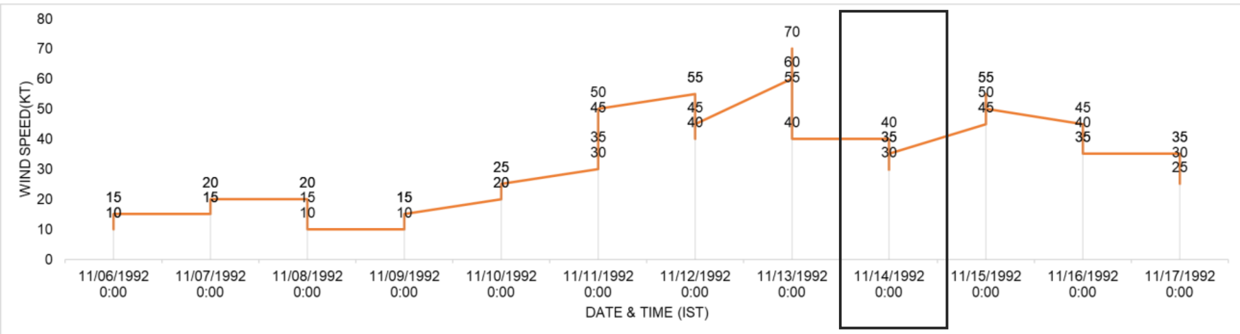

Figure 32 Observed variation of Wind speed

f) Hourly Meteorological Changes - Cyclone 1993

Cyclone of November 1993 initially developed on 5th November 1993 over the Arabian Sea (path shown in Figure 24), with sustained wind speeds of approximately 37 km/h (20 kt), corresponding to a depression stage as per IMD classification. From 5–10th November, the system maintained relatively weak intensity, with wind speeds fluctuating between 37 and 56 km/h (20–30 kt). This indicates a slow and gradual organization of the system, with limited atmospheric support for intensification. During this phase, rainfall would have been light to moderate and scattered, associated with weak convection and modest moisture convergence. The persistence of low wind speeds suggests minimal pressure gradients and weak vertical uplift. By 11th November, wind speeds remained around 46 km/h (25 kt), indicating continued depression stage with only marginal strengthening. A more noticeable intensification occurred on 12th November, when wind speeds increased from 56 km/h (30 kt) to 65 km/h (35 kt) (as shown in Figure 33), marking the transition to a deep depression. This phase would have been associated with increasing rainfall intensity, reflecting improved convective organization and enhanced moisture inflow. The system continued to intensify further, reaching 74–83 km/h (40–45 kt) by early 13th November 1993, confirming its development into a cyclonic storm. This strengthening phase likely resulted in moderate to heavy rainfall, driven by stronger cyclonic circulation, increased vertical uplift, and better-organized cloud bands.

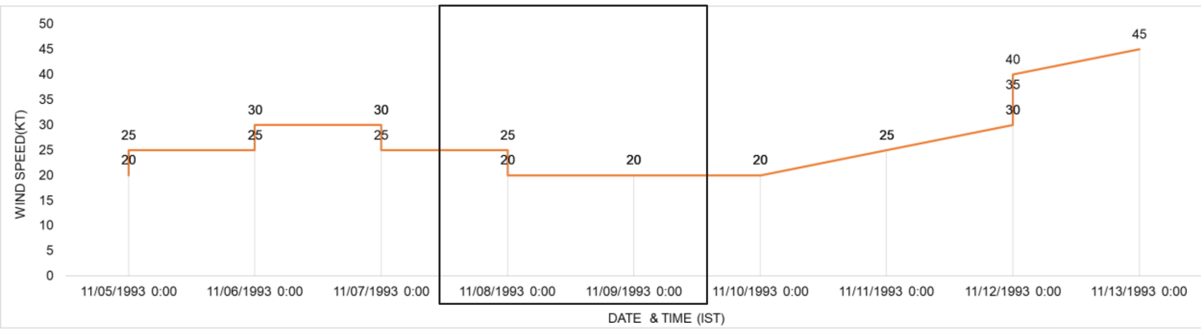

Figure 33 Observed variation of Wind speed

g) Hourly Meteorological Changes - Cyclone 1997

Cyclone of November 1997 initially developed on 2nd November 1997 over the Arabian Sea (path shown in Figure 25), with sustained wind speeds of approximately 28 km/h (15 kt), indicating a system below depression intensity as per IMD classification. From 2nd to 7th November, the system remained weak and relatively stable, maintaining wind speeds between 28 and 37 km/h (15–20 kt). This phase represents a slowly organizing low-pressure system with minimal convective activity, resulting in light and scattered rainfall due to weak moisture convergence and limited vertical uplift. During 8th and 9th November, the system gradually intensified, with wind speeds increasing to 46–56 km/h (25–30 kt), marking the formation of a depression. This strengthening phase suggests improved cyclonic circulation and enhanced convection, likely leading to moderate and more organized rainfall compared to the earlier stage. A significant intensification phase occurred on 10th November, when wind speeds reached 65 km/h (35 kt), indicating the transition to a deep depression. This stage would have been associated with increasing rainfall intensity, supported by stronger upward motion, better cloud organization, and increased moisture inflow. The cyclone continued to strengthen and reached its maximum intensity between 11th and 12th November, with sustained wind speeds of approximately 102 km/h (55 kt), classifying it as a cyclonic storm under IMD standards. This peak phase would have corresponded to maximum rainfall activity, characterized by well-developed cloud bands, strong convection, and enhanced moisture convergence. Following this peak, the cyclone gradually weakened, with wind speeds decreasing to 93 km/h (50 kt) on 12 November and further to 65–74 km/h (35–40 kt) by 13th November, reverting to a Deep Depression. During this weakening phase, rainfall intensity would have declined, becoming less organized as convection weakened and central pressure began to rise. By the evening of 13th November, the system weakened further into a Depression, with wind speeds around 56 km/h (30 kt), and continued to decay by 14th November 1997 (shown in Figure 34). At this stage, the cyclone lost its organized structure, resulting in light and scattered rainfall, indicating the dissipation phase of the system.

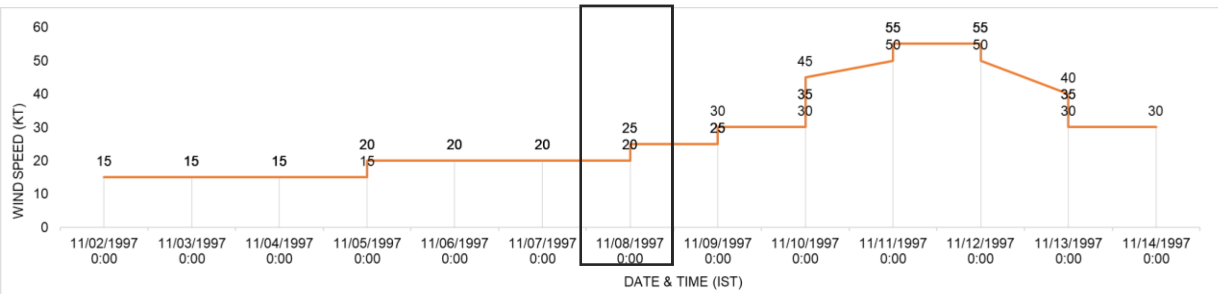

Figure 34 Observed variation of Wind speed

h) Hourly Meteorological Changes – Fanoos (2005)

Cyclone Fanoos developed over the Bay of Bengal (Figure 13) in early December 2005. According to cyclone records, the system initially formed as a tropical depression on 4 December 2005, with sustained wind speeds of about 20 kt and a central pressure of approximately 1004 mb. Gradual intensification occurred on 5 December, as wind speeds increased to 30 kt while the central pressure decreased to around 1000 mb, indicating strengthening of the low-pressure system. By 6 December, the cyclone intensified further and reached the tropical storm stage, with wind speeds increasing from 35 kt to 50 kt and pressure dropping to 987 mb. The system continued to intensify on 7–8 December, maintaining tropical storm intensity with sustained winds of approximately 55 kt and central pressure around 984 mb. The cyclone reached its maximum intensity on 9 December, when wind speeds increased to about 60 kt, and the central pressure dropped to 980 mb, representing the strongest phase of the storm. After reaching peak intensity, the cyclone began to weaken. On 10 December, wind speeds gradually decreased from 55 kt to 45 kt, accompanied by a rise in central pressure (Figure 35). On the evening of December 10th, the system weakened to a tropical depression (30 kt). The weakening trend continued through 11–12 December, with wind speeds decreasing to 15–25 kt and pressure rising to around 1006 mb, indicating the dissipation stage of Cyclone Fanoos (Figure 36). The inverse relationship between wind speed and central pressure observed in the dataset clearly illustrates the intensification and weakening phases of the cyclone during its lifecycle.

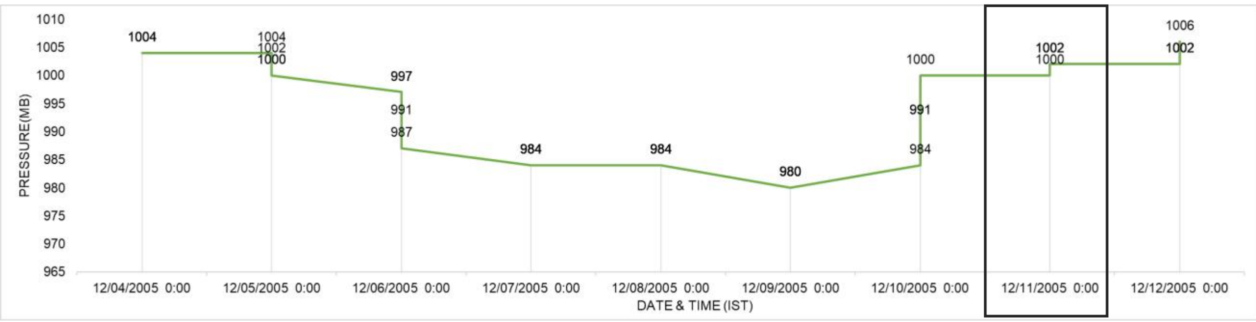

Figure 35 Observed variation of Pressure

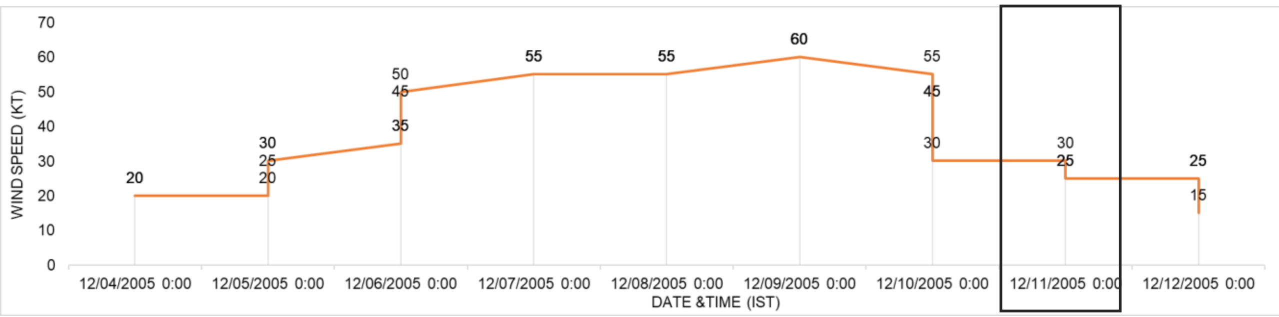

Figure 36 Observed variation of Wind speed

i) Hourly Meteorological Changes – Cyclone Gaja (2018)

Cyclone Gaja formed over the Bay of Bengal in November 2018. The system initially developed as a tropical depression on 10 November 2018 (Figure 4), with wind speeds around 25–30 kt and central pressure close to 1003–1004 mb. By 10 November evening, the system intensified into a tropical storm, with wind speeds increasing to 35 kt and central pressure decreasing to 1000 mb. During 11–12 November, the cyclone maintained moderate intensity with winds around 35 kt, although slight fluctuations in pressure indicated temporary weakening and reorganization of the system. A renewed intensification phase began on 13–14 November, when wind speeds gradually increased from 35 kt to 50 kt, accompanied by a significant drop in central pressure from 1003 mb to 985 mb. The cyclone intensified further on 15 November, reaching hurricane strength (Category 1) with wind speeds of 65–80 kt and a minimum central pressure of about 963 mb, representing the peak intensity of Cyclone Gaja. After reaching peak strength, the cyclone began to weaken on 16 November, as wind speeds decreased from 70 kt to 55 kt and pressure increased. The system continued weakening through 17 November, remaining in the tropical storm stage with wind speeds around 35–40 kt. By 18 November, the cyclone weakened into a tropical depression, with wind speeds decreasing to 20–30 kt and pressure rising above 1006 mb, indicating the dissipation phase of the system (Figure 37 and 38). The observed inverse relationship between central pressure and wind speed clearly reflects the formation, intensification, peak, and weakening stages of Cyclone Gaja during its lifecycle.

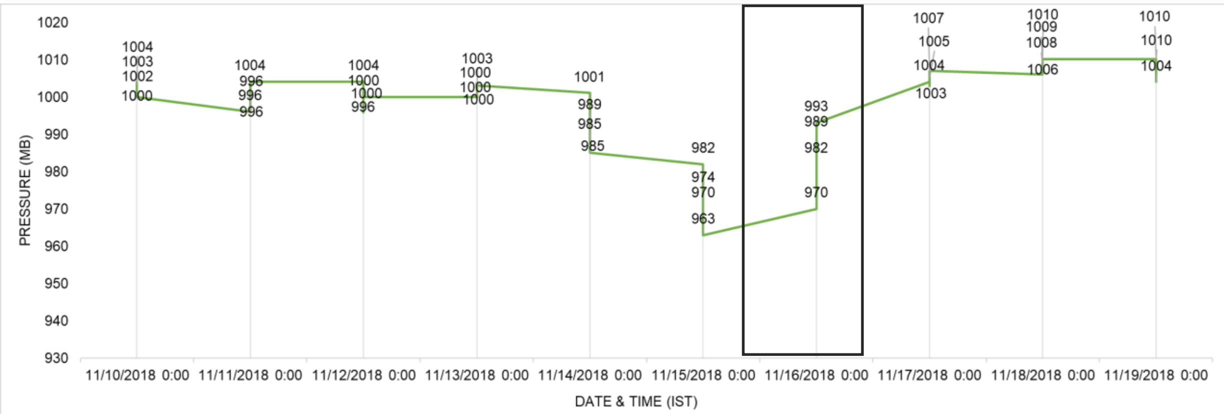

Figure 37 Observed variation of Pressure

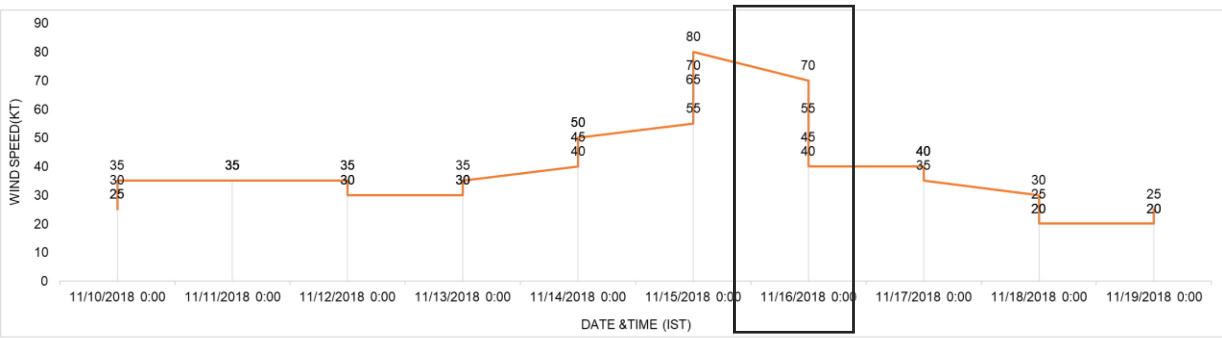

Figure 38 Observed variation of Wind speed

8.2 Variation of Meteorological Parameters During Land Interaction Over the Basin

Hourly land surface meteorological data were obtained from the ERA5-Land Reanalysis dataset, developed by the European Centre for Medium-Range Weather Forecasts. ERA5-Land provides meteorological variables at a spatial resolution of 0.1° × 0.1° (https://cds.climate.copernicus.eu/datasets/reanalysis-era5-single-levels), which enables detailed analysis of land surface conditions during extreme weather events. Within the Periyar River Basin, 43 grid points corresponding to the ERA5-Land dataset were selected to represent basin-scale meteorological conditions. For each identified cyclone event from the NOAA Cyclone Dataset, a 10-day analysis window consisting of five days before and five days after the event was considered to capture the pre-cyclone, cyclone interaction, and post-cyclone phases. The variables extracted include precipitation, near-surface temperature, wind speed, and surface pressure, which are key indicators of cyclone influence over land. Variations in these parameters help identify characteristic cyclone patterns, such as increased rainfall due to organized convection, stronger surface winds associated with cyclone circulation, a decrease in surface pressure indicating the presence of a low-pressure system, and temperature changes resulting from cloud cover and intense precipitation during cyclone interaction with the land region.

Among the identified cyclone events, the last event corresponds to Cyclone Gaja (2018). Figure 39 represents the hourly spatial variation of meteorological parameters on the day the cyclone made landfall over the Periyar river basin, showing a pronounced and basin-wide drop in surface pressure during the central hours, clearly indicating the influence of a strong low-pressure system associated with the cyclone. Concurrently, wind speed increases significantly, particularly during the peak interaction period, reflecting intensified cyclonic circulation over the region. Precipitation exhibits a sharp and widespread rise across almost all grid points, suggesting strong and sustained convective activity during landfall. Near-surface temperature shows a noticeable decline, primarily due to dense cloud cover, reduced solar radiation, and rainfall-induced cooling effects. The hourly progression of these parameters captures the dynamic nature of the cyclone's interaction with land, highlighting the peak impact period followed by gradual stabilization, thereby clearly illustrating the meteorological signature of Cyclone Gaja during its landfall over the basin. *(The details of the spatial plots corresponding to the remaining identified cyclone events are provided in Annexure 1).*

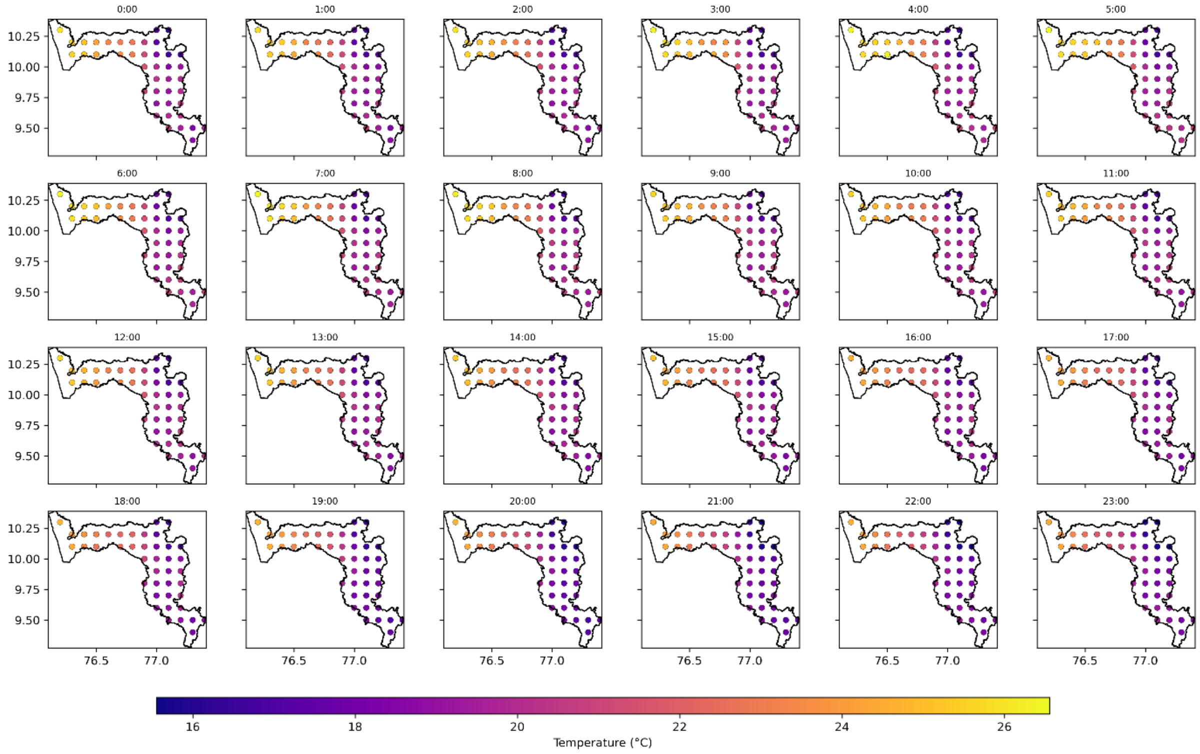
0:00
1:00
2:00
3:00
4:00
5:00
6:00
7:00
8:00
9:00
10:00
11:00
12:00
13:00
14:00
15:00
16:00
17:00
18:00
19:00
20:00
21:00
22:00
23:00
10.25
10.00
9.75
9.50
76.5
77.0
16
18
20
22
24
26
Temperature (°C)

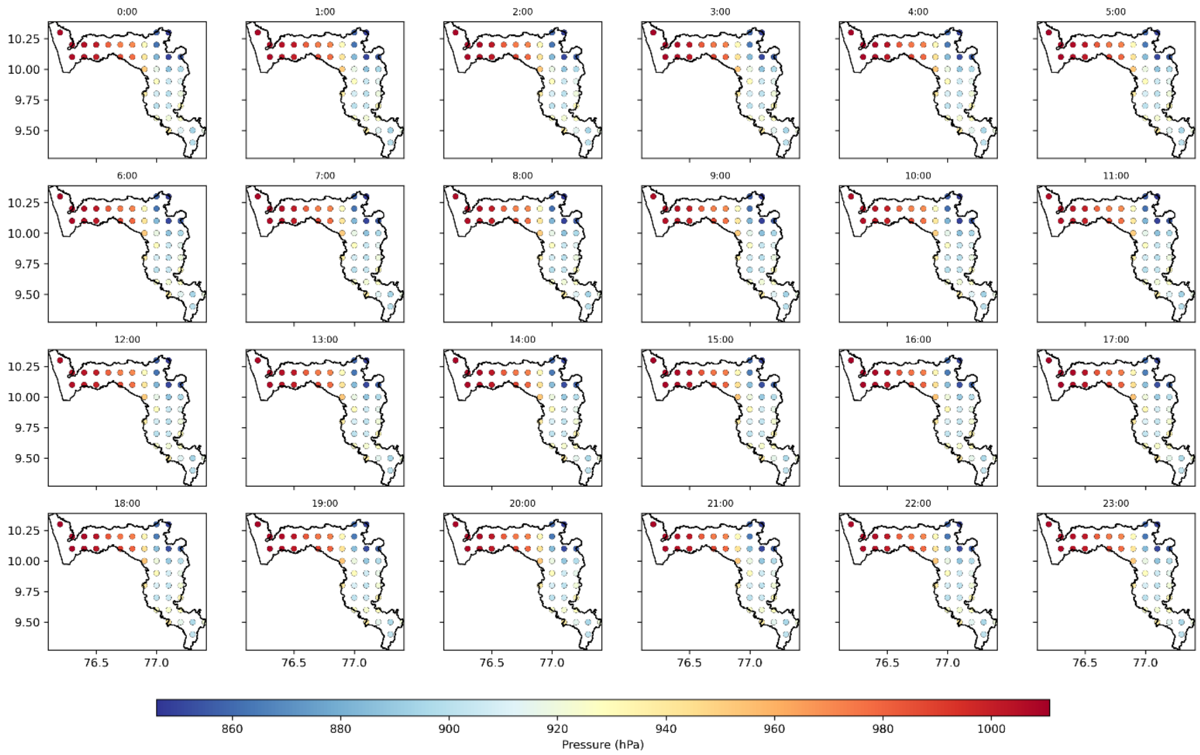
0:00
1:00
2:00
3:00
4:00
5:00
6:00
7:00
8:00
9:00
10:00
11:00
12:00
13:00
14:00
15:00
16:00
17:00
18:00
19:00
20:00
21:00
22:00
23:00
10.25
10.00
9.75
9.50
76.5
77.0
860
880
900
920
940
960
980
1000
Pressure (hPa)

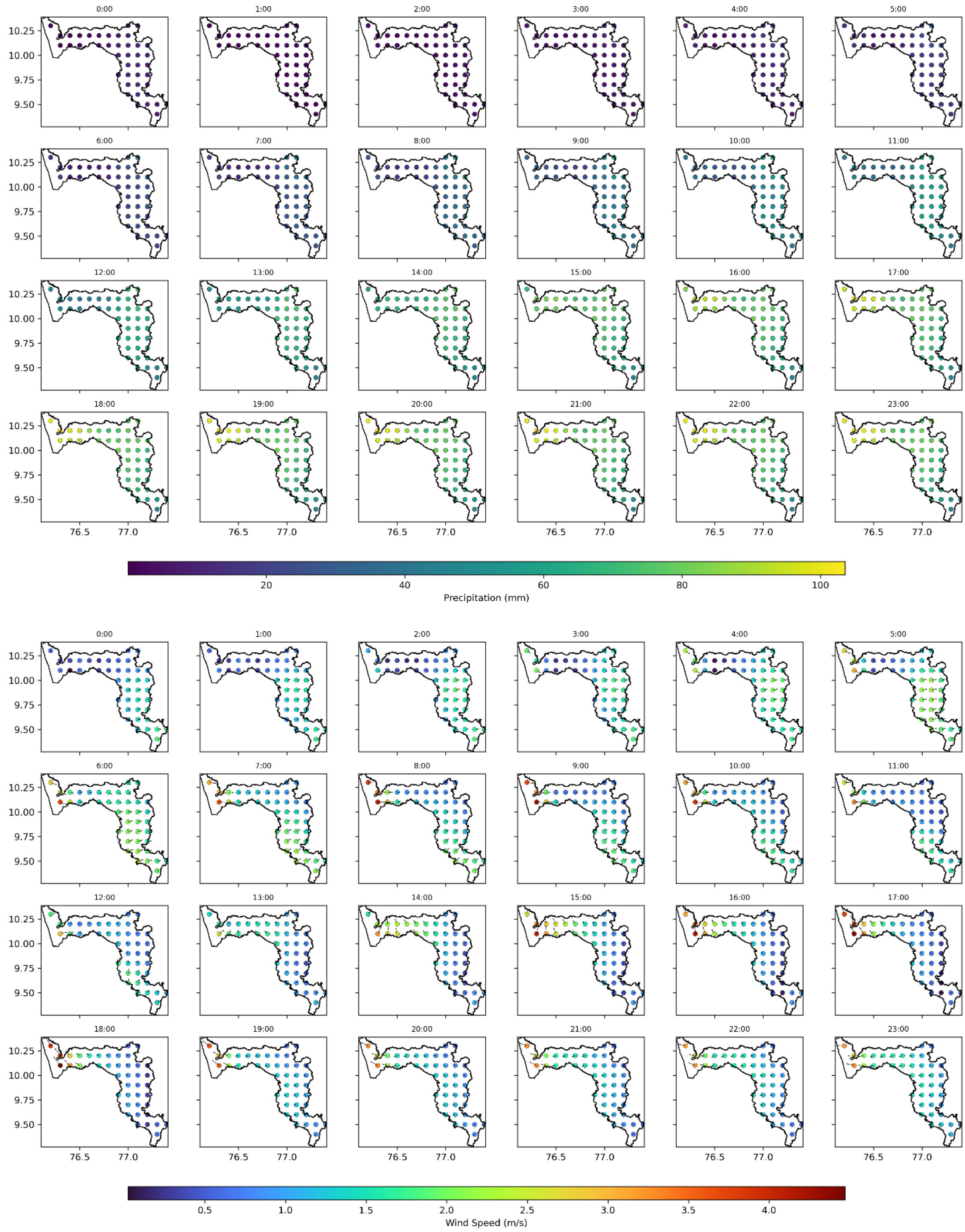

Figure 39 Spatio-temporal variation of the Surface pressure, Temperature, Precipitation and Wind speed corresponds to the cyclone Gaja 2018

8.3 Variation of Meteorological Parameters Within the 500 km Coastal Influence Zone of Kerala

To analyze the atmospheric conditions associated with the cyclones affecting the e Periyar River Basin during cyclone events (as identified in Section 6), data were obtained from the ERA5 Reanalysis with a spatial resolution of 0.25° × 0.25° (https://cds.climate.copernicus.eu/datasets/reanalysis-era5-land). A 500 km buffer from the basin boundary was considered to represent the coastal influence zone surrounding Kerala, covering parts of the Arabian Sea and adjacent coastal regions. The selected spatial domain is shown in Figure 40. The choice of a 500 km distance is based on the typical spatial extent of tropical cyclone circulation, where wind and pressure anomalies can extend several hundred kilometers from the cyclone centre, influencing surrounding regions before land interaction. For each cyclone event identified in Section 6, a 10-day analysis period consisting of five days before and five days after the event was considered in order to capture the atmospheric conditions during the pre-cyclone, active cyclone, and post-cyclone phases. The parameters analyzed include surface pressure and wind speed, which are key indicators of cyclone structure and movement. Surface pressure helps identify the presence and intensity of the cyclone through the formation of a low-pressure system, while wind speed represents the strength of cyclone-induced circulation over the surrounding region.

Among the identified cyclone events, the last event corresponds to Cyclone Gaja (2018), and Figure 41 indicates the hourly spatial variation of wind speed and surface pressure within the 500 km coastal influence zone on the day of its landfall. The wind field clearly shows the development and movement of a well-organized cyclonic circulation, with increasing wind speeds and a distinct rotational pattern becoming more prominent during the central hours, especially over the Arabian Sea and adjoining coastal regions. Simultaneously, surface pressure exhibits a noticeable decrease toward the cyclone centre, forming a well-defined low-pressure core that intensifies during the peak interaction period. The spatial gradient of pressure from the centre toward the periphery highlights the strength and structure of the cyclone system. As the hours progress, both wind intensity and pressure gradients gradually weaken, indicating the movement and dissipation of the cyclone after land interaction.

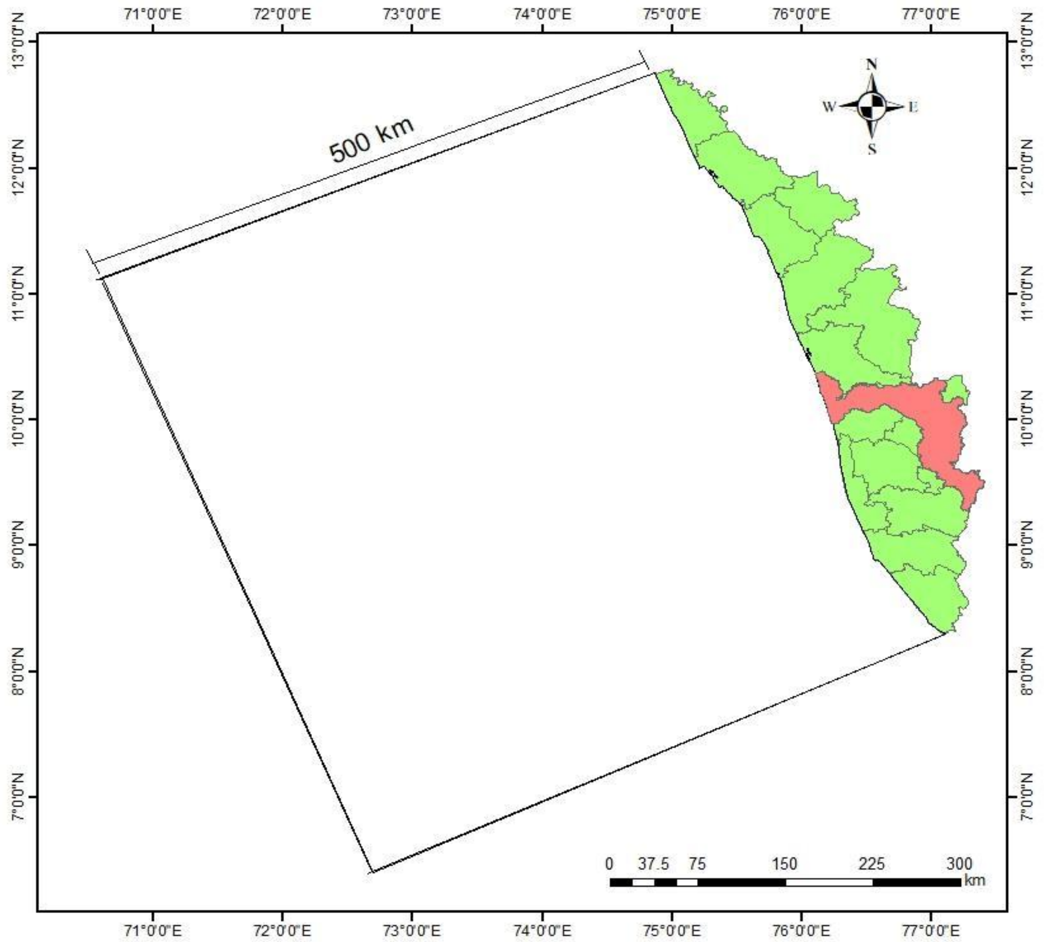

Figure 40 Spatial extent of the 500 km coastal influence zone

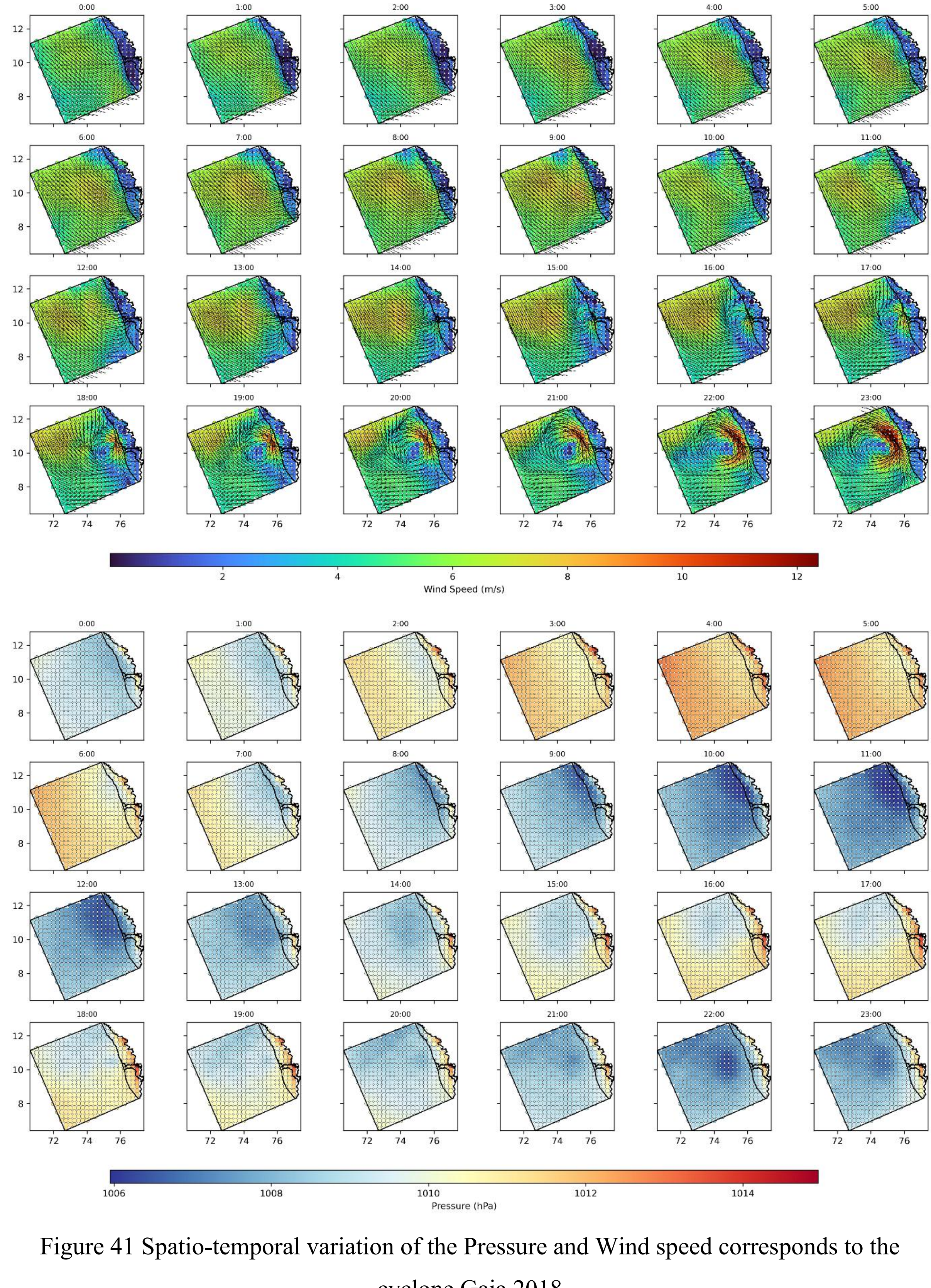

Figure 41 Spatio-temporal variation of the Pressure and Wind speed corresponds to the cyclone Gaja 2018

8.4 Vertical Variation of Meteorological Parameters Across Different Pressure Levels

To examine the vertical atmospheric structure associated with cyclone events affecting the Periyar river basin, atmospheric variables were obtained from the ERA5 Reanalysis pressure-level dataset with a spatial resolution of 0.25° × 0.25° and hourly temporal resolution (https://cds.climate.copernicus.eu/datasets/reanalysis-era5-pressure-levels). For each identified cyclone event, a 10-day analysis period consisting of five days before and five days after the event was considered in order to capture the atmospheric conditions during the pre-cyclone, active cyclone, and post-cyclone phases. The parameters analyzed include geopotential, temperature, relative humidity, specific humidity, u-component of wind, v-component of wind, vertical velocity, vorticity, and divergence. These variables describe the thermal, moisture, and dynamic structure of the atmosphere associated with cyclone systems. Geopotential represents the height of pressure surfaces and helps identify large-scale circulation patterns, while temperature and humidity parameters indicate the thermodynamic conditions that support convection and moisture availability. The u and v wind components describe horizontal wind circulation, which is essential for understanding cyclone movement and wind structure. Vertical velocity represents upward or downward air motion associated with convection, whereas vorticity indicates the rotational characteristics of the atmosphere related to cyclonic circulation. Divergence represents the spreading or convergence of air, which influences vertical motion and cyclone development.

The analysis was conducted at 925, 850, 500, 300, and 200 hPa pressure levels, representing different layers of the troposphere. The 925 hPa and 850 hPa levels correspond to the lower troposphere where moisture transport and low-level cyclone circulation are prominent. The 500 hPa level represents the mid-troposphere and is important for understanding large-scale atmospheric circulation and steering mechanisms. The 300 hPa and 200 hPa levels represent the upper troposphere, where divergence and upper-level outflow play an important role in sustaining cyclone development. Analyzing meteorological parameters across these pressure levels helps to understand the vertical structure and evolution of cyclone systems influencing the region.

The spatial patterns on the landfall day of Cyclone Gaja (2018) over the Periyar river basin reveal a strongly coupled vertical structure with distinct signatures across all pressure levels. In the lower troposphere (925 and 850 hPa), wind speeds are relatively high with clear spatial gradients, indicating intensified low-level circulation and moisture convergence. Specific humidity is notably elevated and uniformly distributed, highlighting abundant moisture availability and active inflow into the system. Temperature at these levels remains warm, supporting instability and enhancing convective processes during landfall.

At the mid-tropospheric level (500 hPa), the circulation appears well organized, with geopotential height fields showing a coherent structure that reflects the cyclone's influence on large-scale atmospheric flow. Wind patterns remain aligned, indicating sustained medium-level support to the system, while moisture, though reduced compared to lower levels, still contributes to maintaining vertical continuity of convection.

In the upper troposphere (300 and 200 hPa), the presence of strong geopotential gradients and organized wind flow indicates active upper-level divergence and efficient outflow. These features are crucial during landfall, as they facilitate upward motion and help sustain the cyclone's intensity even as it interacts with land. The temperature fields are comparatively cooler, reinforcing vertical instability through a strong lapse rate. The vertical distribution of meteorological parameters during Cyclone Gaja (2018) over the Periyar River Basin clearly illustrates a well-structured and dynamically evolving cyclone with strong vertical coupling across atmospheric layers. In the lower troposphere (925 and 850 hPa), wind fields show pronounced intensification during the active phase (around day 0 to +2), accompanied by high specific humidity, indicating strong moisture transport and low-level convergence. The spatial patterns suggest enhanced moisture accumulation and convergence zones, which favor deep convection. Temperature at these levels remains relatively warm, supporting atmospheric instability and sustained convective activity.

At the mid-tropospheric level (500 hPa), the system exhibits a more organized circulation pattern, with geopotential height fields indicating a distinct trough-like structure that plays a key role in steering the cyclone. Although moisture content decreases compared to lower levels, the alignment of wind fields and geopotential contours suggests a coherent mid-level circulation that supports the vertical structure of the cyclone. This layer acts as a bridge between lower-level moisture processes and upper-level dynamics. In the upper troposphere (300 and 200 hPa), strong geopotential gradients and wind patterns indicate the presence of pronounced upper-level divergence and outflow. These features are critical for cyclone intensification, as they facilitate upward motion from the lower layers. The temperature fields at these levels are relatively cooler, enhancing vertical instability through a strong lapse rate. The wind structure shows organized outflow, typical of a mature cyclone, which helps sustain convection and maintain the system's strength.

Temporally, the evolution from pre-cyclone to post-cyclone phases shows a clear progression: initial strengthening characterized by increasing moisture and wind intensity, peak organization with strong vertical coherence across all levels, and subsequent weakening marked by reduced wind speeds, declining moisture, and less organized spatial patterns. The plots (Figure 42 to 46) demonstrate a vertically aligned and dynamically consistent cyclone structure, where low-level moisture convergence, mid-level circulation, and upper-level divergence work together to control the development and evolution of the cyclone over the basin.

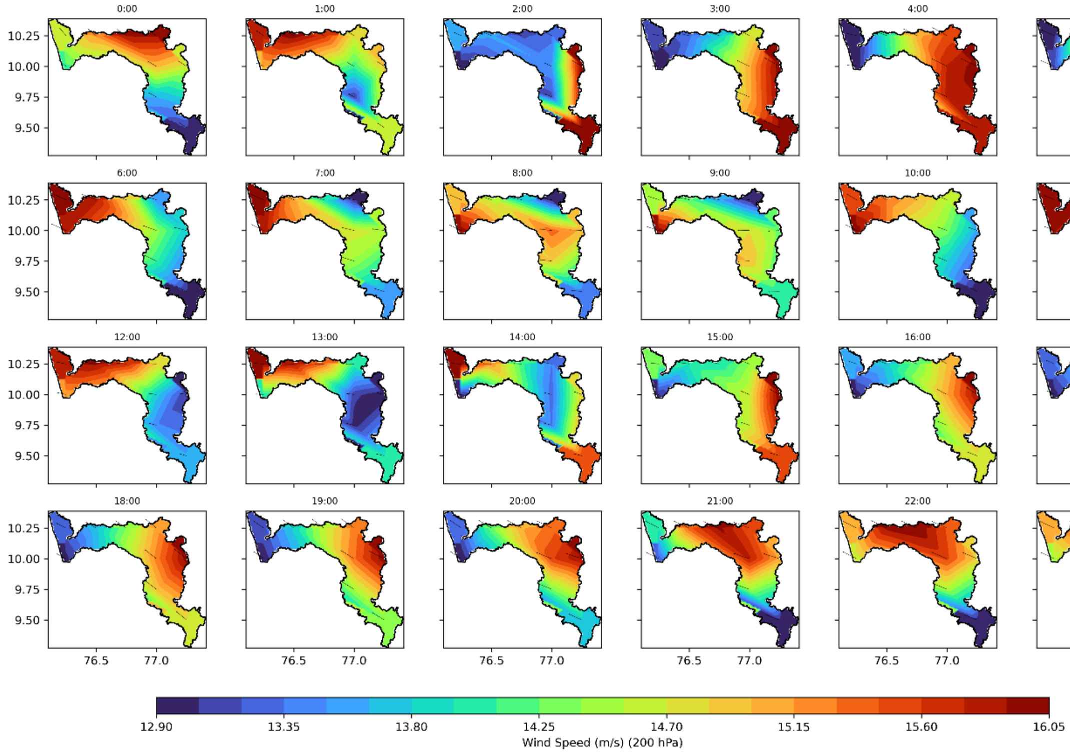

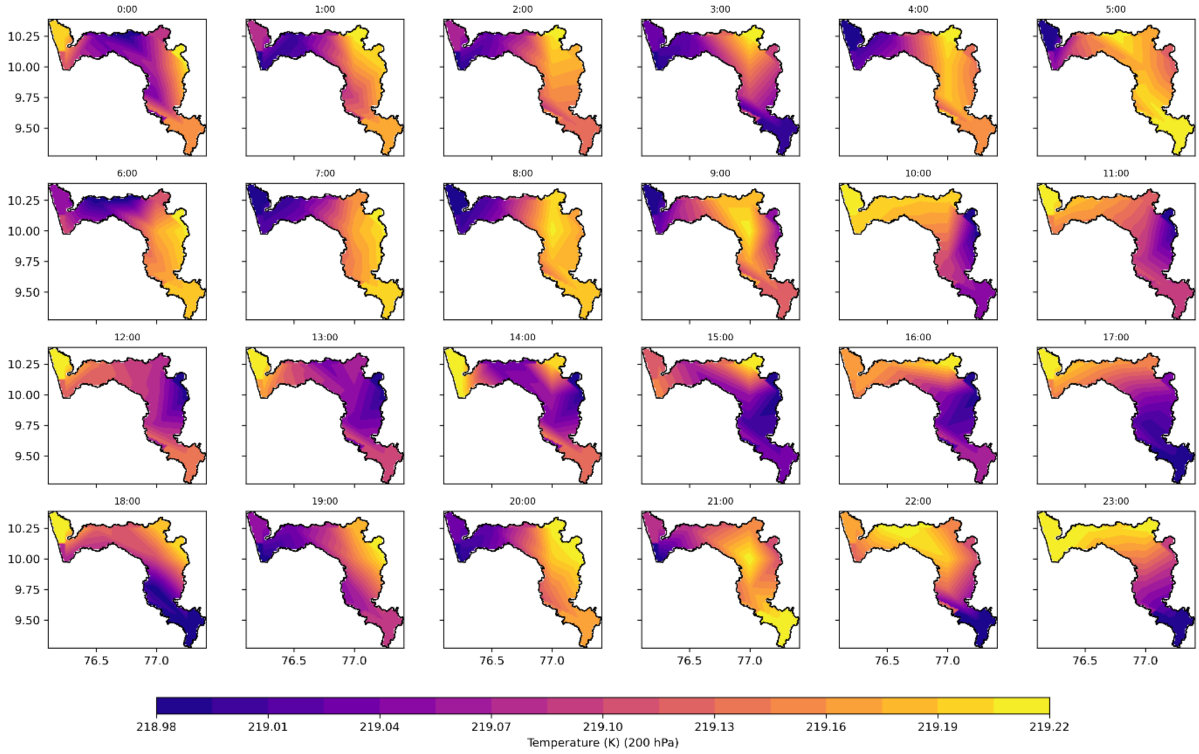
0:00
1:00
2:00
3:00
4:00
5:00
6:00
7:00
8:00
9:00
10:00
11:00
12:00
13:00
14:00
15:00
16:00
17:00
18:00
19:00
20:00
21:00
22:00
23:00
10.25
10.00
9.75
9.50
76.5
77.0
218.98
219.01
219.04
219.07
219.10
219.13
219.16
219.19
219.22
Temperature (K) (200 hPa)

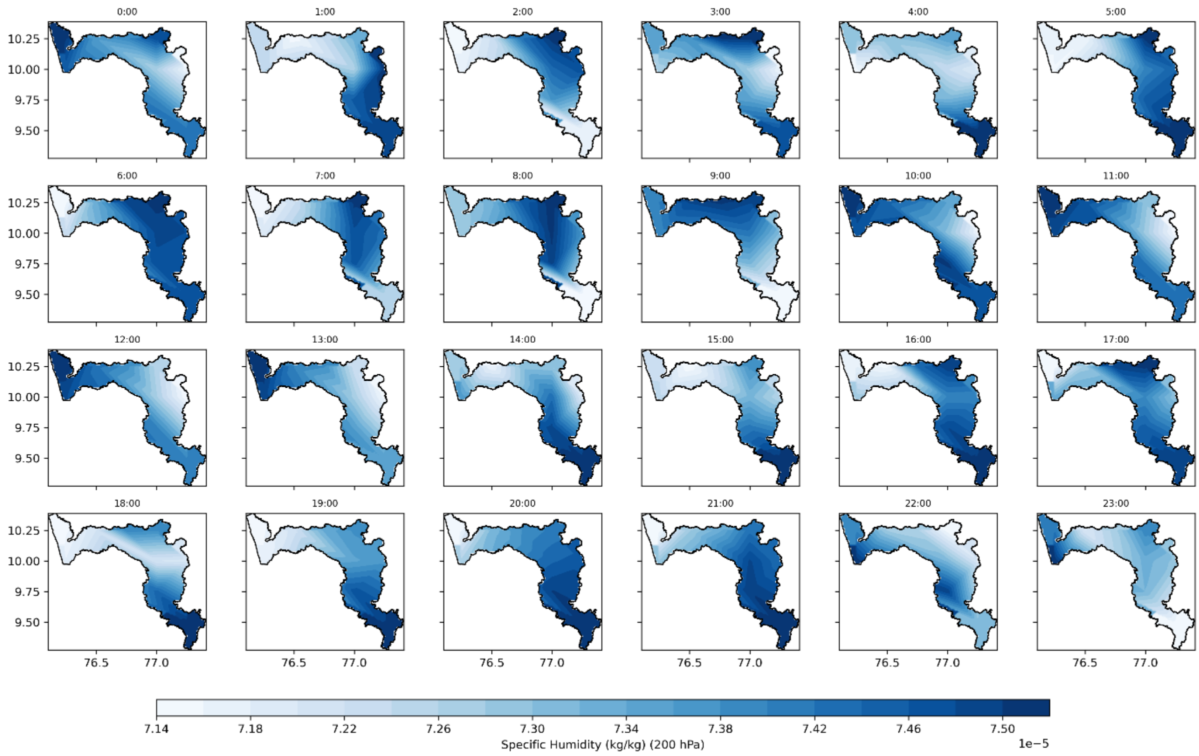
0:00
1:00
2:00
3:00
4:00
5:00
6:00
7:00
8:00
9:00
10:00
11:00
12:00
13:00
14:00
15:00
16:00
17:00
18:00
19:00
20:00
21:00
22:00
23:00
10.25
10.00
9.75
9.50
76.5
77.0
7.14
7.18
7.22
7.26
7.30
7.34
7.38
7.42
7.46
7.50
Specific Humidity (kg/kg) (200 hPa)
1e−5

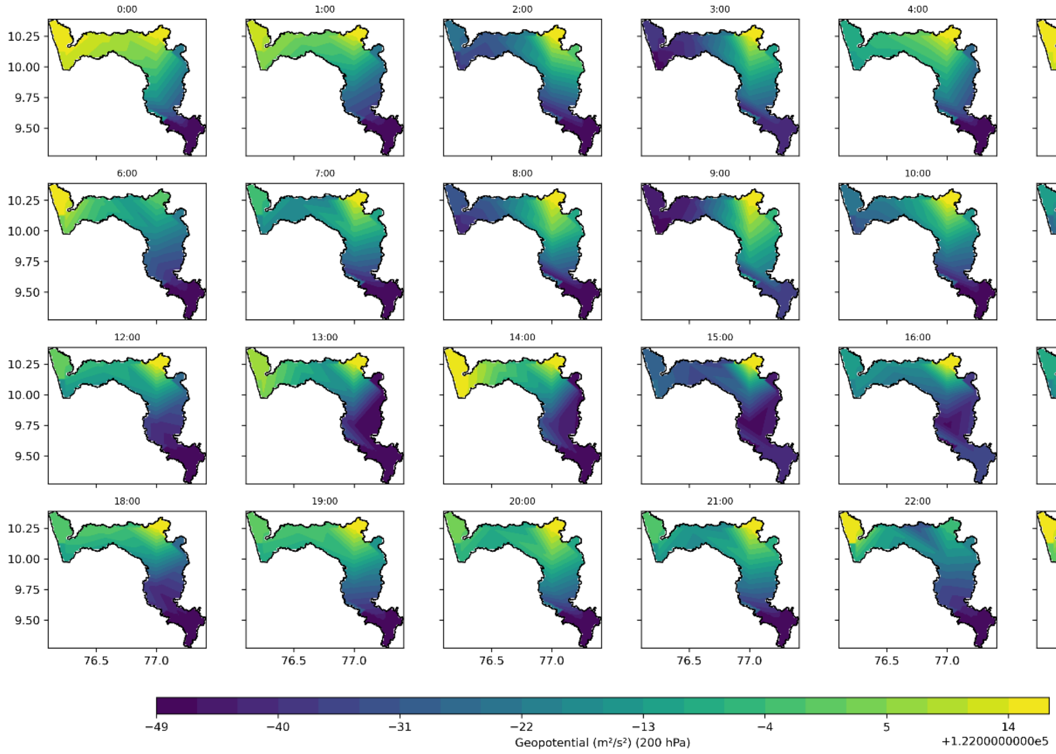

Figure 42 Spatio-temporal variation of the Wind speed, Temperature, Specific humidity, Geopotential at 200hPa corresponds to the cyclone Gaja 2018

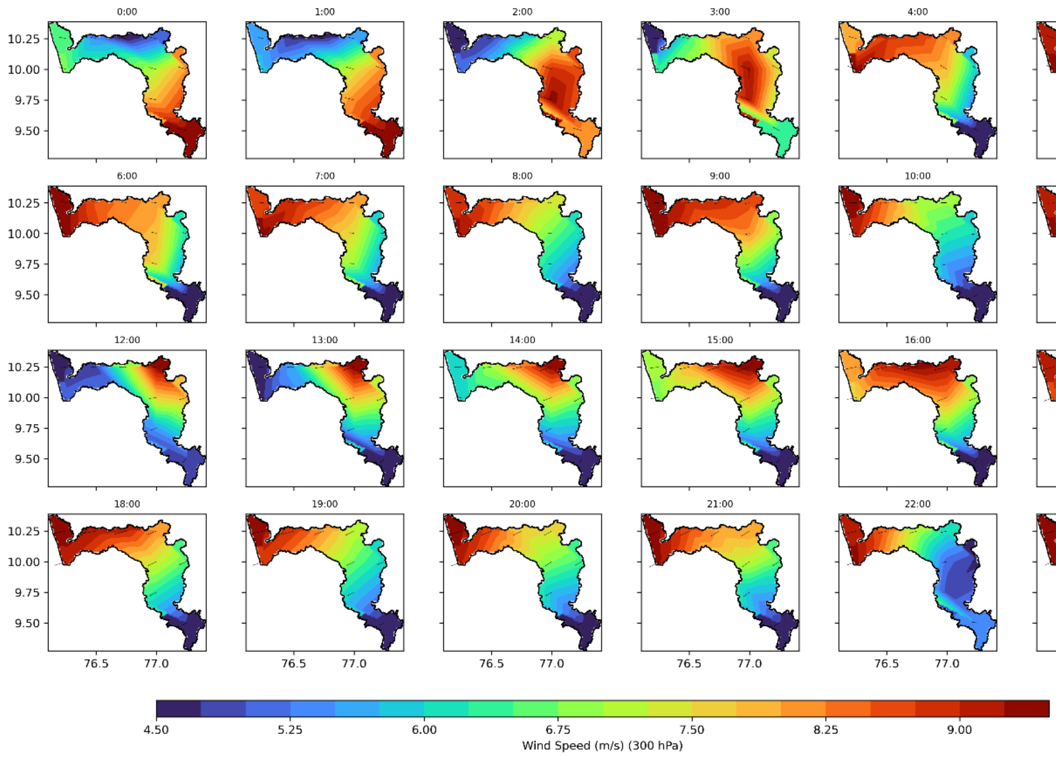

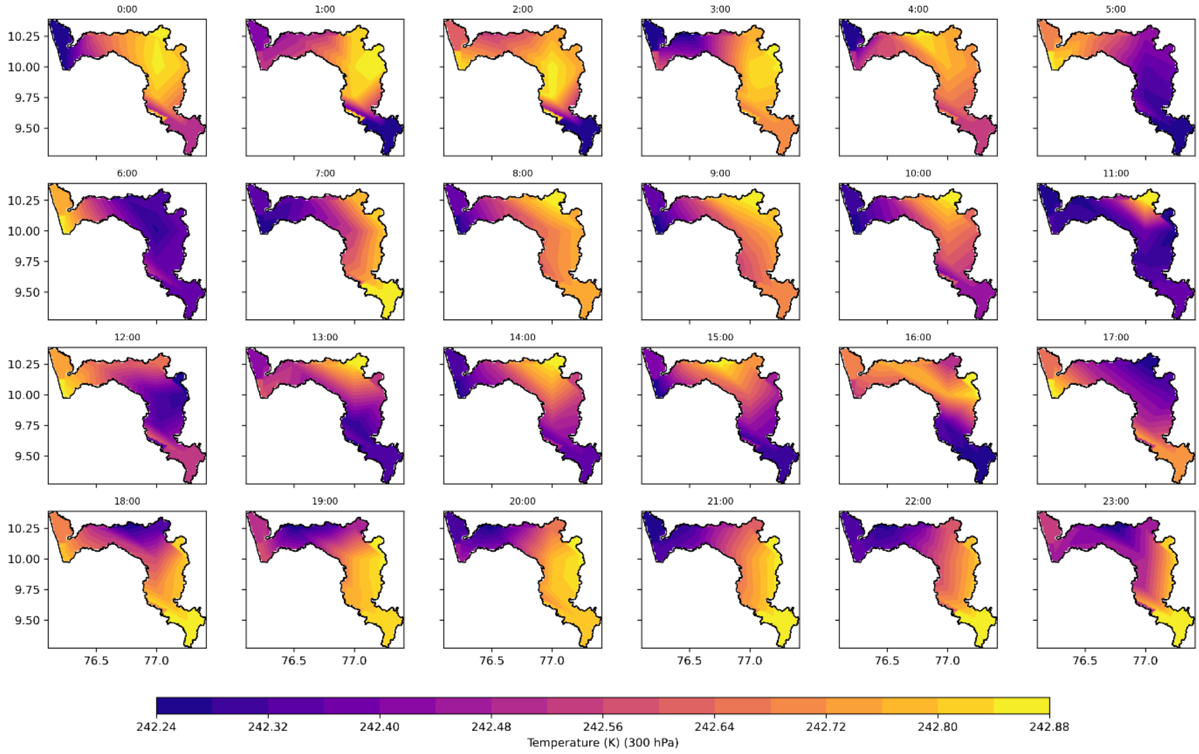
0:00
1:00
2:00
3:00
4:00
5:00
6:00
7:00
8:00
9:00
10:00
11:00
12:00
13:00
14:00
15:00
16:00
17:00
18:00
19:00
20:00
21:00
22:00
23:00
10.25
10.00
9.75
9.50
76.5
77.0
242.24
242.32
242.40
242.48
242.56
242.64
242.72
242.80
242.88
Temperature (K) (300 hPa)

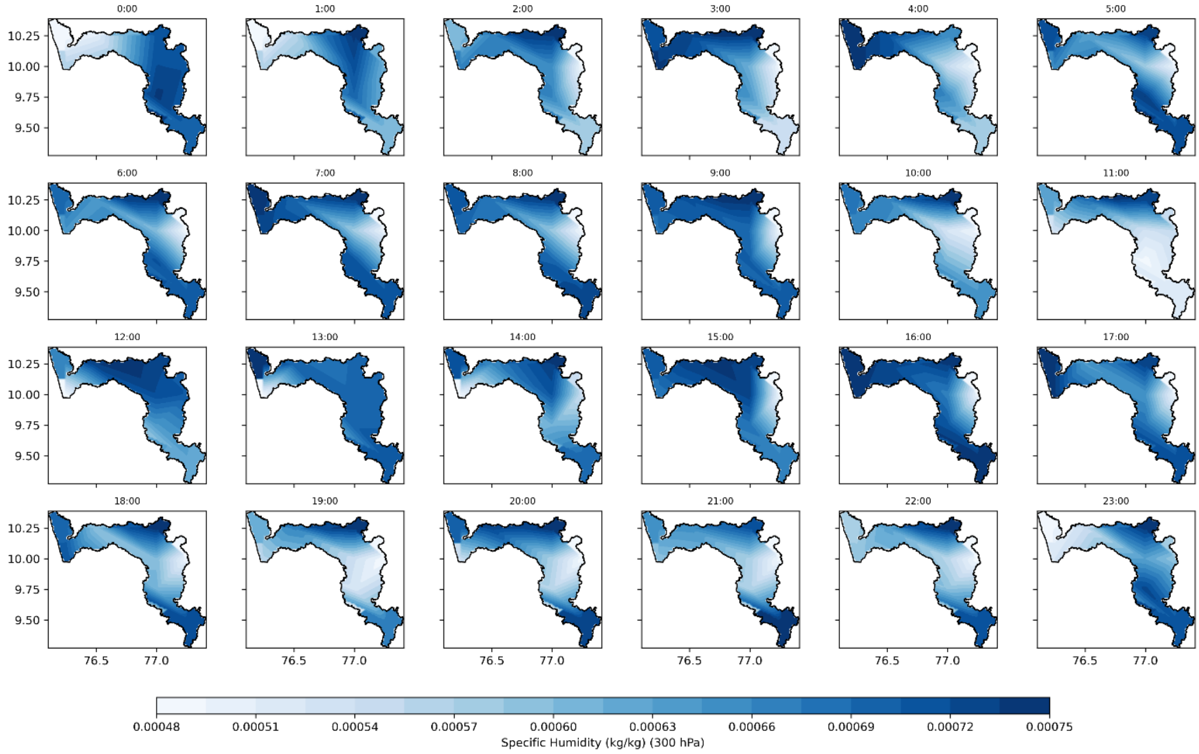
0:00
1:00
2:00
3:00
4:00
5:00
6:00
7:00
8:00
9:00
10:00
11:00
12:00
13:00
14:00
15:00
16:00
17:00
18:00
19:00
20:00
21:00
22:00
23:00
10.25
10.00
9.75
9.50
76.5
77.0
0.00048
0.00051
0.00054
0.00057
0.00060
0.00063
0.00066
0.00069
0.00072
0.00075
Specific Humidity (kg/kg) (300 hPa)

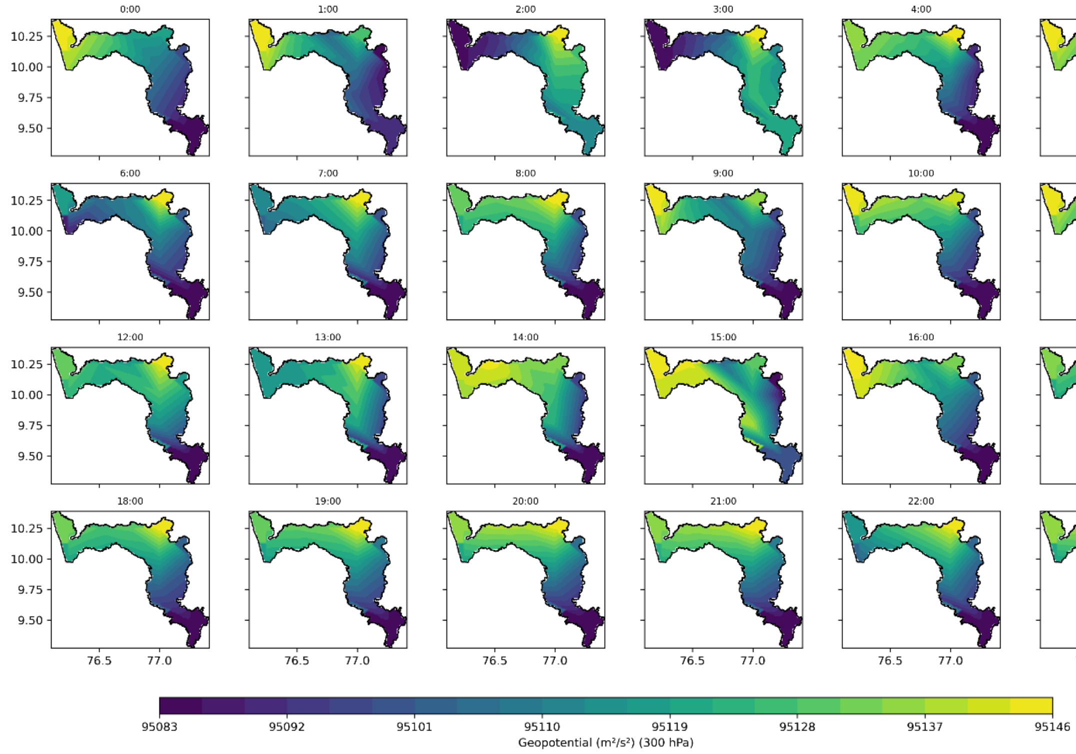

Figure 43 Spatio-temporal variation of the Wind speed, Temperature, Specific humidity, Geopotential at 300hPa corresponds to the cyclone Gaja 2018

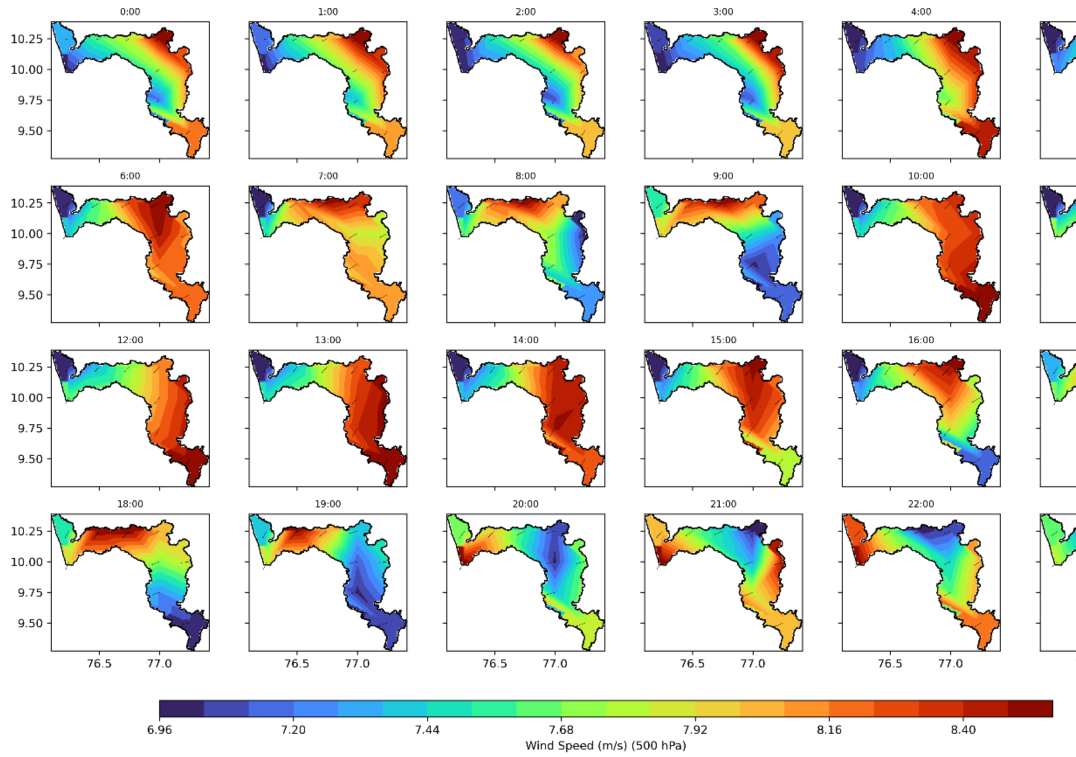

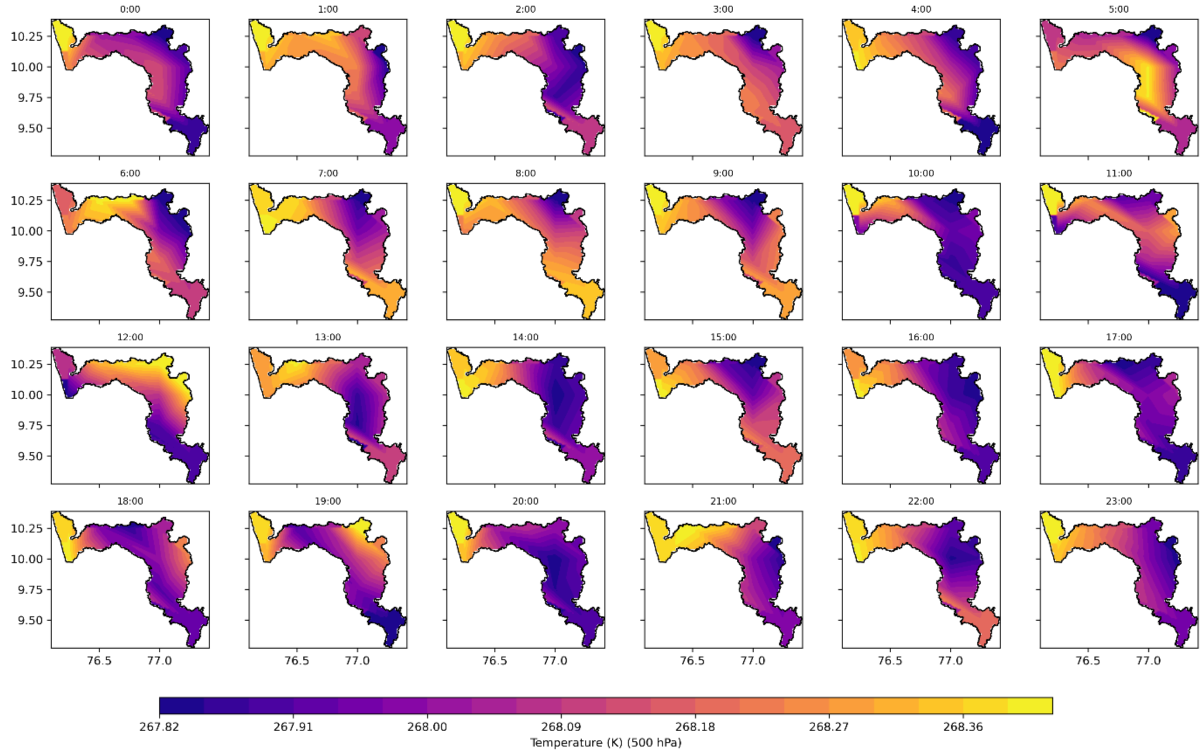
0:00
1:00
2:00
3:00
4:00
5:00
6:00
7:00
8:00
9:00
10:00
11:00
12:00
13:00
14:00
15:00
16:00
17:00
18:00
19:00
20:00
21:00
22:00
23:00
10.25
10.00
9.75
9.50
76.5
77.0
267.82
267.91
268.00
268.09
268.18
268.27
268.36
Temperature (K) (500 hPa)

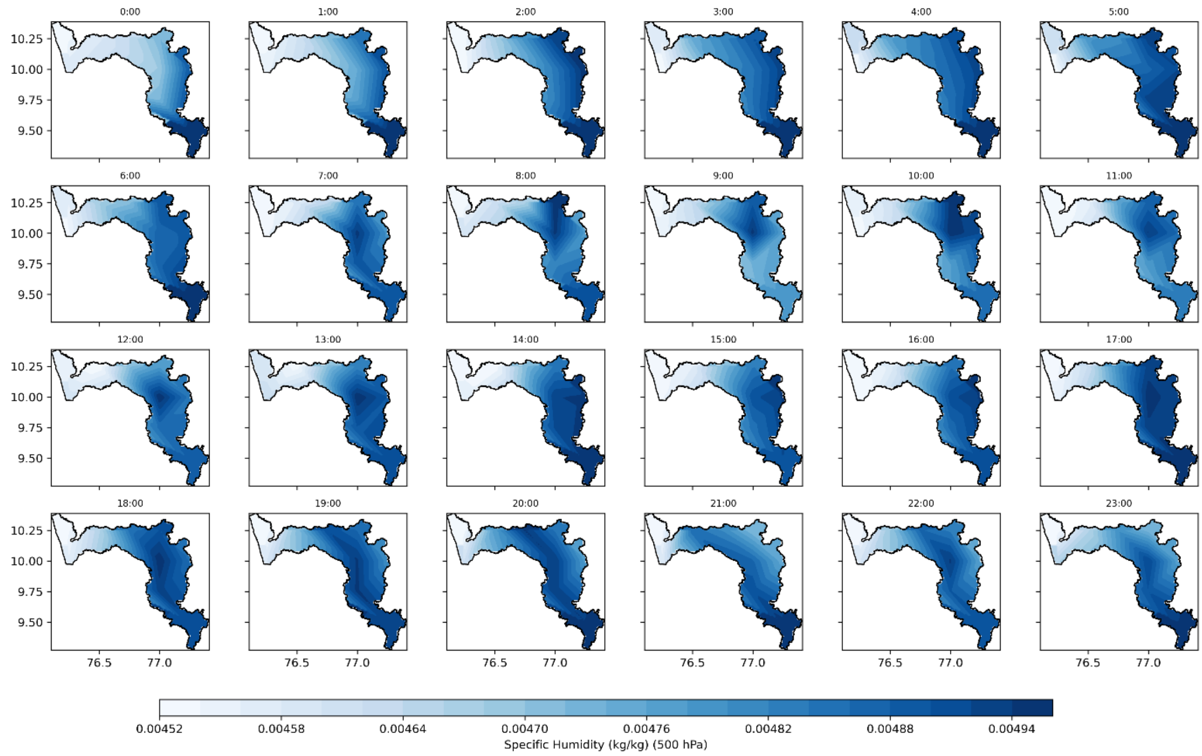
0:00
1:00
2:00
3:00
4:00
5:00
6:00
7:00
8:00
9:00
10:00
11:00
12:00
13:00
14:00
15:00
16:00
17:00
18:00
19:00
20:00
21:00
22:00
23:00
10.25
10.00
9.75
9.50
76.5
77.0
0.00452
0.00458
0.00464
0.00470
0.00476
0.00482
0.00488
0.00494
Specific Humidity (kg/kg) (500 hPa)

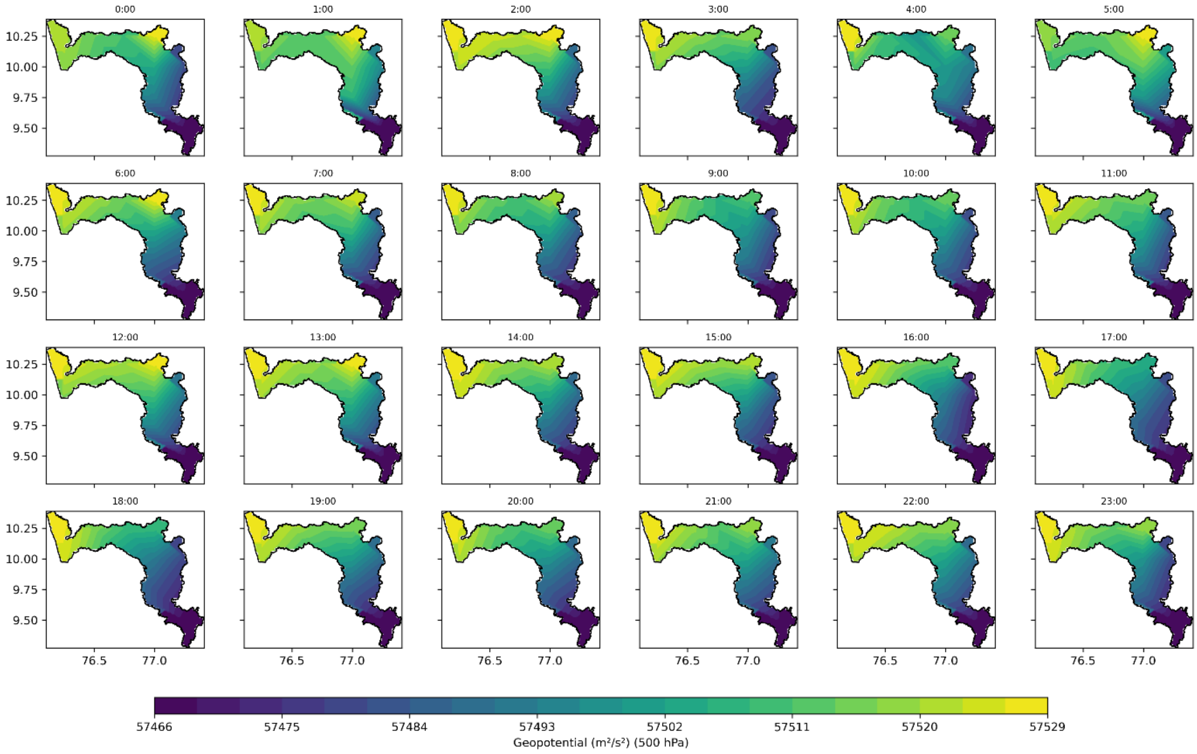

Figure 44 Spatio-temporal variation of the Wind speed, Temperature, Specific humidity, Geopotential at 500hPa corresponds to the cyclone Gaja 2018

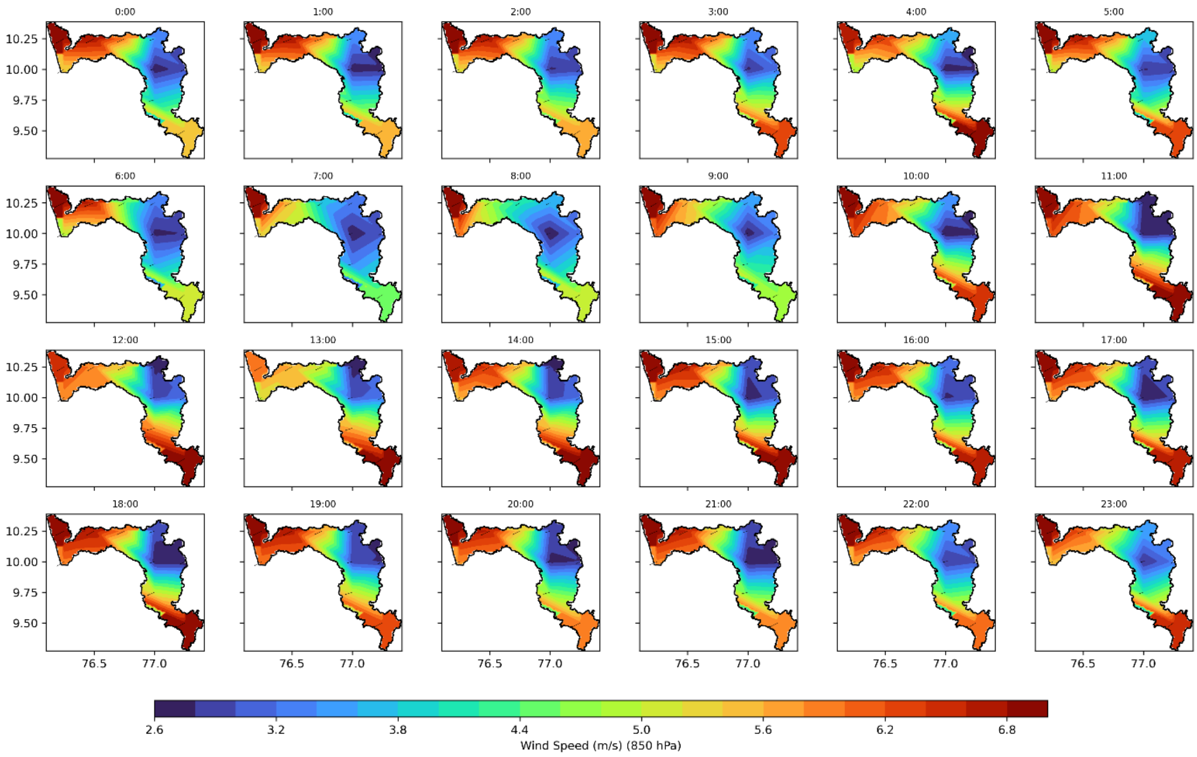

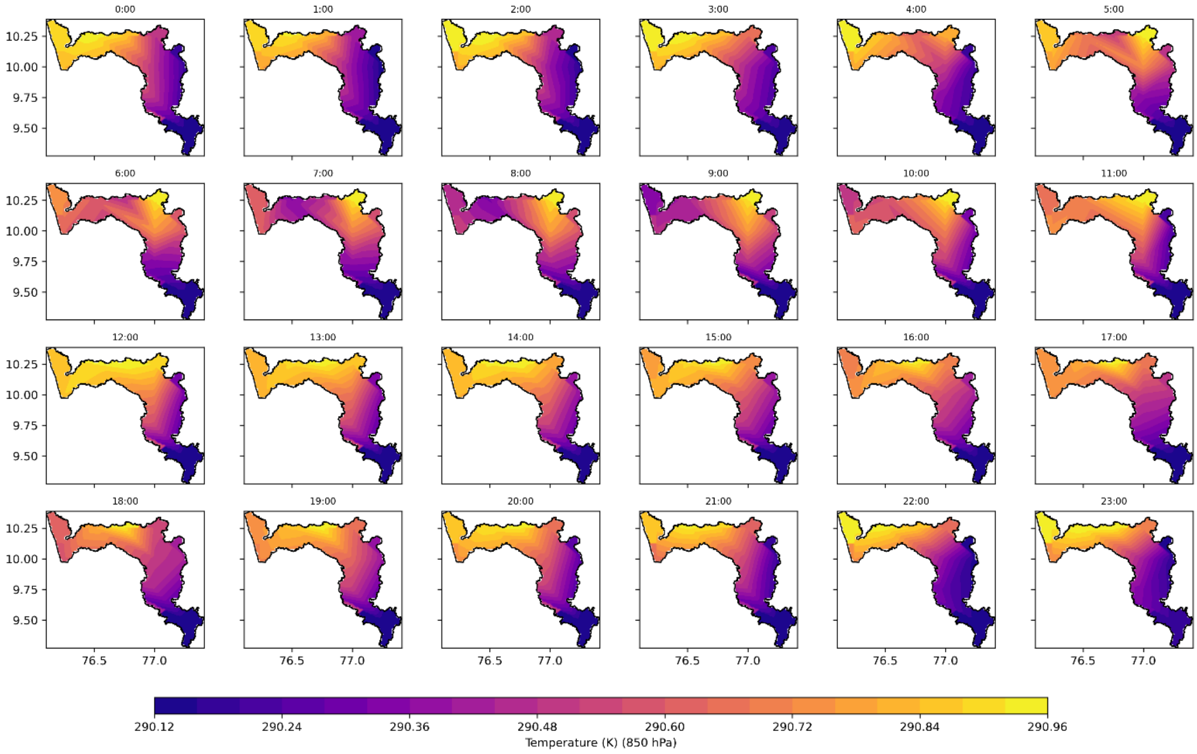
0:00
1:00
2:00
3:00
4:00
5:00
6:00
7:00
8:00
9:00
10:00
11:00
12:00
13:00
14:00
15:00
16:00
17:00
18:00
19:00
20:00
21:00
22:00
23:00
10.25
10.00
9.75
9.50
76.5
77.0
290.12
290.24
290.36
290.48
290.60
290.72
290.84
290.96
Temperature (K) (850 hPa)

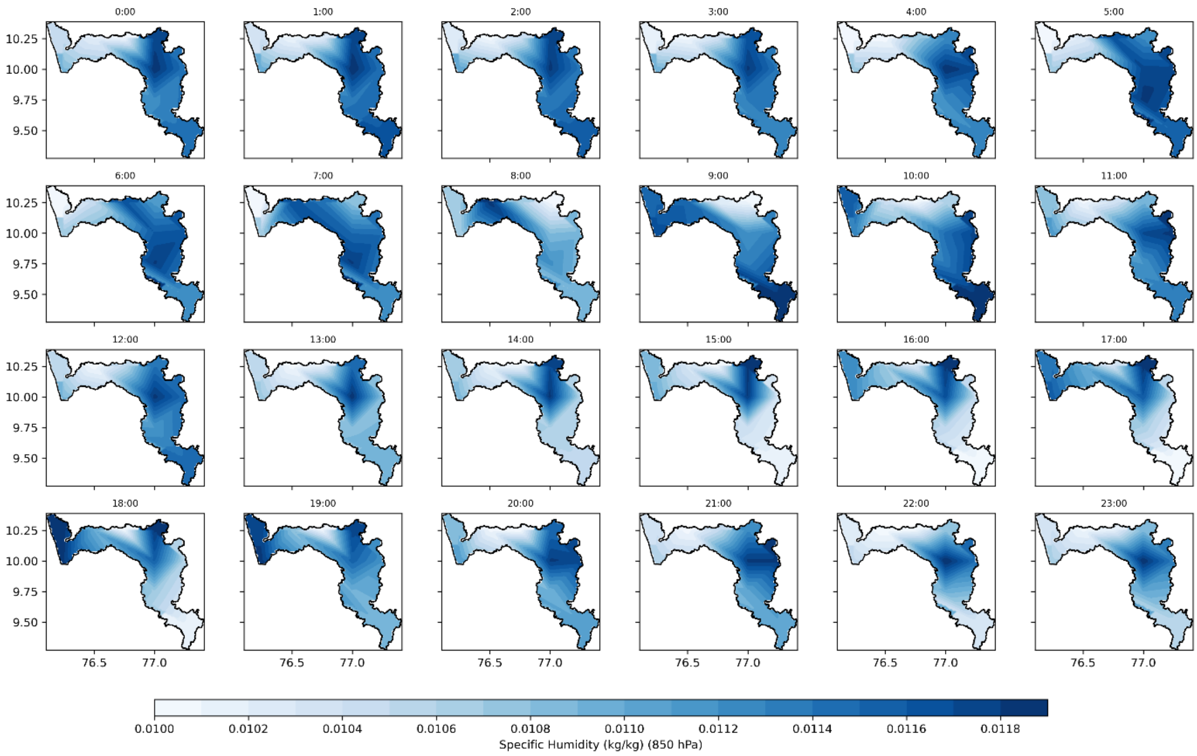
0:00
1:00
2:00
3:00
4:00
5:00
6:00
7:00
8:00
9:00
10:00
11:00
12:00
13:00
14:00
15:00
16:00
17:00
18:00
19:00
20:00
21:00
22:00
23:00
10.25
10.00
9.75
9.50
76.5
77.0
0.0100
0.0102
0.0104
0.0106
0.0108
0.0110
0.0112
0.0114
0.0116
0.0118
Specific Humidity (kg/kg) (850 hPa)

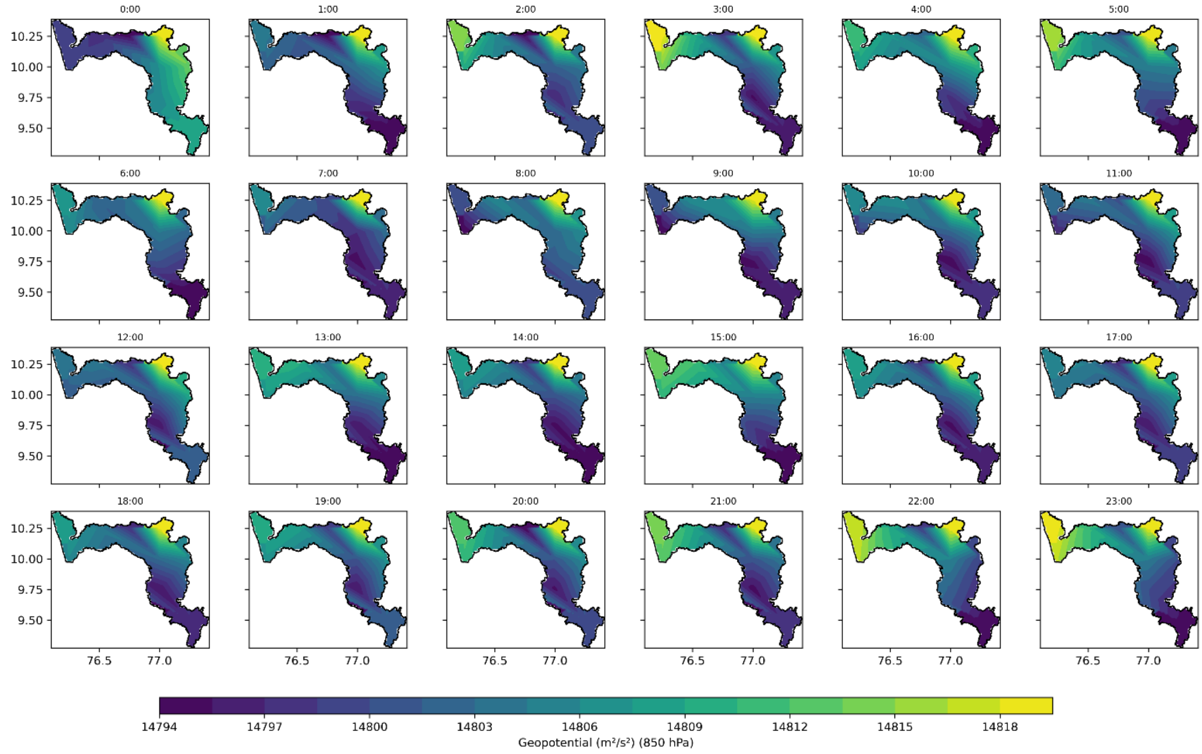

Figure 45 Spatio-temporal variation of the Wind speed, Temperature, Specific humidity, Geopotential at 850hPa corresponds to the cyclone Gaja 2018

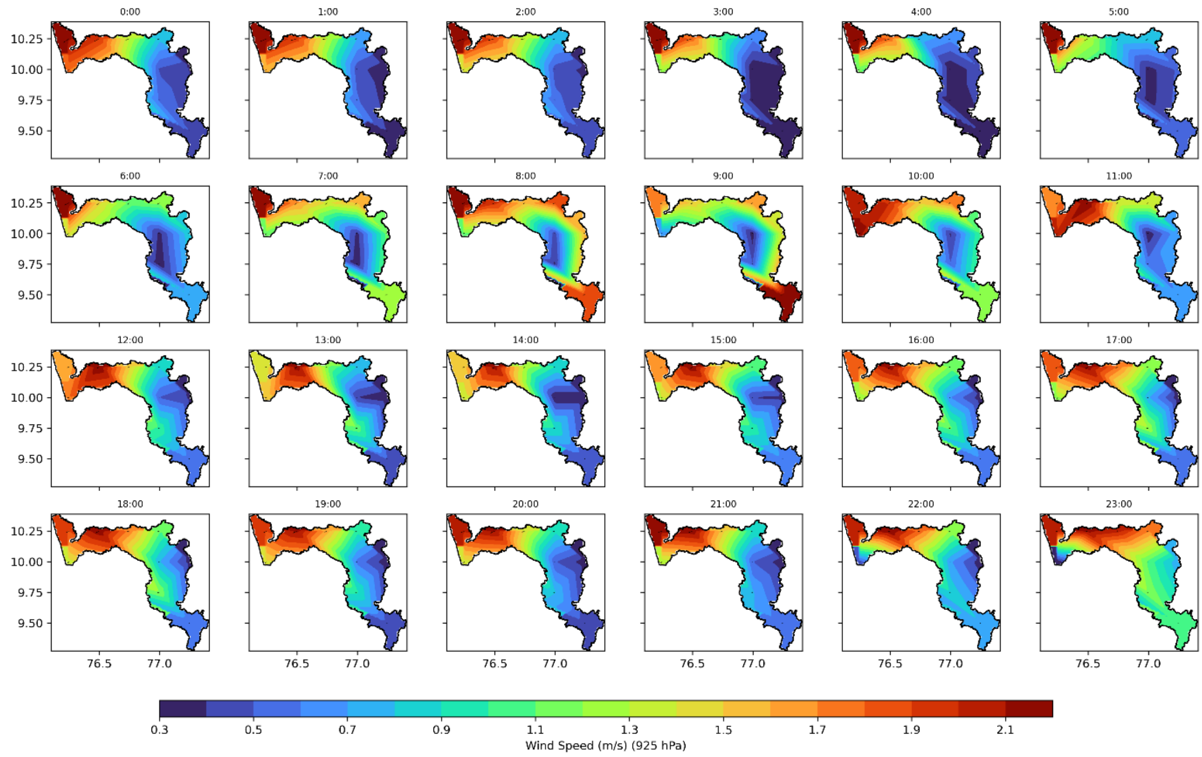

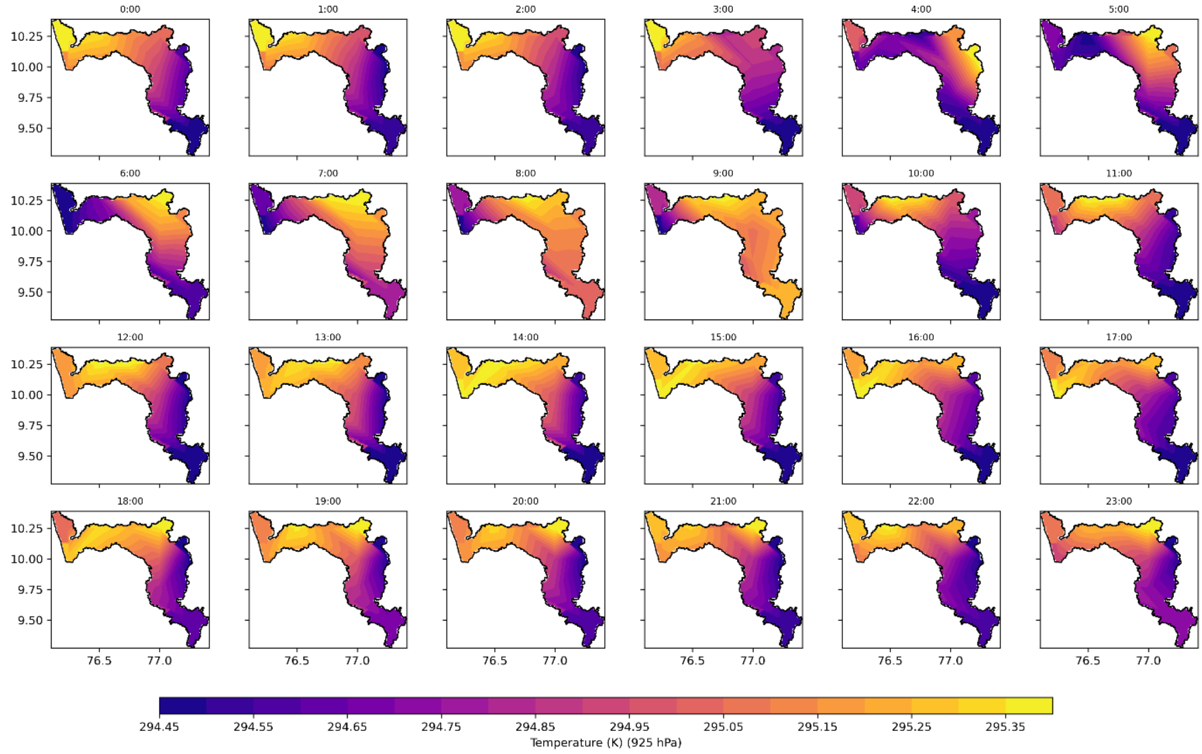
0:00
1:00
2:00
3:00
4:00
5:00
6:00
7:00
8:00
9:00
10:00
11:00
12:00
13:00
14:00
15:00
16:00
17:00
18:00
19:00
20:00
21:00
22:00
23:00
10.25
10.00
9.75
9.50
76.5
77.0
294.45
294.55
294.65
294.75
294.85
294.95
295.05
295.15
295.25
295.35
Temperature (K) (925 hPa)

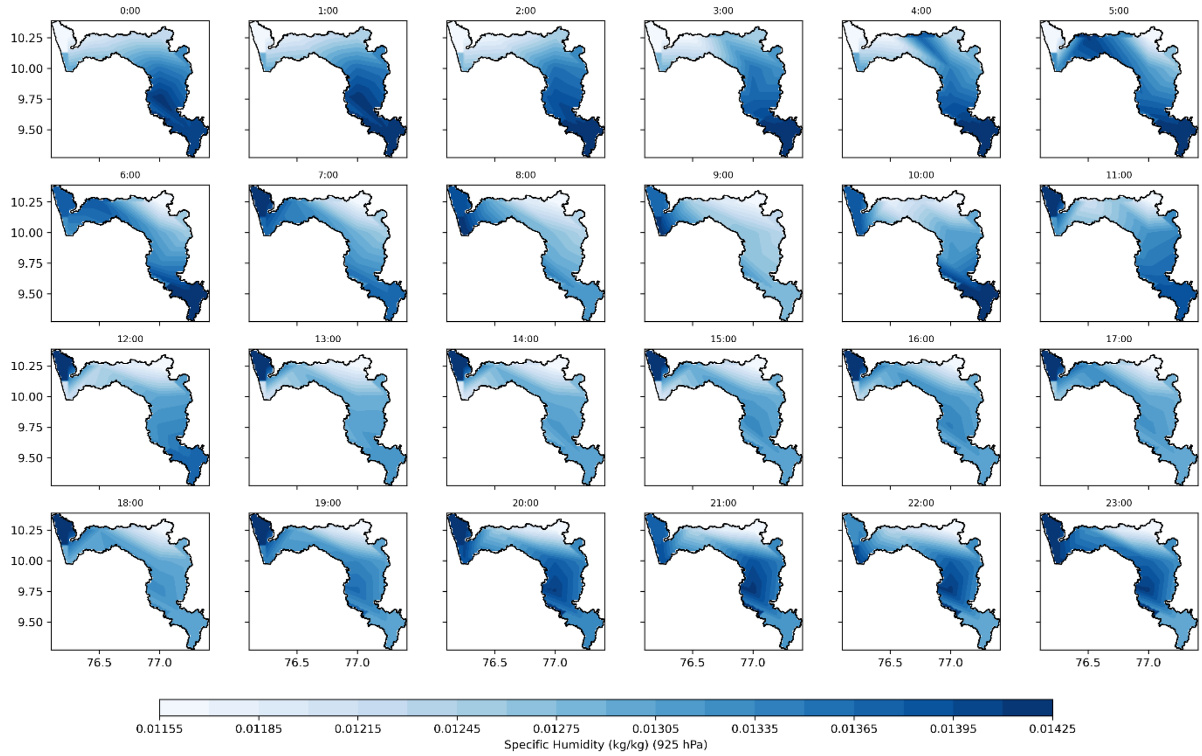
0:00
1:00
2:00
3:00
4:00
5:00
6:00
7:00
8:00
9:00
10:00
11:00
12:00
13:00
14:00
15:00
16:00
17:00
18:00
19:00
20:00
21:00
22:00
23:00
10.25
10.00
9.75
9.50
76.5
77.0
0.01155
0.01185
0.01215
0.01245
0.01275
0.01305
0.01335
0.01365
0.01395
0.01425
Specific Humidity (kg/kg) (925 hPa)

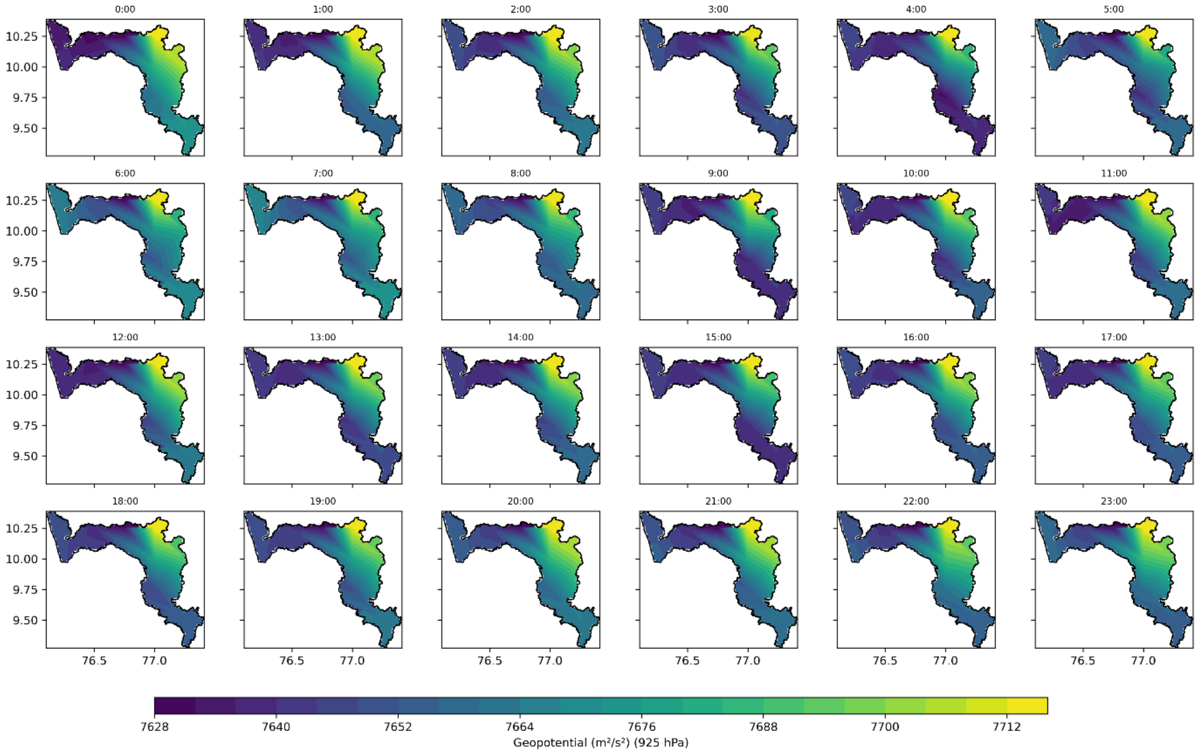

Figure 46 Spatio-temporal variation of the Wind speed, Temperature, Specific humidity, Geopotential at 925hPa corresponds to the cyclone Gaja 2018

9. Conclusions

The major cyclonic events that affected Kerala include Cyclone Gaja, Cyclone Ockhi, Cyclone Tauktae, Cyclone Fannos and other unnamed cyclones. Although the Periyar River Basin is categorized under low to moderate cyclone proneness, it remains highly vulnerable to indirect cyclonic impacts. Even without direct landfall, these systems produced intense rainfall, resulting in rapid surface runoff, increased river discharge, higher reservoir inflows, localized flooding, and slope instability across Idukki, Ernakulam, and parts of Thrissur Districts. The vulnerability of the basin is largely controlled by its physiographic and climatic characteristics. The upper catchment lies within the steep, high-relief terrain of the Western Ghats, where orographic lifting during cyclonic circulation enhances rainfall intensity. The Periyar River Basin exhibits moderate wind hazard risk but high rainfall-induced hazard sensitivity, particularly in the highland catchment regions.

10. Recommendations & Role of stakeholders

The analysis of all identified cyclone events over the Periyar River Basin shows recurring patterns of intense short-duration rainfall, rapid drops in surface pressure, strong wind fields, and vertically coherent atmospheric structures extending from lower to upper tropospheric levels. These consistent characteristics indicate the need for a basin-specific, impact-oriented cyclone management strategy. It is recommended to strengthen early warning systems through the use of high-resolution, real-time meteorological data and improved forecasting techniques to enhance lead time and spatial accuracy. Forecast outputs should be directly linked with flood assessment frameworks to enable timely identification of high-risk zones and potential inundation areas. In addition, development of dense observation networks and real-time monitoring systems within the basin will improve both early warning and post-event analysis.

From a planning perspective, cyclone risk must be integrated into basin management by identifying vulnerable regions, particularly low-lying and flood-prone areas, and regulating land use accordingly. Improving drainage capacity, maintaining river channels, and protecting natural buffers such as wetlands and floodplains are critical for reducing flood peaks and enhancing resilience. Infrastructure planning should also account for cyclone-induced stresses, especially in terms of wind damage and extreme rainfall impacts.

The role of stakeholders is central to effective implementation. Meteorological and disaster management agencies should ensure timely, accurate, and location-specific warnings, along with clear communication of risk levels. Water resource authorities must incorporate forecast information into reservoir operations and flood mitigation strategies to manage sudden inflows. Local governments and district administrations are responsible for translating warnings into actionable measures, including evacuation planning, emergency response, and public awareness campaigns. Research and academic institutions should focus on improving understanding of cyclone behavior, basin response, and long-term climate variability. At the community level, active participation in preparedness measures, adherence to warnings, and sustainable land and water management practices are essential.

References

Ashrit, R., Sharma, K., Kumar, S., Dube, A., Karunasagar, S., Arulalan, T., Mamgain, A., Chakraborty, P., Kumar, S., Lodh, A., Dutta, D., Momin, I., Bushair, M. T., Prakash, B. J., Jayakumar, A., & Rajagopal, E. N. (2020). Prediction of the August 2018 heavy rainfall events over Kerala with high-resolution NWP models. Meteorological Applications. https://doi.org/10.1002/met.1906

Bell, M. M., & Montgomery, M. T. (2008). Observed structure, evolution, and potential intensity of Category 5 Hurricane Isabel (2003) from 12 to 14 September. Monthly Weather Review, 136(6), 2023–2046. https://doi.org/10.1175/2007MWR1858.1

Colomb, A., Veremes, H., Bonnardot, F., Jumaux, G., Langlade, S., & Malardel, S. (2025). Evaluating monthly tropical cyclone forecasts through the lens of track clustering over the Southwest Indian Ocean. Meteorological Applications, 32, e70120. https://doi.org/10.1002/met.70120

Dean R. Morford. (1979). North Indian Ocean tropical cyclones (Section 3.2). In 1978 annual tropical cyclone report. Joint Typhoon Warning Center, United States Navy & United States Air Force.

India Meteorological Department. (1980). Cyclones and depressions in the Indian seas, 1978. Mausam, 31(4), 495–506. https://doi.org/10.54302/mausam.v31i4.3444

Deshpande, M., Singh, V. K., Ganadhi, M. K., Roxy, M. K., Emmanuel, R., & Kumar, U. (2021). Changing status of tropical cyclones over the north Indian Ocean. *Climate Dynamics*. Springer-Verlag GmbH Germany, part of Springer Nature. Published online July 17, 2021.

Gupta, S., Jain, I., Johari, P., & Lal, M. (2019). Impact of climate change on tropical cyclones frequency and intensity on Indian coasts. In P. Rao, K. Rao, & S. Kubo (Eds.), *Proceedings of the International Conference on Remote Sensing for Disaster Management* (Springer Series in Geomechanics and Geoengineering).

India Meteorological Department. (2013). *Cyclone warning in India: Standard operating procedure* (July 2013). Ministry of Earth Sciences, Government of India.

India Meteorological Department. (2018). *Very severe cyclonic storm "Gaja" over southeast Bay of Bengal (10–19 November 2018): A report*. Cyclone Warning Division, Ministry of Earth Sciences, Government of India.

India Meteorological Department. (2018). *Very severe cyclonic storm "Ockhi" over the Bay of Bengal (29 November–05 December 2017): A report*. Cyclone Warning Division, Ministry of Earth Sciences, Government of India.

India Meteorological Department. (2021). Cyclone warning in India: Standard operating procedure. Ministry of Earth Sciences, Government of India.

India Meteorological Department. (2021). *Extremely severe cyclonic storm "Tauktae" over the Arabian Sea (14–19 May 2021): A report*. Cyclone Warning Division, Ministry of Earth Sciences, Government of India.

India Meteorological Department (IMD), 2023. *Cyclone Hazard Climatology*. New Delhi: India Meteorological Department, June 2023.

IPCC. (2019). IPCC special report on the ocean and cryosphere in a changing climate (H.-O. Pörtner, D. C. Roberts, V. Masson-Delmotte, P. Zhai, M. Tignor, E. Poloczanska, K.

Mintenbeck, A. Alegría, M. Nicolai, A. Okem, J. Petzold, B. Rama, & N. M. Weyer, Eds.). Intergovernmental Panel on Climate Change.

IPCC. (2021). Climate Change 2021: The Physical Science Basis. Contribution of Working Group I to the Sixth Assessment Report. Cambridge University Press.

Joint Typhoon Warning Center. (1993). Annual tropical cyclone report: 1993. United States Navy & United States Air Force.

Joint Typhoon Warning Center. (1997). Annual tropical cyclone report: 1997.

Kannaujiya, V. K., Rai, A. K., & Malakar, S. (2024). Nature and impact of extremely severe cyclone Tauktae over India. *Discover Oceans*.

Kerala State Disaster Management Authority. (2015). *District disaster management plan: Idukki district*. Government of Kerala.

Kerala State Disaster Management Authority. (2015). *District disaster management plan: Ernakulam district*. Government of Kerala.

Kerala State Disaster Management Authority. (2016). *Kerala state disaster management plan 2016*. Kerala State Disaster Management Authority.

Kerala State Disaster Management Authority. (2021). *An integrated approach to the preparedness and mitigation of Cyclone Tauktae: The case of Kerala*. Government of Kerala.

Kotal, S. D., Bhattacharya, S. K., & Roy Bhowmik, S. K. (2014). Development of NWP based objective cyclone prediction system (CPS) for North Indian Ocean tropical cyclones — evaluation of performance. Theoretical and Computational Research in Radar Meteorology. https://doi.org/10.6057/2014TCRR03.03

Kumar, A., & Gupta, S. (2023). A review paper on tropical cyclone center detection. *International Journal of Scientific Development and Research (IJSDR)*, 8(7), 416–422.

Kumar, S., Verma, S., & Lodh, A. (2025). Unravelling the dynamical characteristics of tropical cyclones: Amphan and Nisarga using ERA5 reanalysis. Frontiers in Environmental Science, 12, 1475324. https://doi.org/10.3389/fenvs.2024.1475324

Mashao, F. M., Demoz, B., Kifle, Y., Klopper, D., Chikoore, H., Sakai, R. K., & Ayisi, K. K. (2024). An Appraisal of the Progress in Utilizing Radiosondes and Satellites for Monitoring Upper Air Temperature Profiles. *Atmosphere*, *15*(3), 387. https://doi.org/10.3390/atmos15030387

National Disaster Management Authority. (2019). *National disaster management plan (2019)*. Government of India.

National Disaster Management Authority. (2008). *National disaster management guidelines: Management of cyclones*. Government of India.

Niyas, N. T., Srivastava, A. K., & Hatwar, H. R. (2009). *Variability and trend in the cyclonic storms over the North Indian Ocean* (Meteorological Monograph No.). India Meteorological Department.

Priya, P., Pattnaik, S., & Trivedi, D. (2022). Characteristics of the tropical cyclones over the North Indian Ocean basins from the long-term datasets. Meteorology and Atmospheric Physics, 134, 65. https://doi.org/10.1007/s00703-022-00904-7.

Rao, S. R., Krishna, K. M., & Kumar, O. S. R. U. B. (2009). Study of tropical cyclone "Fanoos" using MM5 model: A case study. Natural Hazards and Earth System Sciences, 9, 43–51. https://doi.org/10.5194/nhess-9-43-2009

Salim, S. S., & Monolisha, S. (2022). Very severe cyclonic storm "Gaja" and its impact off the Tamil Nadu coastline. Indian Journal of Geo Marine Sciences, 51(08), 671–679. https://doi.org/10.56042/ijms.v51i08.68866

Sharma, M., Mohapatra, M., & Suneetha, P. (2025). *Evaluation of operational extended range forecast of cyclogenesis over the North Indian Ocean.* Advance online publication.

Singh, V., Koll, R. M., & Deshpande, M. (2020). The unusual long track and rapid intensification of very severe cyclone Ockhi. *Current Science, 119*(5), 771–779. https://doi.org/10.18520/cs/v119/i5/771-779

Singh, V. K., & Roxy, M. K. (2022). *A review of ocean–atmosphere interactions during tropical cyclones in the North Indian Ocean.*

Srivastava, K., & Bhardwaj, R. (2014). Assimilation of Doppler weather radar data in WRF model for simulation of Tropical Cyclone Aila. *Pure and Applied Geophysics, 171*(8), 2043–2057. https://doi.org/10.1007/s00024-013-0723-5

Tallapragada, V., et al. (2014). Hurricane Weather Research and Forecasting (HWRF) model: 2014 scientific documentation. NOAA/NCEP

Thenmozhi, M., Sujatha, M., Kavitha, M., Senthilraja, S., Babu, M., & Priya, V. (2024). Assessment of cyclone risk and case study of Gaja cyclone using GIS techniques and machine learning algorithms in coastal zone of Tamil Nadu, India. Environmental Research, 246, 118089. https://doi.org/10.1016/j.envres.2024.118089

Wang, S., Murakami, H., & Cooke, W. F. (2023). Anthropogenic forcing changes coastal tropical cyclone frequency. npj Climate and Atmospheric Science, 6, 187. https://doi.org/10.1038/s41612-023-00516-x

Wu, L., Zhao, H., Wang, C., et al. (2022). Understanding of the effect of climate change on tropical cyclone intensity: A review. Advances in Atmospheric Sciences, 39, 205–221. https://doi.org/10.1007/s00376-021-1026-x

Yip, K.H., Lui, Y.S., Chan, W.S., Kwok, Y.T., Chow, W., Lee, S.H., He, Y.H. and Chan, P.W., 2026. Advances in Tropical Cyclone Monitoring and Forecasting in Hong Kong Using Ensemble Predictions and Artificial Intelligence. *Tropical Cyclone Research and Review*.

Zhang, J., Chen, H., Zhu, Y., Shi, H., Zheng, Y., Xia, X., Teng, Y., Wang, F., Han, X., Li, J. and Xuan, Y., 2019. A novel method for estimating the vertical velocity of air with a descending radiosonde system. *Remote Sensing*, *11*(13), p.1538.

Zhao, K., Li, X., Xue, M., Jou, B.J.D. and Lee, W.C., 2012. Short-term forecasting through intermittent assimilation of data from Taiwan and mainland China coastal radars for Typhoon Meranti (2010) at landfall. *Journal of Geophysical Research: Atmospheres*, *117*(D6).

Annexure A: Data Availability

All datasets mentioned in the report are provided in the project folder for reference and reproducibility. These include shapefiles corresponding to each identified cyclone track; ERA5-Land, ERA5 surface, and ERA5 pressure-level datasets associated with the analyzed cyclone events; as well as the generated spatial maps (hourly meteorological variation maps, cumulative rainfall maps, coastal influence zone maps, and vertical profile plots). The data and outputs are systematically organized based on cyclone events, time periods, dataset types, and analysis categories, in alignment with the methodology described in the respective sections of the report.